Title of Investigation: Design Data Collection with Skylab/EREP Microwave Instrument S-193

Title of Report: A Survey of Terrain Radar Backscatter Coefficient Measurement Programs by C. King and R. K. Moore

CRES Technical Report 243-2

December, 1973

NASA Contract NAS 9-13331

Prepared for:

Principal Investigations Management Office
Technical Monitor: Mr. Larry B. York
NASA Lyndon B. Johnson Space Center
Houston, Texas 77058

Prepared by:

Richard K. Moore, Principal Investigator
University of Kansas Center for Research, Inc.
Remote Sensing Laboratory
Lawrence, Kansas 66045

Type of Report: Advance Report of Significant Results

THE UNIVERSITY OF KANSAS CENTER FOR RESEARCH, INC.
2385 Irving Hill Rd.—Campus West Lawrence, Kansas 66044

THE UNIVERSITY OF KANSAS / CENTER FOR RESEARCH, INC.

Irving Hill Rd.— Campus West Lawrence, Kansas 66044

A SURVEY OF TERRAIN RADAR BACKSCATTER COEFFICIENT MEASUREMENT PROGRAMS

CRES Technical Report 243-2

C. King

R. K. Moore

December, 1973

Supported by:

NATIONAL AERONAUTICS AND SPACE ADMINISTRATION
Lyndon B. Johnson Space Center
Houston, Texas 77058
CONTRACT NAS 9-13331

TABLE OF CONTENTS

LIST OF FIGURES

LIST OF FIGURES (Continued)

LIST OF FIGURES (Continued)

LIST OF FIGURES (Continued)

ABSTRACT

Backscatter cross-section data from the literature are summarized for different land targets for frequency and angle ranges near those of the S-193 radiometer-scatterometer on Skylab. The following formats are used: original data with reported absolute values, relative σ^o normalized to one incident angle, and relative σ^o normalized to one terrain category at a particular incident angle.

1.0 INTRODUCTION

Radar backscatter measurements have been made since the 1940's in numerous individual programs. The S-193 radscat sensor on Skylab, however, provides an opportunity for measuring the scattering properties of a larger variety of target areas than any of the individual previous programs because of the great speed with which the spacecraft can move over the ground. This summary has been prepared to serve as a manual of the state of knowledge of terrain backscatter in the pre-Skylab period for comparison with the data obtained from Skylab, and also to serve as a reference in its own right.

Measurements of the radar backscatter from the ground have been made from bridges and truck booms, from low and high altitude aircraft, and once from a rocket. Unfortunately, the absolute calibrations of the various measuring instruments have been inconsistent, so comparison of observations by the different investigators is difficult. Attempts have been made in this study to obtain more consistency by normalizing the data, first to a given angle of incidence (approximately 52°) and then to a given terrain category (cropland). Another inconsistency that made this task more difficult is the lack of uniformity in reporting of target classes and properties; in some cases detailed measurements and photographs are available, but in others only general categories designated by the pilot of a test aircraft were recorded.

The experiments reported here deal with the range of incident angles of the Skylab instrument (vertical out to 52°), although some observations are reported for angles closer to grazing incidence for special categories where measurements are not available in the preferred angular range. The S-193 operates at 13.9 GHz, and frequencies close to this were preferred for this summary report. As with the angular range, however, some observations rather far removed in frequency have been considered where suitable ovservations at nearby frequencies were not available. Unfortunately the only continuous frequency spectral measurements available at the time of writing were at 4-8 GHz, and the nearest frequency at which a complete set of near-vertical measurements could be found was 3.8 GHz.

Differences in terrain backscatter are caused by differences in dielectric properties, roughness of the surface, and inhomogeneities in the subsurface within the range of penetration of the signal. These backscatter properties are also governed

by the sensor parameters: look angle, frequency, polarization, bandwidth, and resolution. Since each program reported on used a different set of these parameters, comparison was often difficult. This fact should be borne in mind in examining the summary graphs and tables.

1.1 Organization

Differences in resolution between the Skylab and the various previous programs pose a problem in categorizing the data. The S-193 has a resolution of from 7 to about 30 km at different angles. The Ohio State University truck-mounted measuring system had a resolution of only about 35 cm. Other programs used resolutions or effective categorizations between these extremes. The only satisfactory approach at category selection seems to be use of rather broad categories appropriate to the Skylab sensor, and this approach has been selected here.

With this in mind, the following categories have been established:

1. Grassland
2. Farmland (cropland)
3. Forest
4. Desert
5. Residential-commercial area
6. Swamps
7. Pavements
8. Volcanic areas
9. Snow-covered terrain

These classifications may not be electromagnetically unique. For example, the class of terrain called "grassland" might have the same backscatter properties as dry cropland and it is shown later in the report that they do indeed appear similar. Use of pavements as a separate category might also be questioned since its contribution to the total return from a resolution cell as large as that of the S-193 is certainly insignificant; however, this category was extensively studied by Ohio State University so it is included for completeness. Since radar is proposed as a sensor to discriminate between crop types, use of "farmland" as a category may seen strange; however, the variation between crops is relatively small compared with the variation between

calibrations of the different programs, so this seems a reasonable category. Even though these faults certainly exist in the categorization scheme, it is used here since it seems best able to match the kinds of identifications given in the various programs referenced.

A brief, but quite comprehensive survey is made of the majority of measurements previously reported in the literature. Particular emphasis, however, is placed on work by four institutions that engaged in long-term measurement programs: U. S. Naval Research Laboratory airborne [1] and bridge-mounted [2] radars, Goodyear Aerospace Corporation airborne radars [3, 4], Ohio State University truck mounted systems [5-8], and NASA/MSC airborne scatterometer [9-15].

Extensive samples of the observations from these programs, and some of the other shorter-duration programs, are first presented. Then summaries of the results, using the calibrations provided, are given. The disparity between calibrations is clearly apparent in this summary. Results from the same terrain class appear to differ by as much as 20 dB!

Next, the backscatter observations are normalized to a single look angle. That is, returns at that angle are considered to be identical, and the variability of the ratios of returns at other angles to returns at this angle is examined. This process reduced the variation of the data considerably, but the various categories of terrain still give such overlapping responses that they are essentially indistinguishable and this is believed due more to differences in measurement techniques and calibrations than to real commonality of the responses.

To improve categorization of the ovservations, the backscatter cross-sections were normalized to one category: farmland. This technique seemed most encouraging even though farmland itself has considerable variability within a given program. Deserts and roads could be separated with this technique, and to some extent volcanic areas also appeared separate. Grasslands and woods could be distinguished from each other.

2.0 SURVEY OF PREVIOUSLY CONDUCTED MEASUREMENTS

2.1 Naval Research Laboratory Measurements

The Naval Research Laboratory has been one of the leading institutions in the measurement programs on radar terrain returns. Their investigations involved the use of both aircraft and ground based stations and these efforts are discussed in turn. Their even more significant research in sea returns is not discussed here, although a part is mentioned briefly in Appendix A.

The aircraft program [1] obtained terrain backscatter data in four frequencies, about 0.4, 1.2, 4.4 and 8.9 GHz; with each frequency, data for all four polarizations were taken. The angles of incidence ranged from vertical to 80° off vertical.

The target areas were identified by pilot comments, having been preselected as relatively homogeneous.

The four major categories of land areas investigated were New Mexico desert land with low sparse vegetation, New Jersey pine trees with heavy under-growth and occasional snow patches, the city of Chicago area including industrial, business and residential structures, and the portion of Lake Michigan immediately adjacent to the city of Chicago. Figures 1A-D show the backscatter coefficient variation as a function of the incidence angle for X band (8.9 GHz) with VV, HH, and cross polarizations respectively. The results for other frequencies are listed in the original report and are not repeated here.

Another Naval Research Laboratory radar terrain backscatter investigation was reported by Grant and Yaplee [2]. Radars operating at wave-lengths of 3.2 cm (X-band), 1.25 cm (K-band), and 8.6 mm (Ka-band) were used to obtain the scattering coefficient of ocean surface under various conditions of wind speed as well as several types of land surfaces with different types of natural vegetation canopy.

The radars were mounted on bridges that had approaches at least 30 meters above the land terrain and 45 meters above the water surface. The discussion here is limited to land observations.

Figure 2A is the backscatter vs viewing angle curve for a tree-covered terrain in full foliage at New Orleans. Figures 2B and 2C shows the contribution of moisture to a terrain in Port Arthur, Texas, with tall weeds and flags. Data from Figure 2B was obtained when the ground was dry and Figure 2C described the same

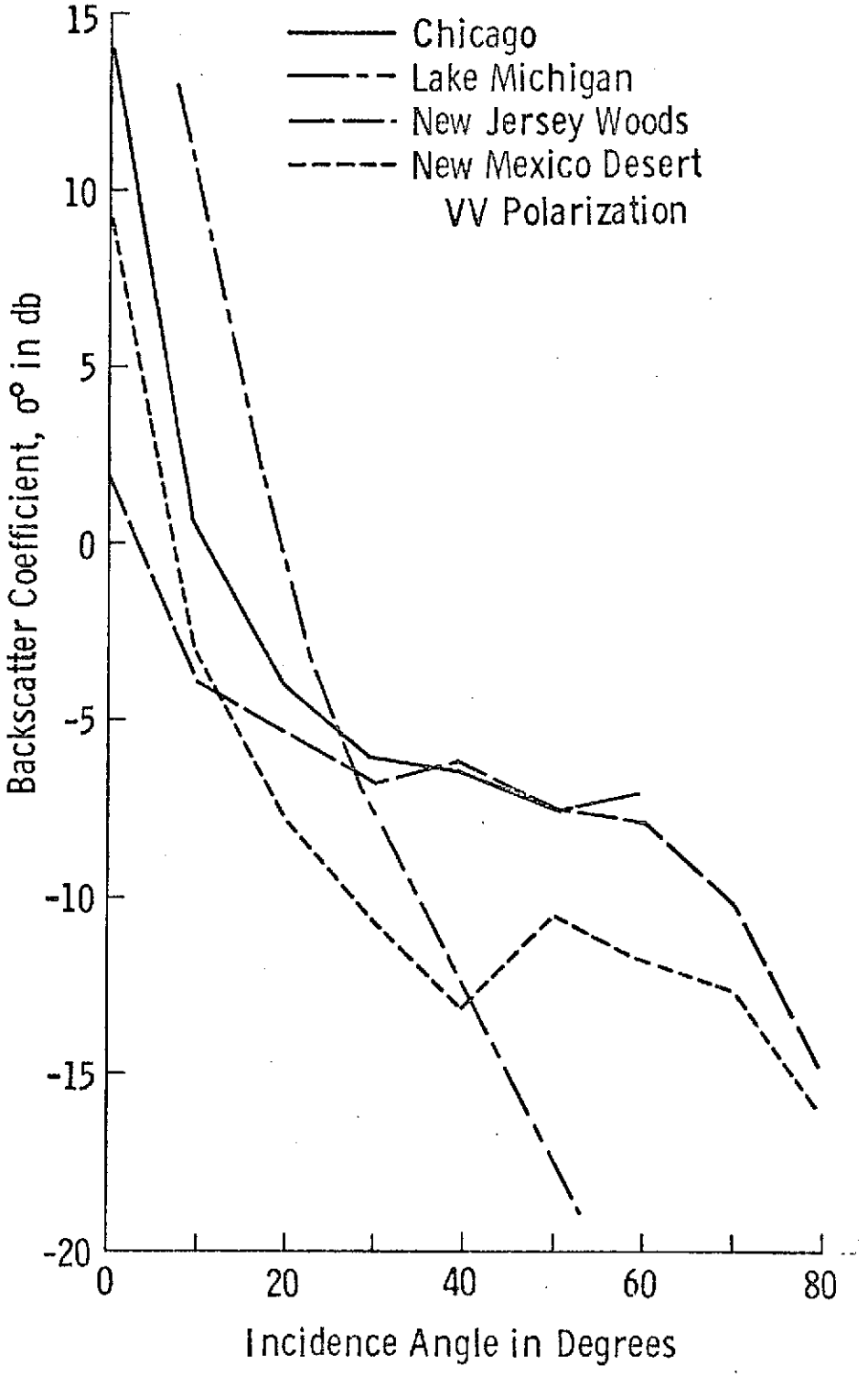

Figure IA. Backscatter Coefficient at X-Band for Four Terrain Targets. (After Ament, et al.)

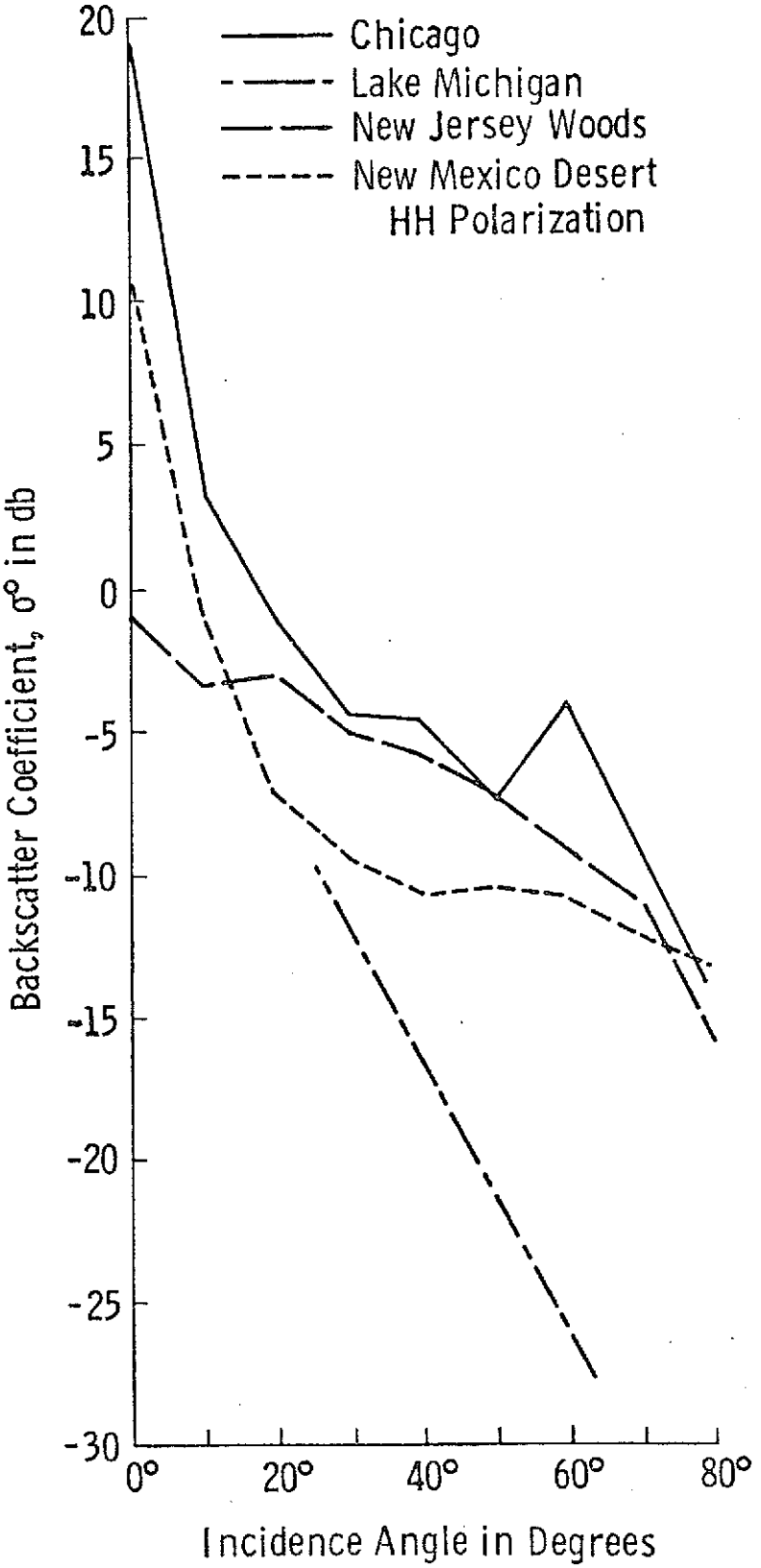

Figure IB. Backscatter Coefficient at X-Band for Four Terrain Targets. (After Ament, et al.)

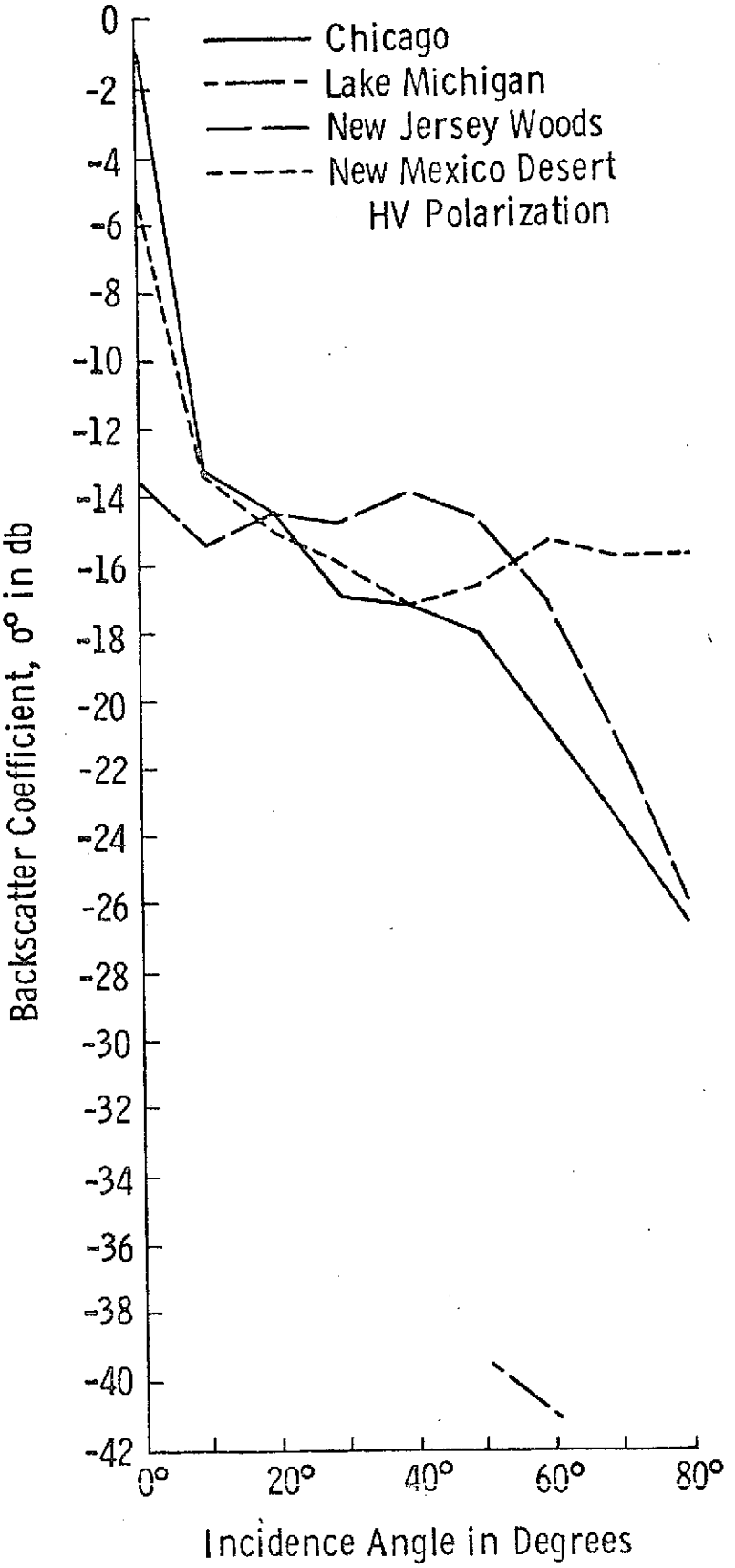

Figure IC. Backscatter Coefficient at X-Band for Four Terrain Targets. (After Ament et al.)

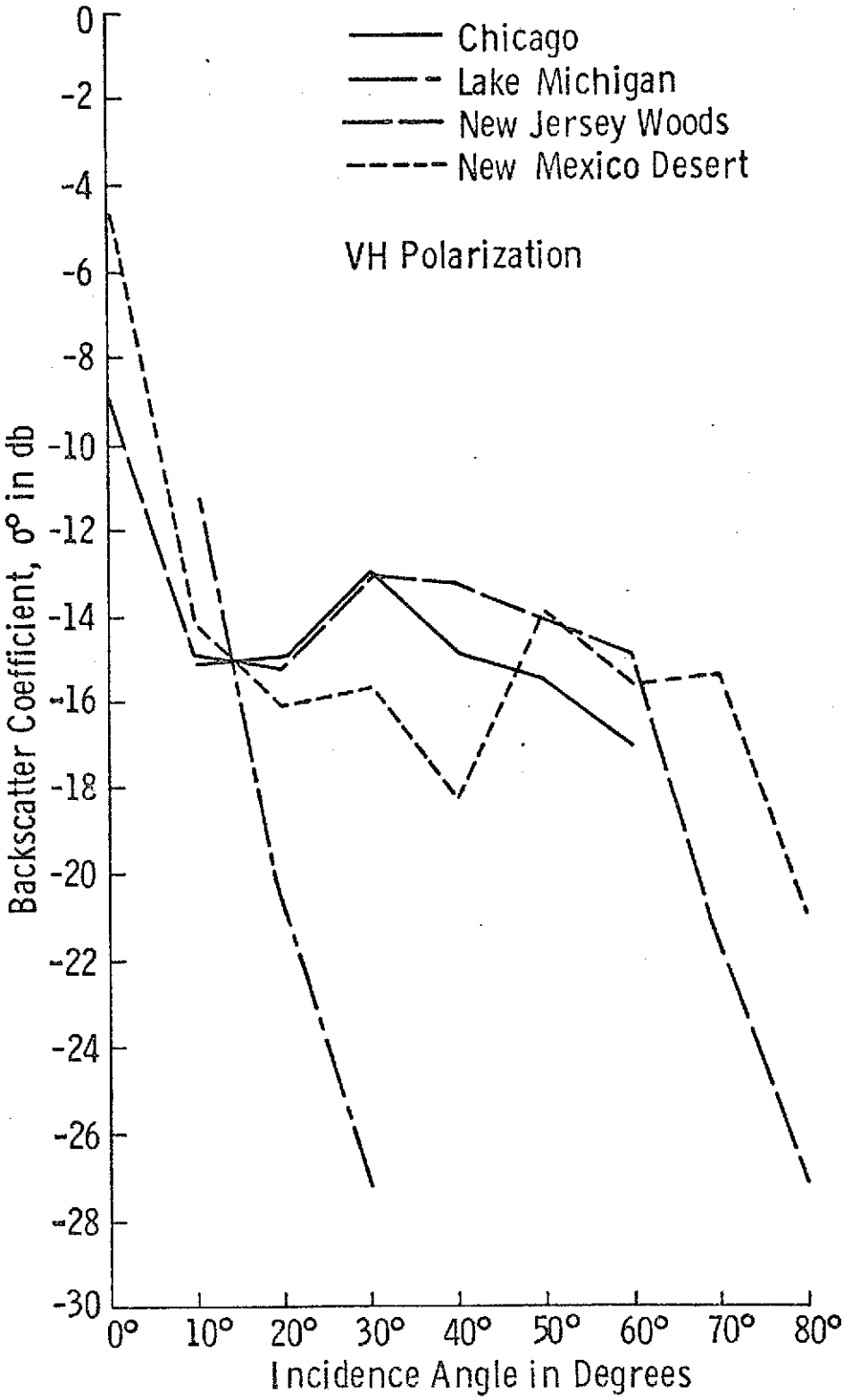

Figure ID. Backscatter Coefficient at X- Band for Four Terrain Targets. (After Ament, et al.)

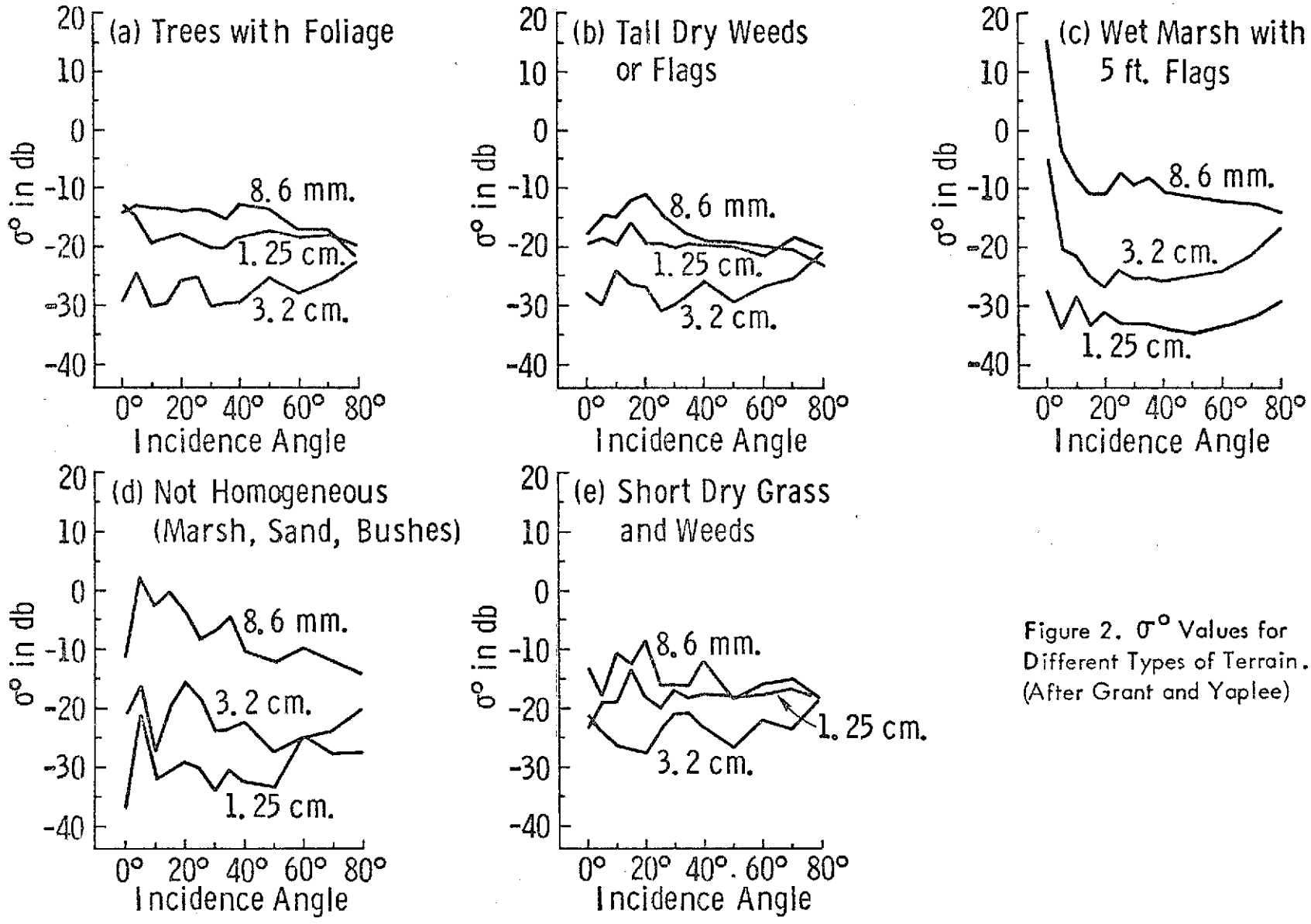

Figure 2. σ° Values for Different Types of Terrain. (After Grant and Yaplee)

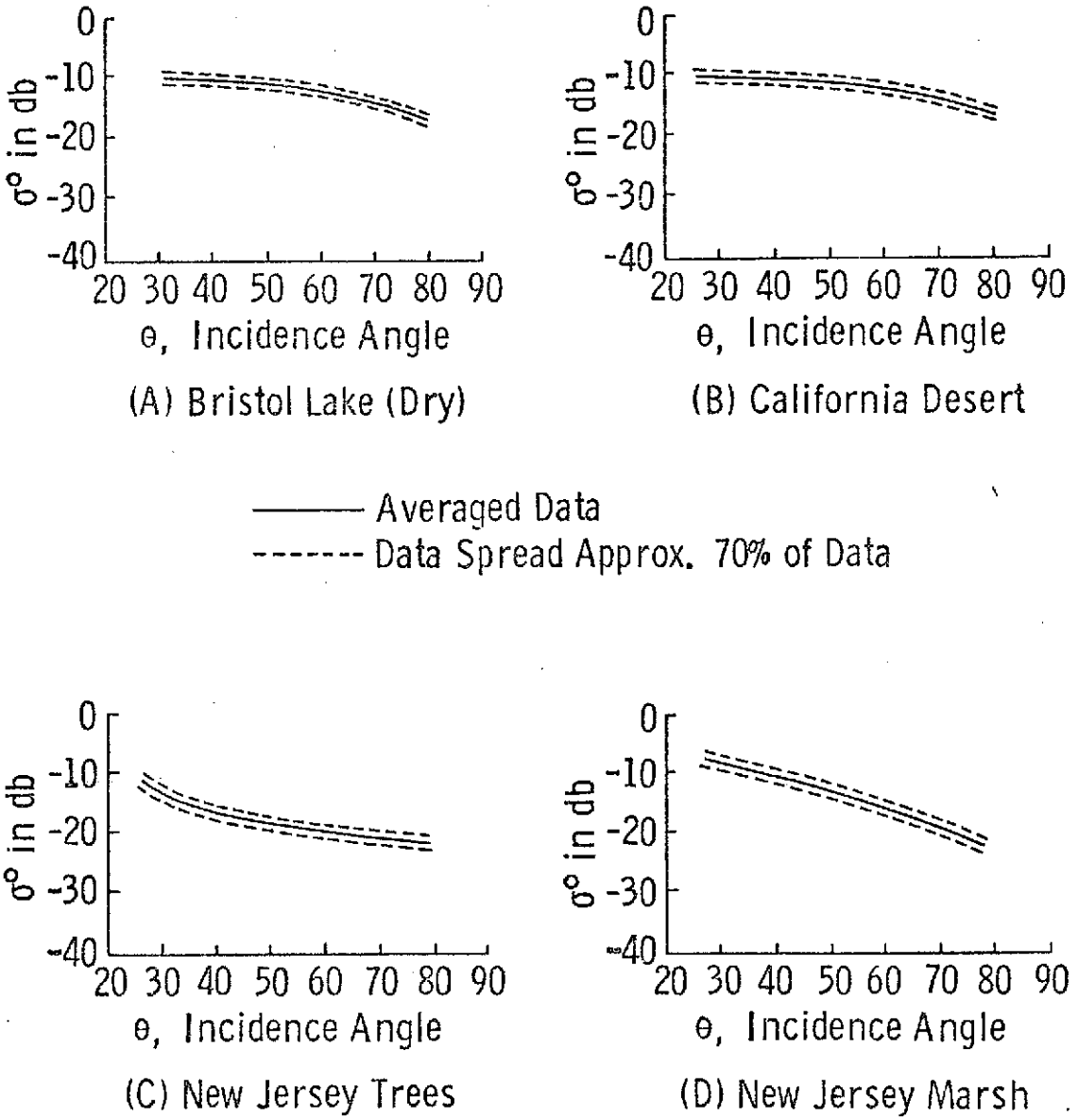

Figure 3. Backscattering Coefficient Vs. Incidence Angle. (After Reitz, et al.[3]) X-Band, Horizontal Polarization.

area wet. The other figures included non-homogeneous terrain composed of marsh, sands and bushes and river levee predominantly covered with grass.

Both the land and aircraft measurements presented above were lacking in detailed ground descriptions. This makes it difficult to compare other results with those obtained by NRL. The NRL results can, however fit into the general categories devised for the S-193.

2.2 Goodyear Aerospace Corporation Measurements

The Goodyear Aerospace Corporation conducted an investigation to obtain scattering coefficient data [3] in which much more complete ground descriptions were obtained. Widely different terrains representing four geographic areas in five states were studied with a modified airborne imaging radar. The imaged areas included irrigated farmland in Arizona, forest and meadows in Minnesota, trees and marsh along the New Jersey coast, mangrove islands and swamps in the Florida Keys, dry pine forest and grassland in Arizona, desert regions in both Arizona and California and the Bristol dry lake bed in California. The ground targets were identified by vertical aerial photos taken inflight and the radar imagery was also used for verification purposes.

Simultaneous pulse-by-pulse recordings of the signals used to produce imagery were made on film and these were used for the computation of back-scattering coefficients. In cases where finer details of the terrain investigated were desired ground photos were also taken.

The radar employed a conventional pulsed transmitter operating at a frequency of 9.375 GHz. The antenna was designed to provide uniform ground illumination over the wide range of depression angles from 10 to 70 degrees.

Figures 3A-3D show some of the results obtained. The solid lines are the average values of the backscatter coefficients and the dashed lines indicate bounds for approximately 70 per cent of the data spread. A more interesting result was that the backscatter coefficients grouped into bands that can be associated with the gross terrain characteristics [4]. Figure 4 shows that all the measured terrain with heavy vegetation cover are limited to a band less than 5 dB wide. The narrow band of broken desert included the dry grassland of Northern Arizona, the desert in Chandler, Arizona and Amboy, California. The sandy desert of Yuma, Arizona contributed to the wide band of arid desert sand.

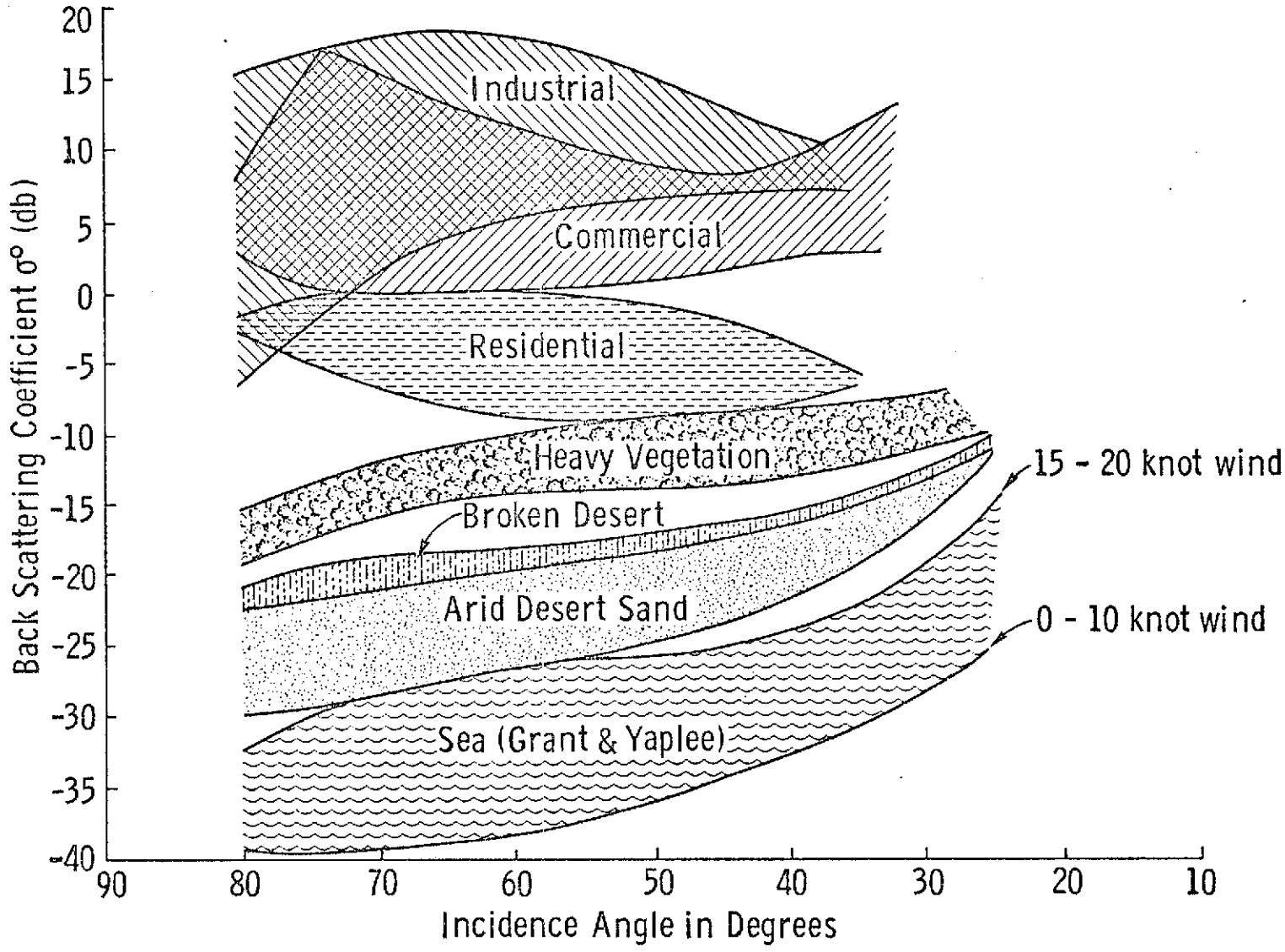

Figure 4. Goodyear X-Band horizontal polarized terrain return analysis program data summary. (After Newbry[4])

For comparison, Grant and Yaplee's ocean surface wind dependence data, which was excluded in previous discussions in this report was included (in reference 4) to emphasize the cluster nature of the data. The areas marked industrial, commercial, and residential come from sketchy data and will only be taken in a relative measure in the sense that cultural areas, in general, fall above the band for heavy vegetation.

It is interesting, at this point, to compare the NRL data with that obtained by Goodyear. To pick a reference, the backscatter coefficient for vegetation (heavy vegetation from Goodyear and New Jersey woods from Ament's NRL results) is arbitarily set to 0 dB at 43° incidence. The returns from the other areas are normalized accordingly. From Figure 5 it can be seen that within the range of antenna viewing angles of the Goodyear system, the backscattering data from NRL followed the same order in terrain return magnitude; i.e. the return from an urban target is higher than the return froma vegetated area, and that, in turn, is higher than the return from desert and water body. Nevertheless, the NRL data did not fall completely in the bands prescribed by Goodyear. The return from Chicago, in particular, was entirely outside of Goodyear's industrial-commercial-residential band.

2.3 Ohio State University Measurements

Since the 50's, the Ohio State University ElectroScience Laboratory has been conducting terrain radar return measurements. The measuring system for the work reported here consisted of four high-gain, narrow beam, CW-Doppler radars operating at L (1.8 GHz), X(10 GHz), Ku (15 GHz), and Ka (35 GHz) bands.

Most of the experiments were conducted with the radars mounted on the hydraulic boom of a truck, and the Doppler signal was generated by driving the truck along the terrain surface to be measured [5, 6, 7]. For some experiments, notably on bistatic return [8], the equipments were set up in the laboratory and the targets were brought in on a movable cart. The Doppler signal, in this case, was generated by pulling the cart across the illuminating beam.

The incidence angles ranged from 10° to 80° and all four polarization were possible. The size of the illuminated area was in the order of 30 cm square; thus limiting the range of terrains studied in the sense that any sort of terrain variability having a large scale could not be observed.

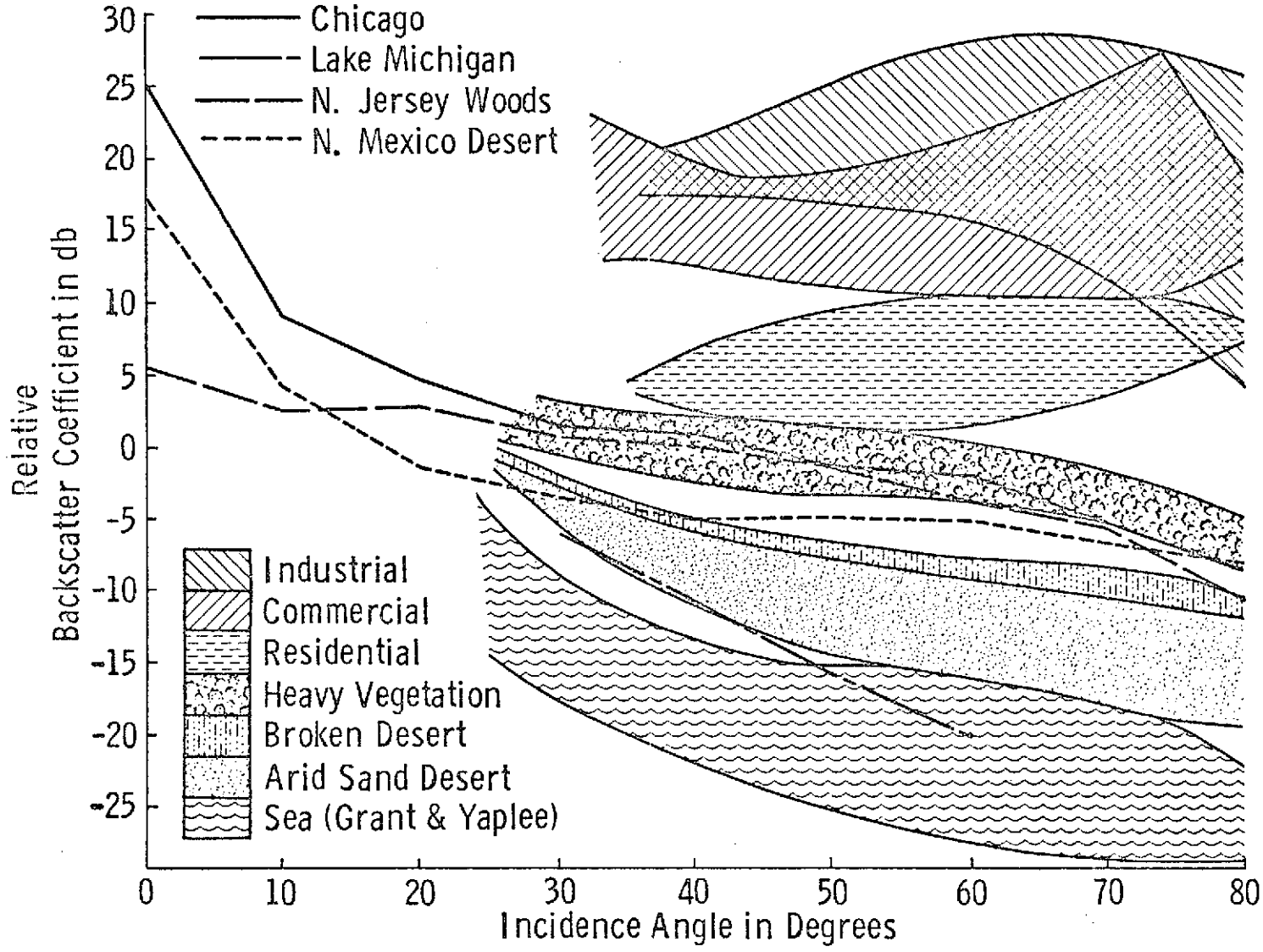

Figure 5. Goodyear Adjusted Data (+11.5 db) HH Polarization. Compared with NRL (Ament, et al.) Data (+6.1 db) Reference of 0 dB for σ° for Heavy Vegetation at 43°.

The Terrain Handbook [5], published in 1959, contained a detailed description of the measurements made by the Ohio State personnel prior to that time. Basically three categories of measurements were made; road surfaces, agricultural terrains and the effect of precipitation on surfaces. The road surfaces examined included pavements of different compositions and degrees of roughness; agricultural terrains consisted of fields of various stages of preparation and crop cover; and both rain and snow effects of backscatter were studied.

Figure 6 shows the backscatter from the different road pavements examined. In general, gravel-topped surfaces gave the highest return followed by asphalt and concrete surfaces respectively. Notice that the data could be grouped into three distinct bands.

On the other hand, the data from farmland were quite different. Figure 7 shows the radar cross sections of the crop as listed in the Terrain Handbook. Only alfalfa, grass, oats, and one bare field were investigated at Ku-band. Additional data available from Oliver and Peake's report [6], are plotted in Figure 8.

From both sets of figures, it is obvious that no definite bands can be ascribed to the crop types. This particular nature of agricultural terrain is also reflected in the June, 1970 Garden City farmland data obtained by the NASA/Ryan scatterometer. A detailed discussion on the NASA data is presented later in this report. On the other hand, NASA imaging radar data, and Kansas University truck-based data, taken later in the season, do show distinctions.

It might be worth noting that the σ^o vs viewing angle plots for agricultural crops tend to curve up beyond 50^o incidence for crops that are in head. The dynamic range of the entire farmland data is around 13 dB and this figure is much greater than the 5 dB range prescribed by Goodyear for all vegetated landscapes.

The effects of precipitation cover on terrain surfaces are equally complex. Figure 9 shows that at X and Ka bands, snow increased the backscatter from grass but the reverse is observed at Ku band. This reversal trend might be an indication of the kind of roles that the indicent wavelength could play. Different formations of snow cover and the depth of snow also caused different return as evidence in Figure 10.

The effects of rain on backscatter are depicted in Figures 11A and 11B. At Ka band, precipitation moisture decreased the backscatter of a relative smooth

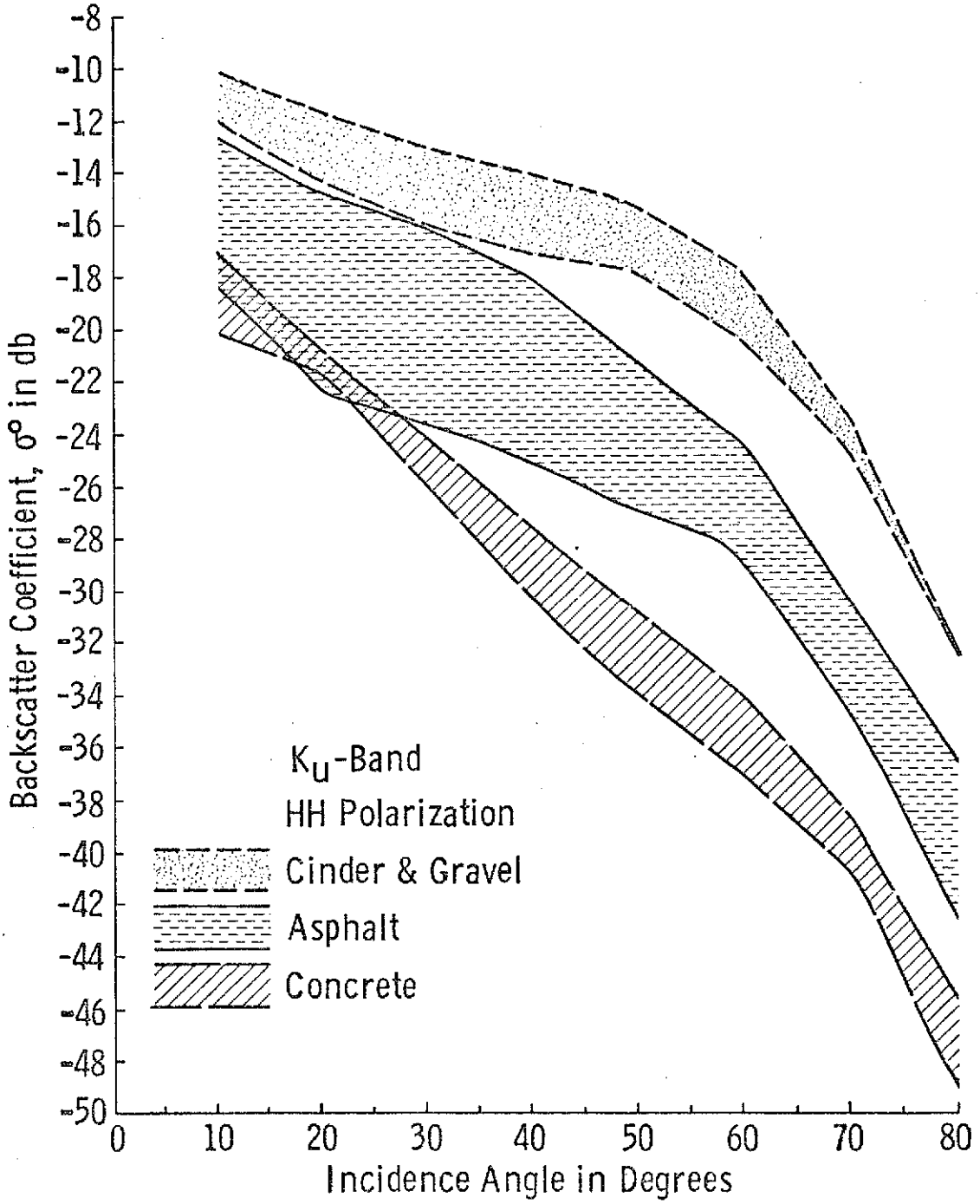

Figure 6A. Backscatter Coefficient of Road Surfaces. (After Cosgriff, et al.)

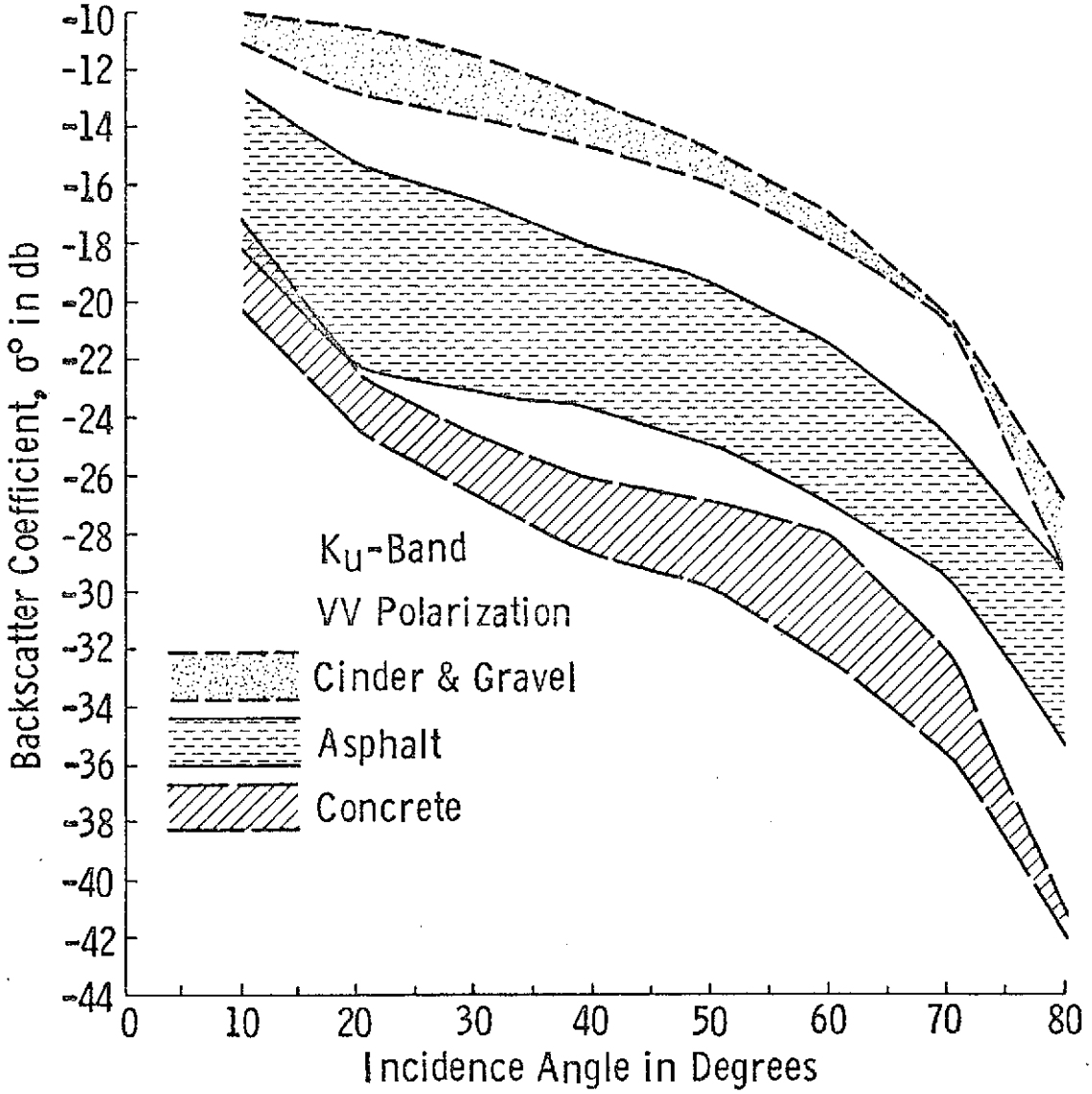

Figure 6B. Backscatter Coefficient of Road Surfaces.
(After Cosgriff, et al.[5])

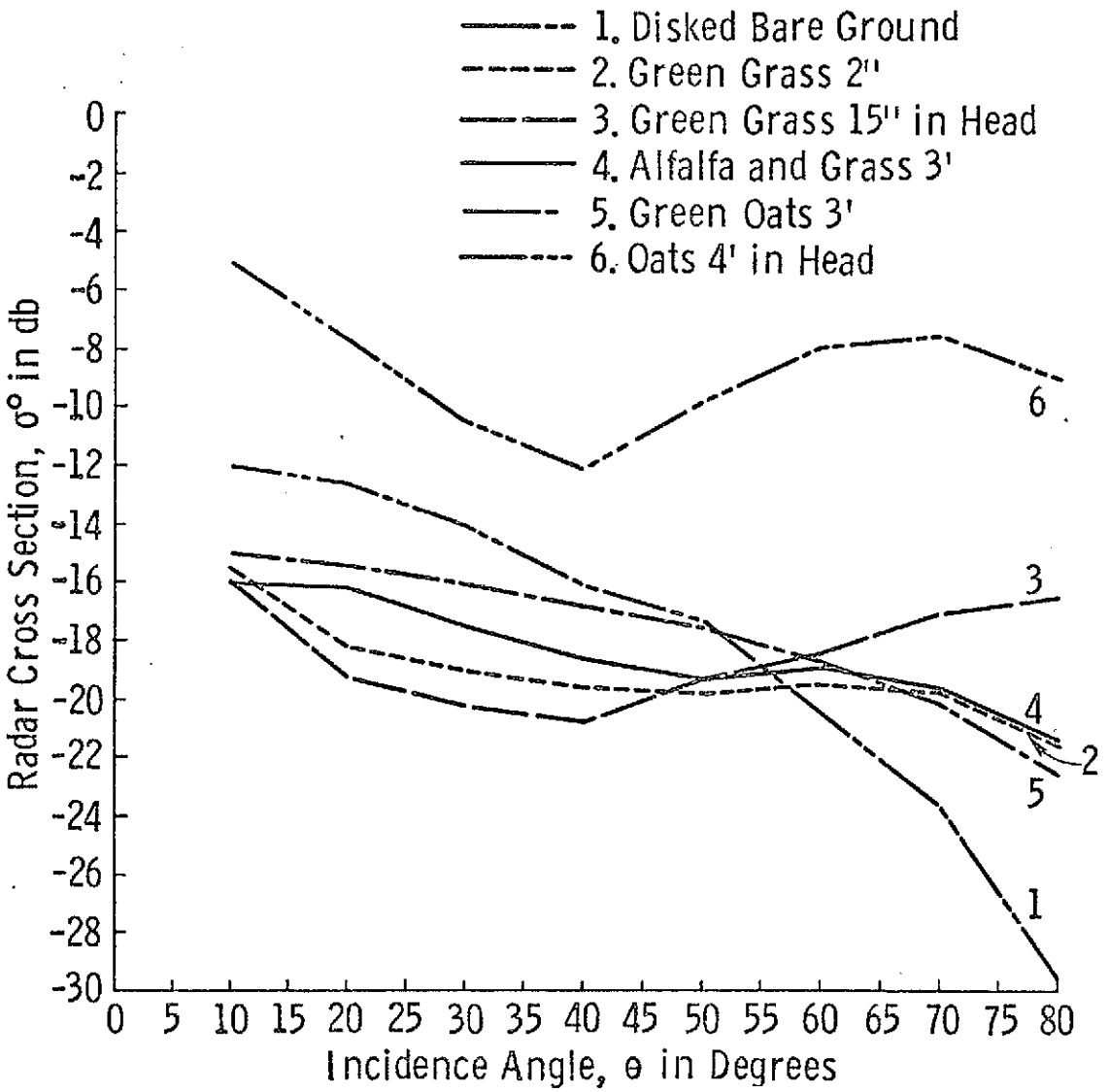

Figure 7A. Ohio State Farmland Data, Ku-Band, Polarization VV. (After Cosgriff, et al.)

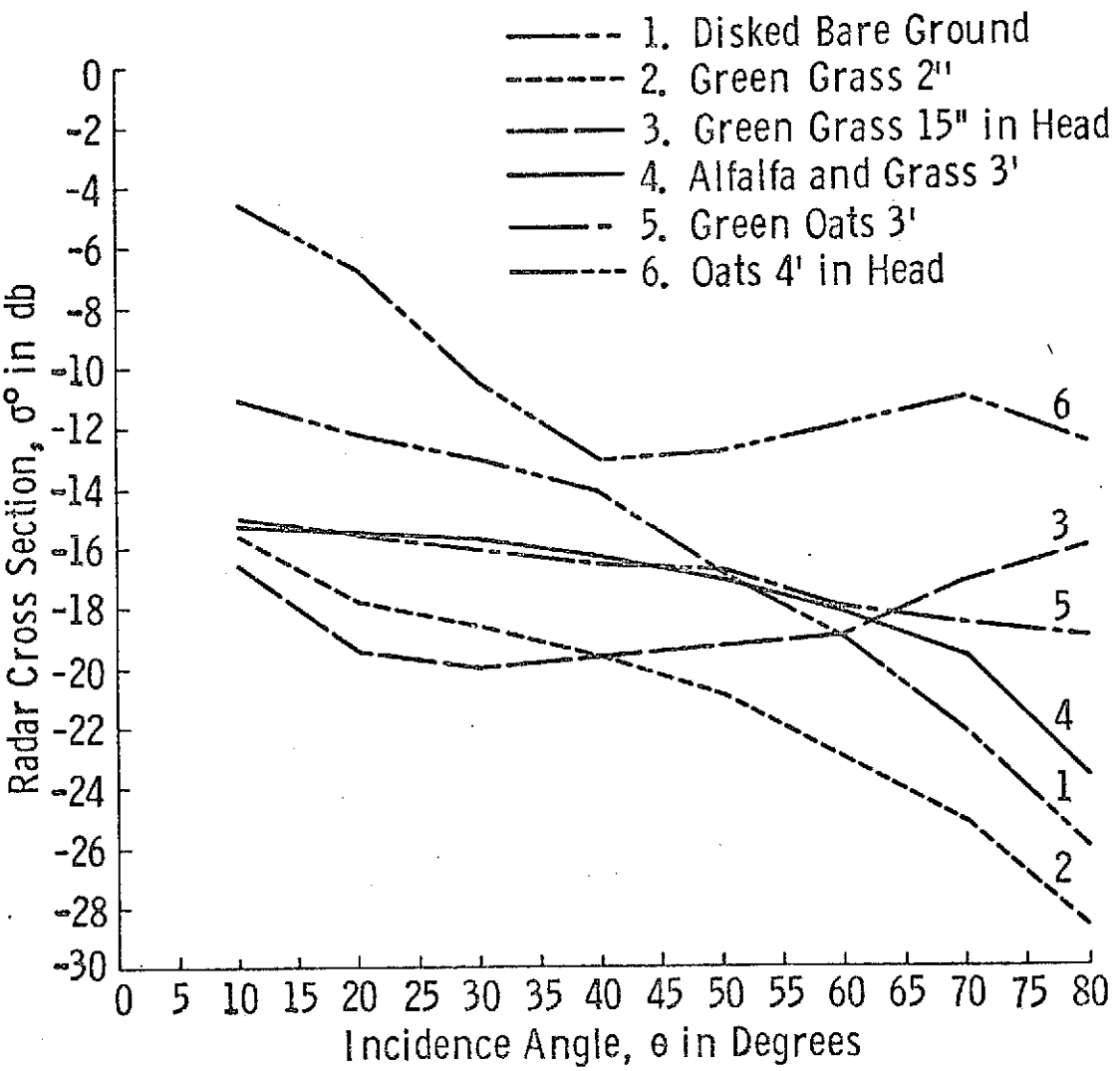

Figure 7B. Ohio State Farmland Data, Ku-Band, Polarization HH. (After Cosgriff, et al.)

310. Wheat, in Head 48"
66. Bulk Wheat, in Head, 32"
103. Wheat Stubble
68. Oats, in Head, 26"
302. Oats, Green, 10"
306. Oats, Green, in Head, 36"
111. Soybeans, 36"
107. Corn, Not in Tassel, 7'
113. Corn, in Tassel, 6'
70. Alfalfa, 12 - 18"
156. Grass, 2"
158. Grass, 2 1/2"

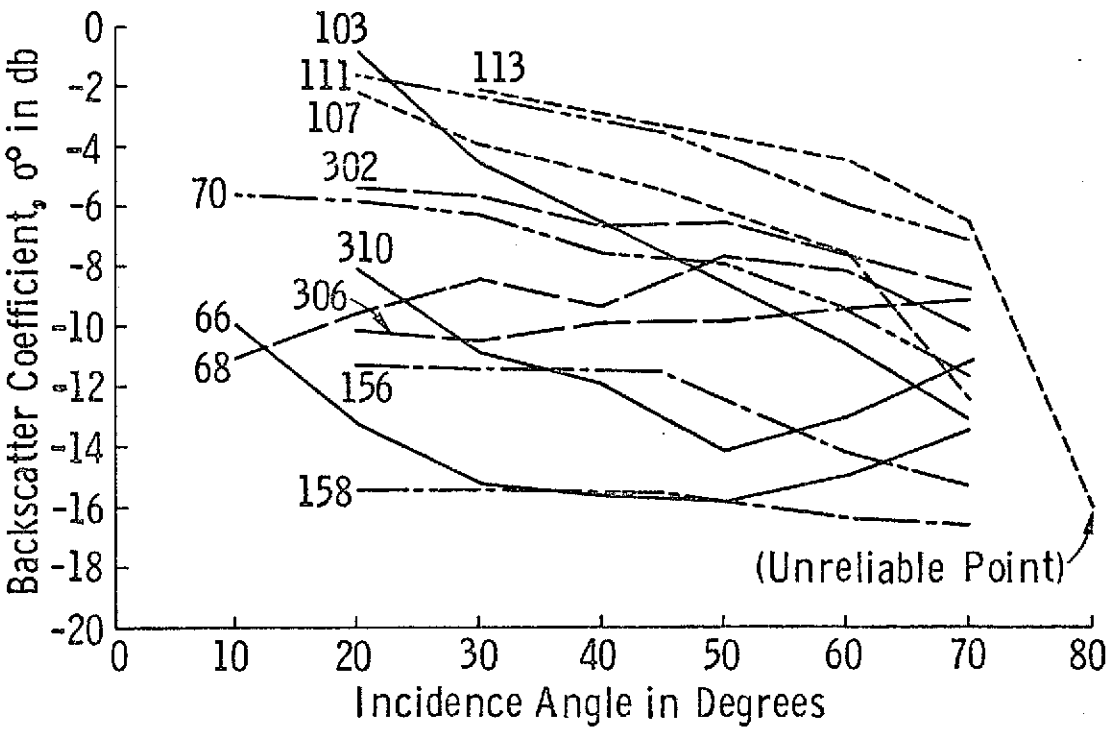

Figure 8A. Backscatter Coefficient for Farmland, Ohio State, Ku-Band, Polarization V. (After Peake and Oliver)

310. Wheat, in Head 48"
66. Bulk Wheat, in Head, 32"
103. Wheat Stubble
68. Oats, in Head, 26"
302. Oats, Green, 10"
306. Oats, Green, in Head, 36"
111. Soybeans, 36"
107. Corn, Not in Tassel, 7'
113. Corn, in Tassel, 6'
70. Alfalfa, 12 - 18"
156. Grass, 2"
158. Grass, 2 1/2"

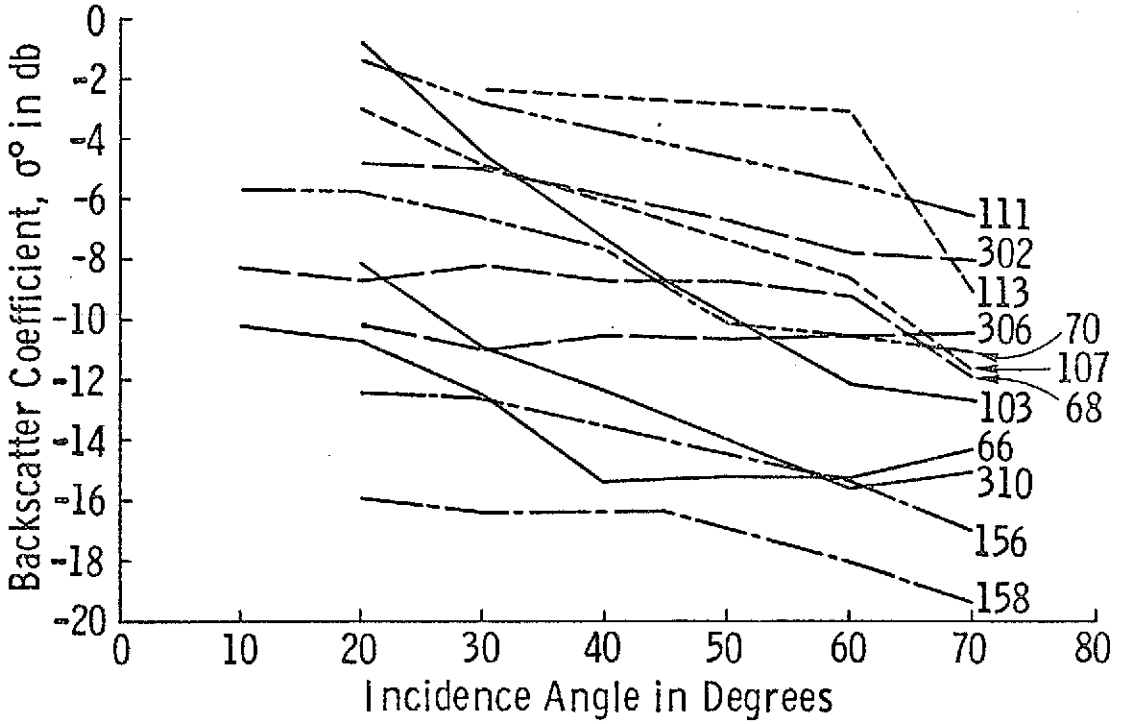

Figure 8B. Scattering Coefficient for Farmland, Ohio State, Ku-Band, Polarization H. (After Peake and Oliver)

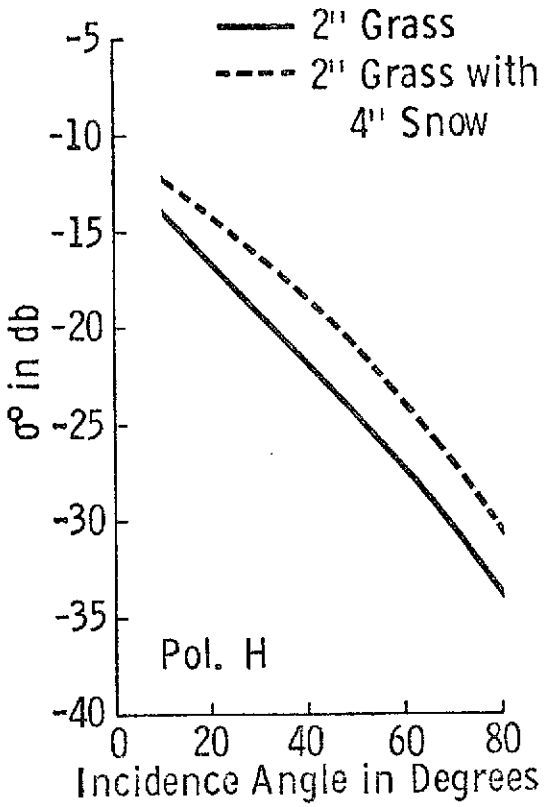

(A) X-Band

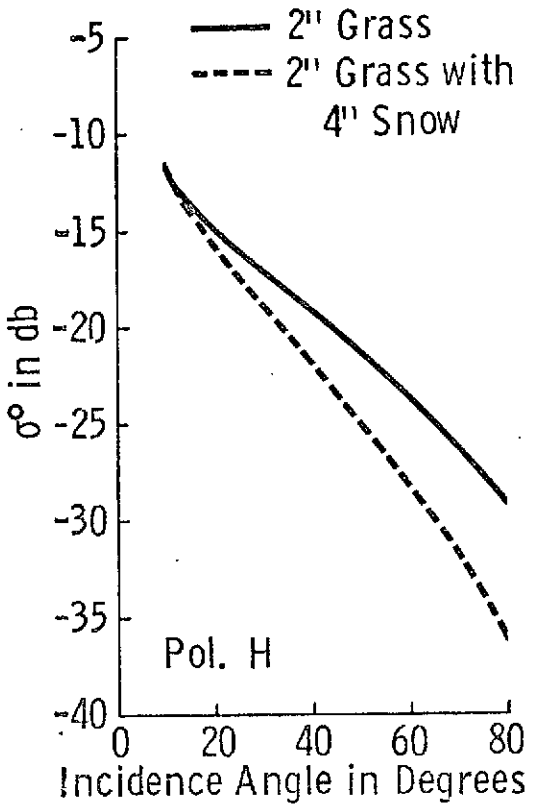

(B) K_U-Band

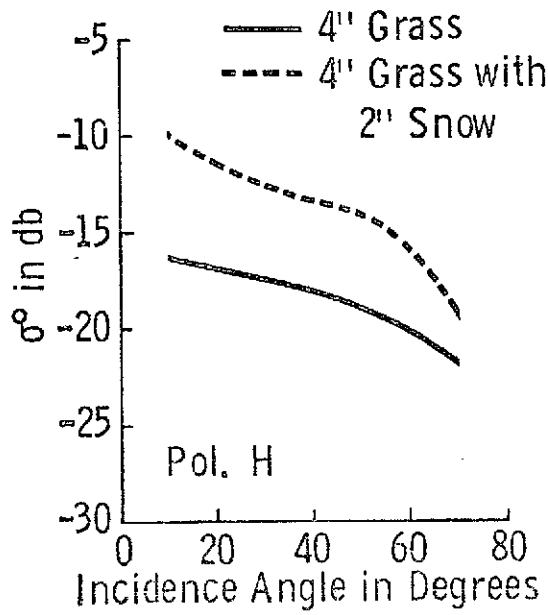

(C) K_a-Band

Figure 9. Effects of Snow Cover on Grass at X, K_U, and K_a-Bands. (After Cosgriff, et al.)

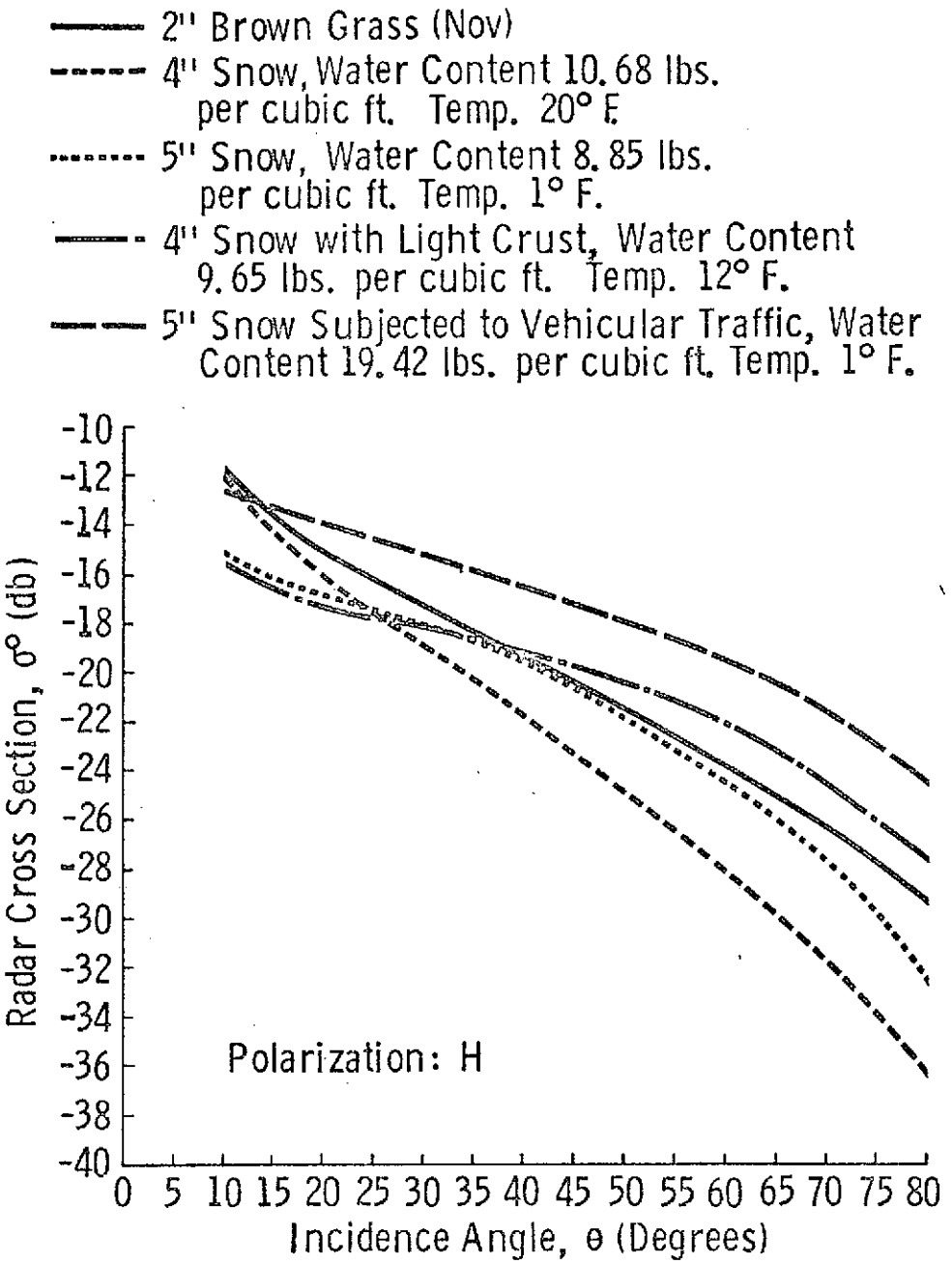

Figure 10. Effects of Various Types of Snow at K_u-Band. (After Cosgriff, et al.)

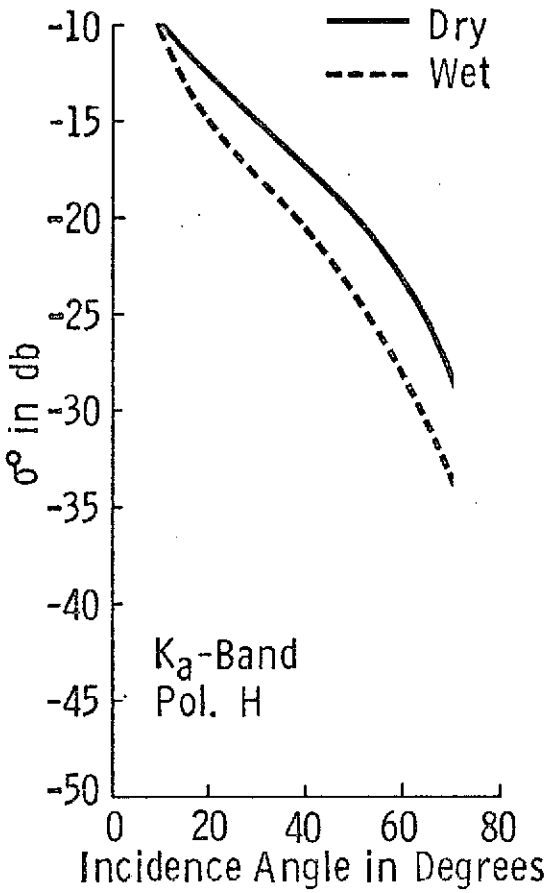

Figure IIA. Effect of Rain on Asphalt Road. (After Cosgriff, et al.)

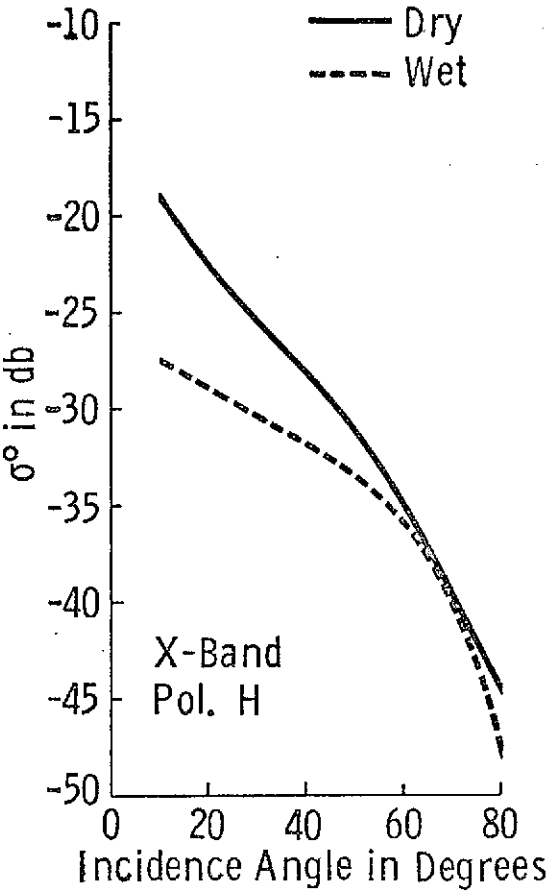

Figure IIB. Effect of Spraying Water on Asphalt Road. (After Cosgriff, et al.)

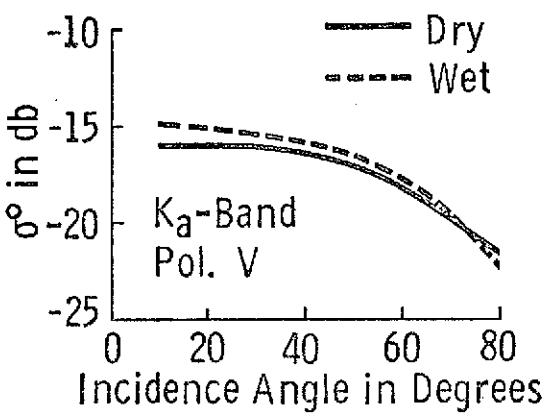

Figure IIC. Effect of Light Rain on 3' Alfalfa and Grass. (After Cosgriff, et al.)

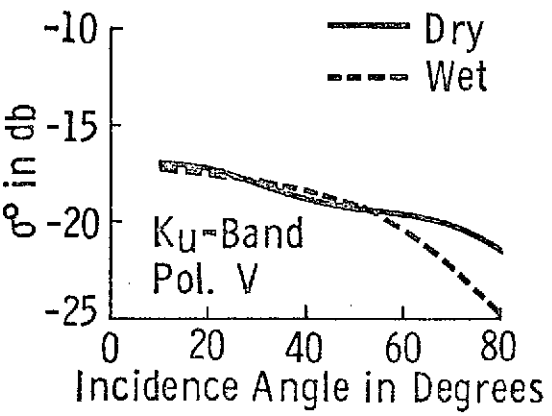

Figure IID. Effect of Light Rain on 3' Alfalfa and Grass (After Cosgriff, et al.)

surface such as asphalt and increased the backscatter from a relative rough surface such as a vegetated field. The same phenomenon was reported at X band. At Ku band, no data was taken for the effects of rain on asphalt road.

In 1965-66, a series of measurements were conducted by the Ohio State researchers to obtain the backscatter information for terrains of geological interest [7]. The terrains investigated included a volcanic area with lava flows and playa in California and limestone quarries in Ohio and Indiana.

The results at Ku band are listed in Figures 12 and 13. Figure 12 shows data from the volcanic area at Pisgah Crater and Figure 13 shows the backscatter cross section of a limestone quarry near Columbus, Ohio.

The Ohio State data discussed so far were all for monostatic systems. A bistatic terrain return experiment was performed by Peake and Cost [8] in the mid-60's using an X band system. The additional variable introduced in this experiment was the receiver azimuth angle. The bistatic experiments explored the effects of surface roughness, the sensor polarization, and also verified the reciprocity theorem.

2.4 NASA/MSC Scatterometer Measurements

The NASA Manned Spacecraft Center,starting from the mid-60's, conducted a series of radar terrain return programs with an airborne Ku band scatterometer. Most of the data were analyzed at The University of Kansas. The three major programs were a geological study at Pisgah Crater in California [9, 10], sea ice studies off Point Barrow, Alaska [11, 12] and an agricultural terrain study in Western Kansas [13, 14, 15].

The NASA experiments are characterized by careful ground study of the regions overflown. Besides supporting materials such as aerial photos and radar images which were taken inflight, ground crews were dispatched to collect information on the ground. Typical information inthe agricultural experiments included ground photos, vegetation types and coverage, stages of crop development, crop vigor, planting direction, and representative soil and plant moisture data.

The NASA/MSC scatterometer operated at 13.3 GHz and was vertically polarized. This CW-Doppler system has a fan beam that spans 60° either side of the vertical along the flight line. At a normal flight altitude of 1 km the half power illuminated cross-track width on the ground was 40 meters.

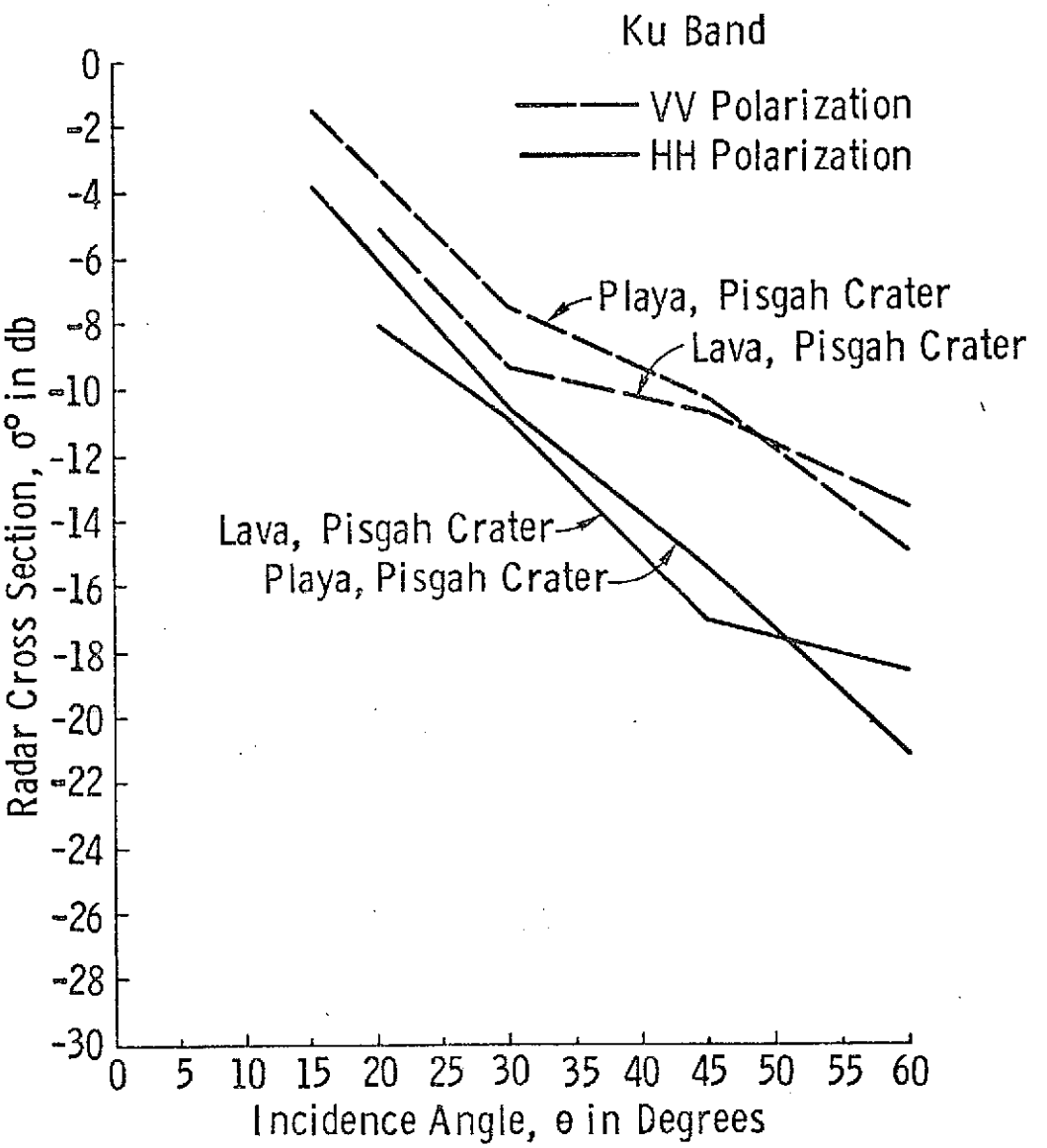

Figure 12. Backscatter Coefficient of Various Volcanic Soils. (After Shultz, et al.)

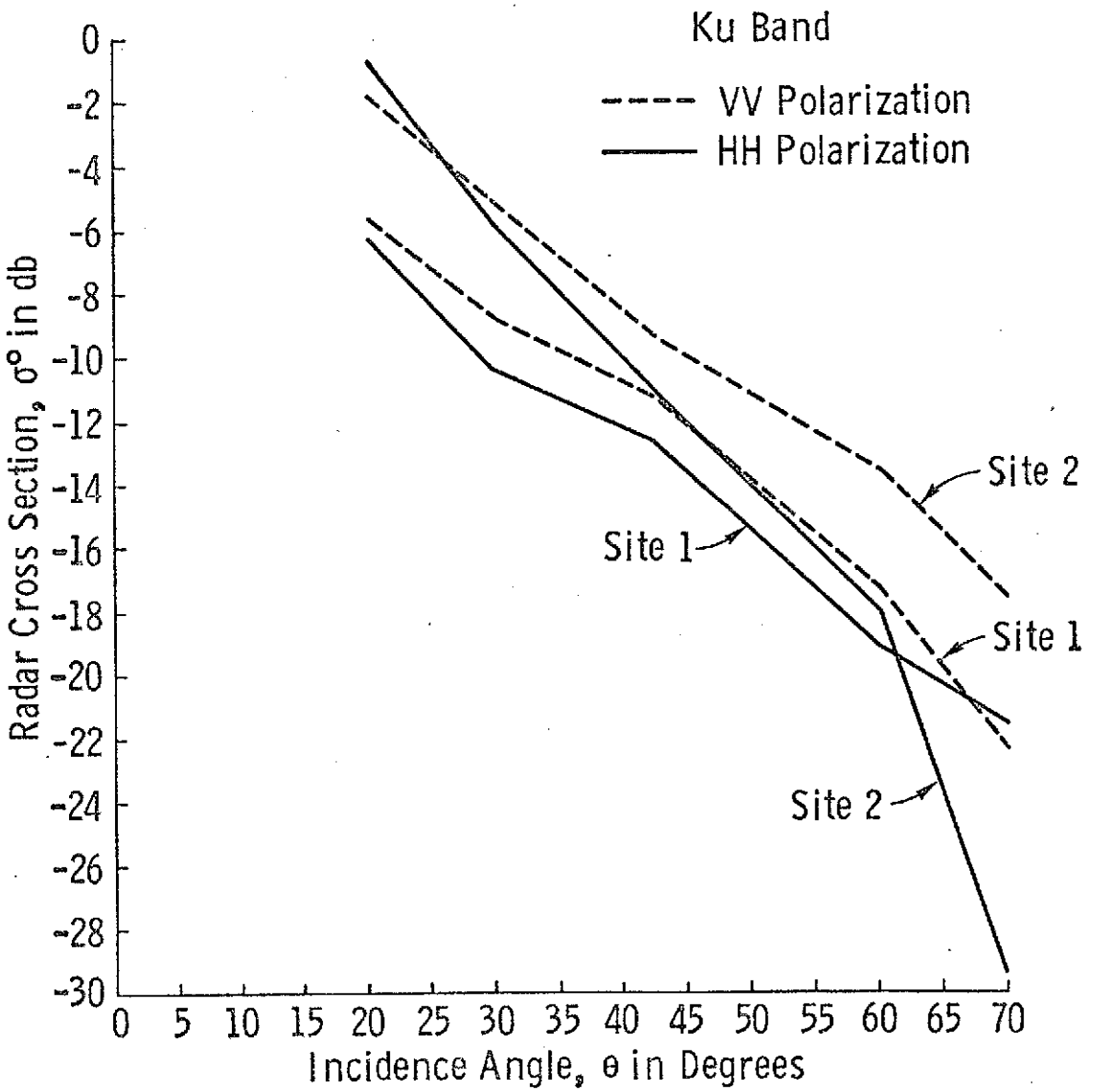

Figure 13. Backscatter of Limestone Quarry Surfaces. (After Shultz, et al.)

In the Pisgah Crater run, the flight path traversed fourteen different geological formations, mostly of volcanic origin [9]. The area where the Ohio State data was gathered was also included. These fourteen areas could be grouped into three more general categories: desert, lava area, and playa. Figure 14 shows the radar cross sections observed at the Pisgah Crater area.

On comparing results with the Ohio State data, it was found that, except for a vertical displacement, the playa surface yielded identical slopes for their respective cross section curves (Figure 15). The encouraging feature was that except for a bias, the two groups of data, although taken years apart by two different systems operating at entirely different platform altitudes yielded the same result.

In the sea ice experiments, the ice formations were first separated into five [11] and then expanded into seven major categories [12] of ice thickness. This identification was made possible from aerial photos which were taken in the same time the experiment was conducted. The backscatter from the different ice types is shown in Figure 16 and it can be seen that except for open water in the range of incidence angles less than 20°, multi-year ice (more than 6 feet thick) gave the strongest return.

Agricultural terrain backscatter data was collected by the same system over a test site northwest of Garden City, Kansas. In this region the terrain is very flat, and the farming is sometimes done with irrigation, but not always. Crops grown include alfalfa, corn, grain sorghum, sugar beets, and wheat.

A recent study conducted by The University of Kansas reported that presence of irrigation water in the fields caused an increase of 5-7 dB in the radar cross section at angles within 45° of the vertical [14] (see Figure 17). Implications for use of radar as a sensor of agricultural areas were that determining soil moisture requires incidence under 45° at that particular frequency, but studying plants requires larger incident angles.

The distinctions among the various crop types were not marked for the observations in June. The average value of σ° for each field in the Garden City test site was computed and histograms were made to show the spread of all the means of the individual fields at each antenna viewing angle [15]. Figures 18A-18F illustrate the spread of the backscatter data at the various angles. Each dot represents the mean value of a field, and the bar is the average all the fields that fall within a particular crop type. The shaded area represents the spread of one standard deviation from the mean.

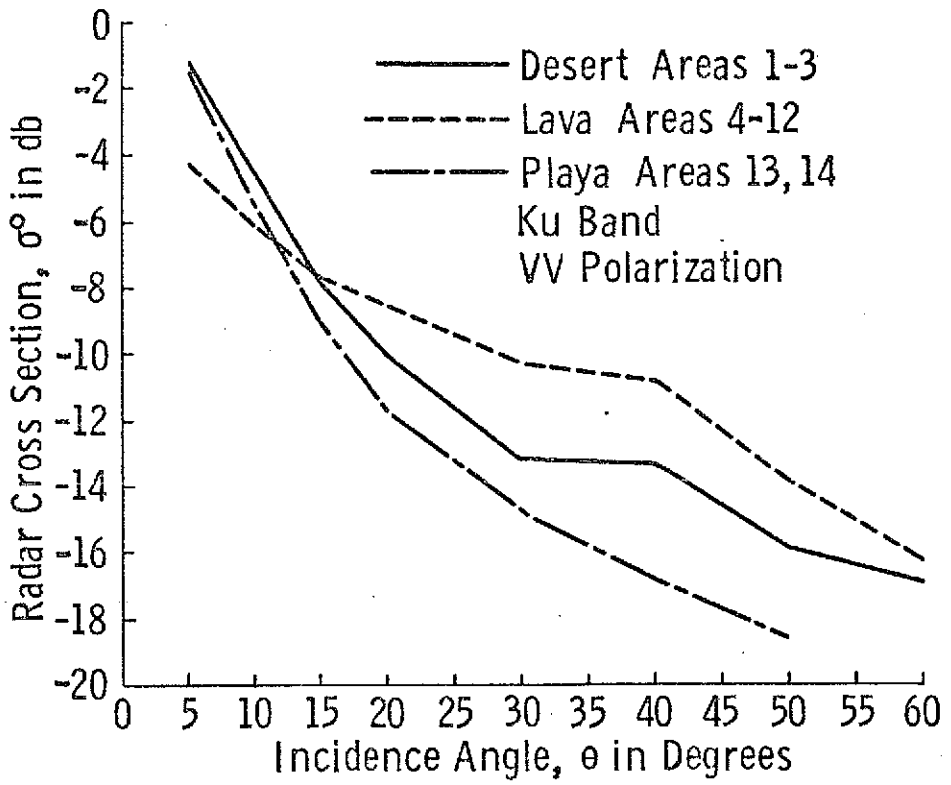

Figure 14. Radar Cross-Section of Pisgah Crater. (After Masenthin)

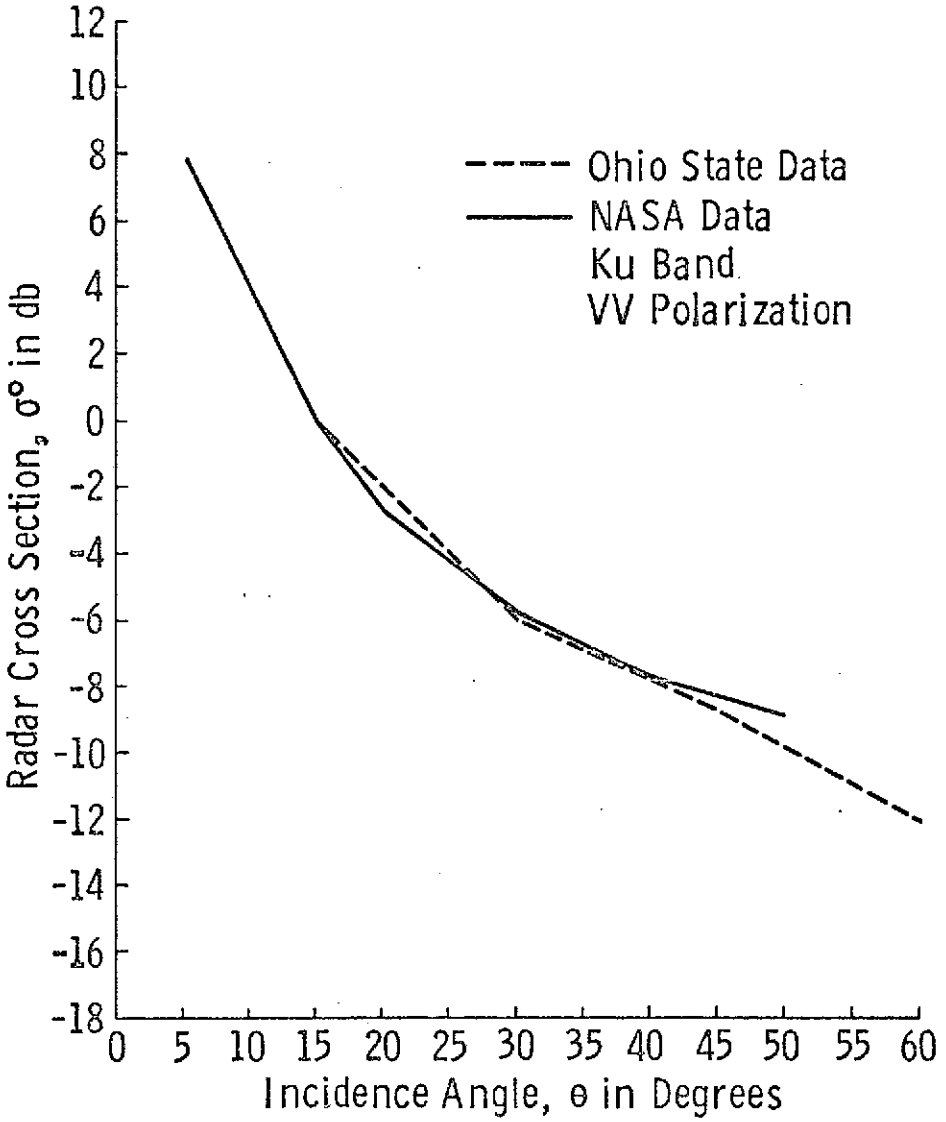

Figure 15. Radar Cross-Section of Playa Surface from Pisgah Crater (Values are Relative).

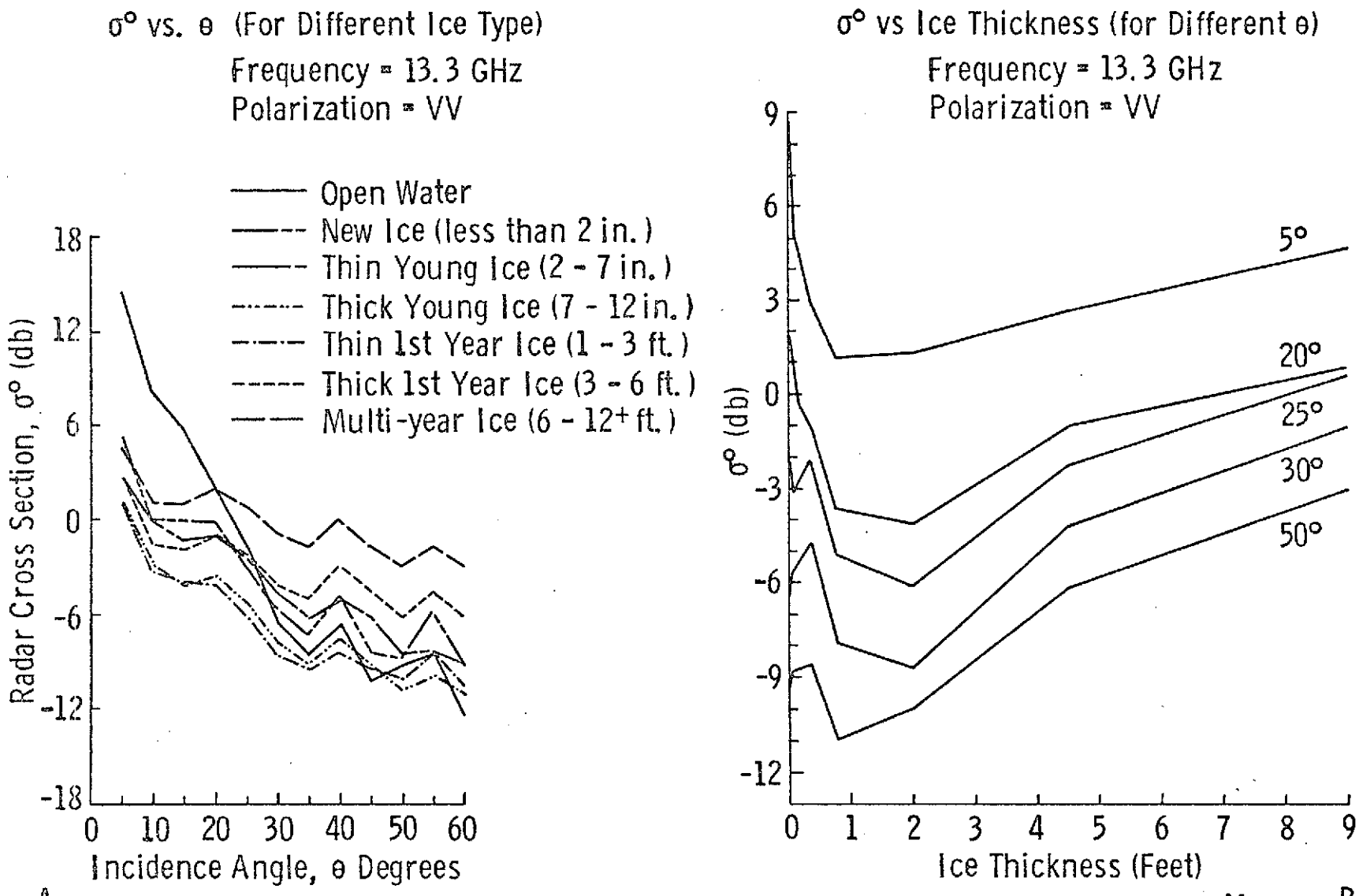

Figure 16. Scattering coefficient for sea ice off Point Barrow, Alaska. (After Parashar.[11])

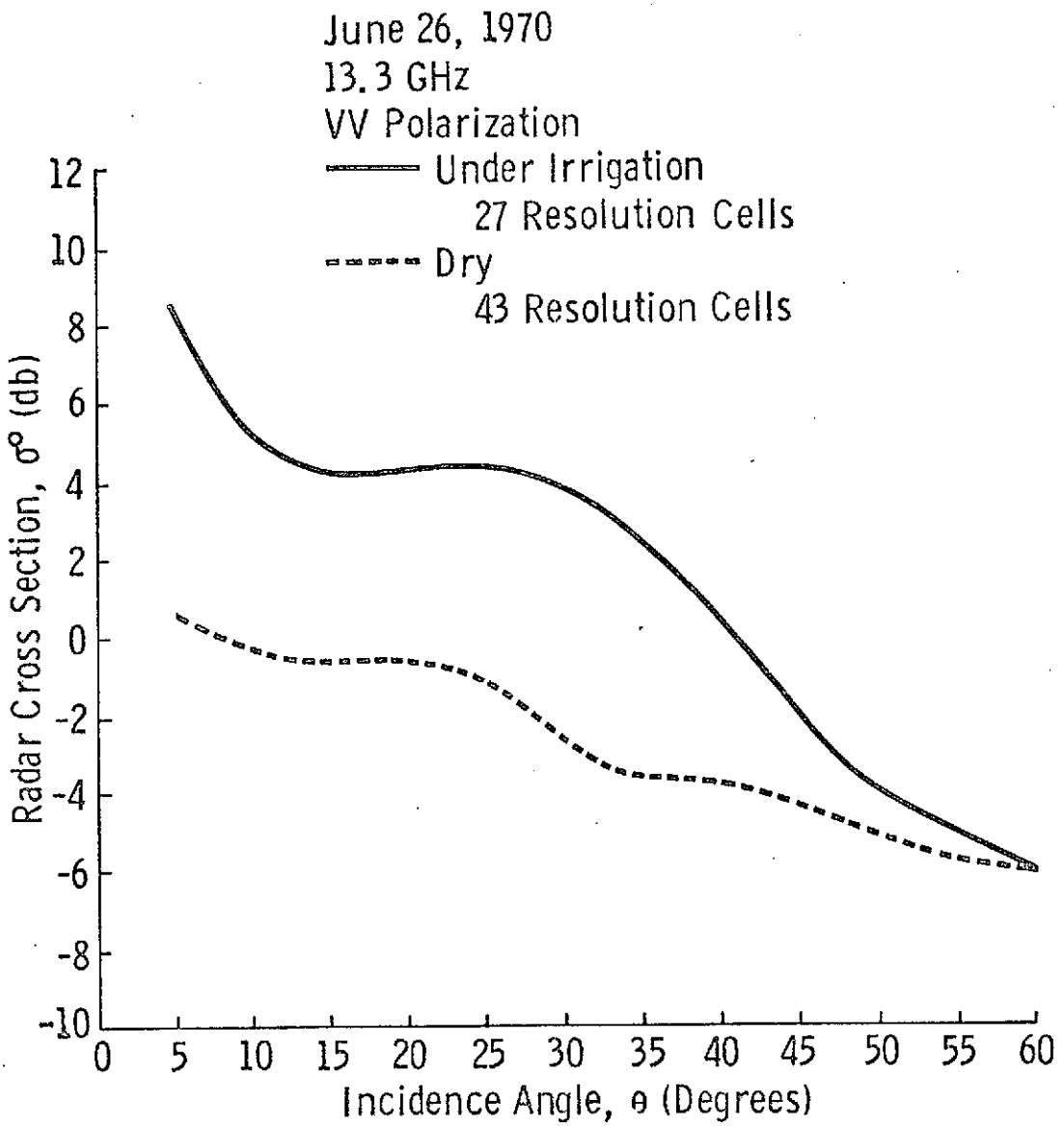

Figure 17. Dry Fields vs. Fields Under Irrigation. (NASA/JSC Data Analyzed at University of Kansas)

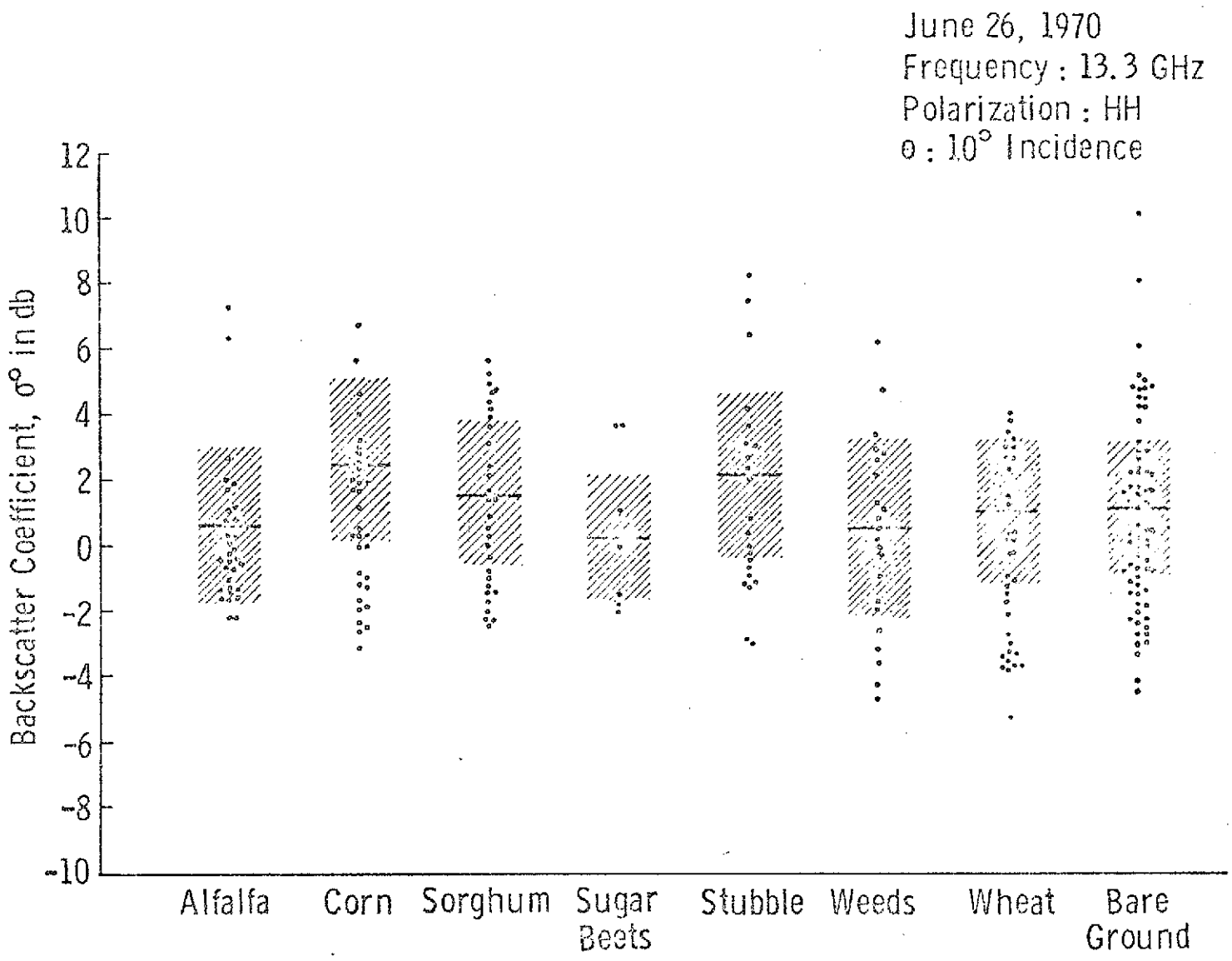

Figure 18A. Distribution of Mean Scattering Coefficients of Agricultural Fields.

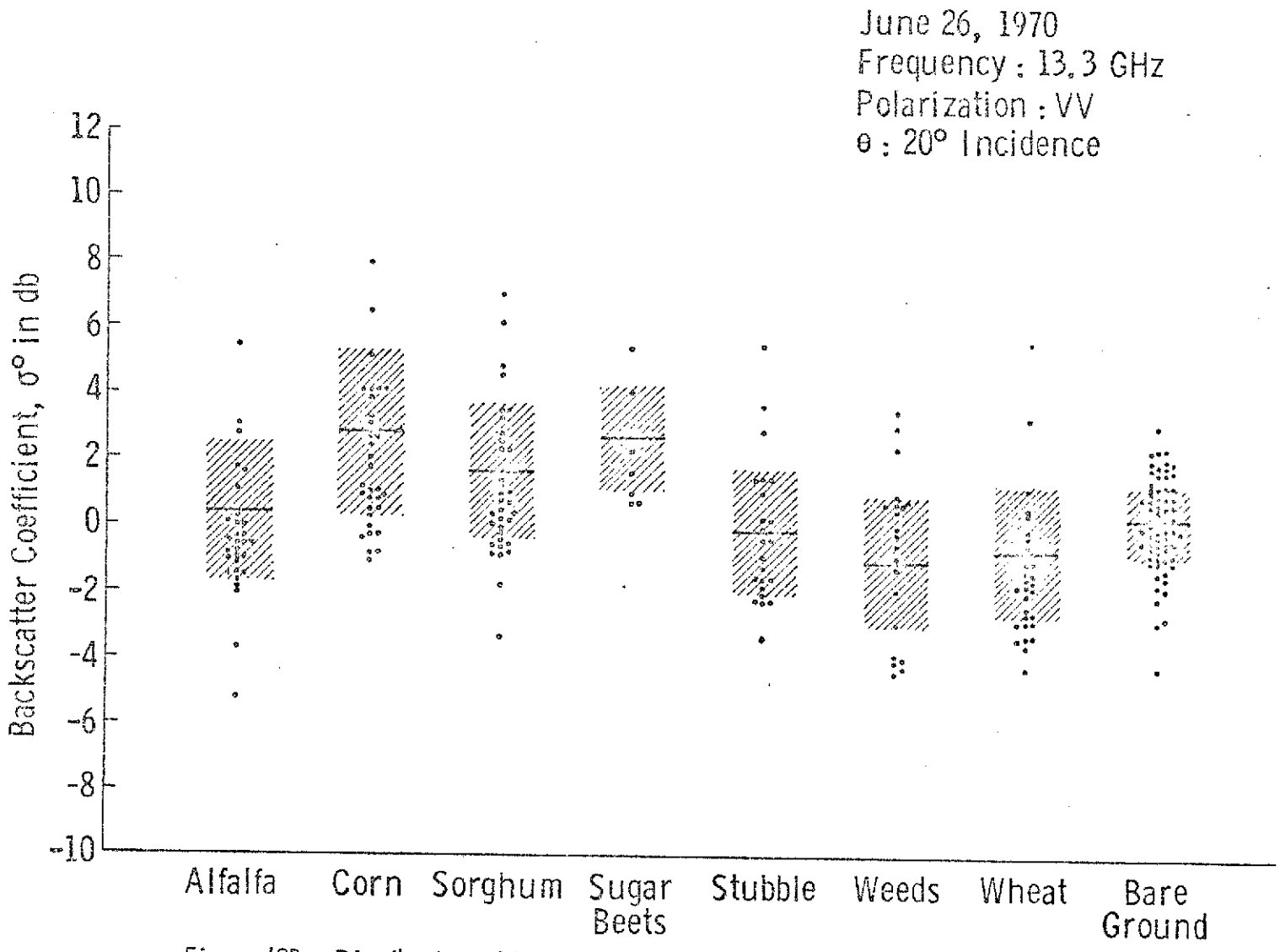

Figure 18B. Distribution of Mean Scattering Coefficients of Agricultural Fields.

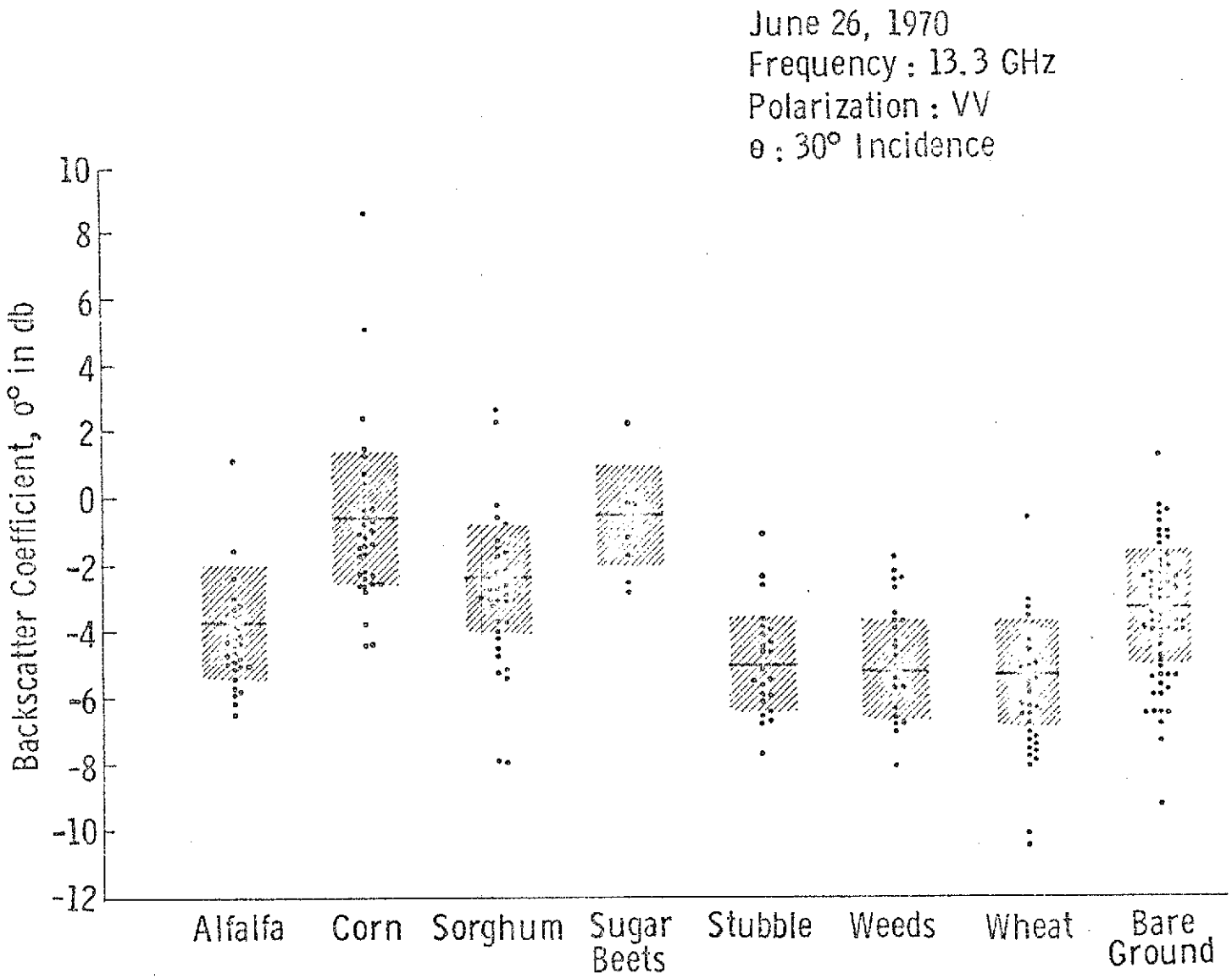

Figure 18C. Distribution of Mean Scattering Coefficients of Agricultural Fields.

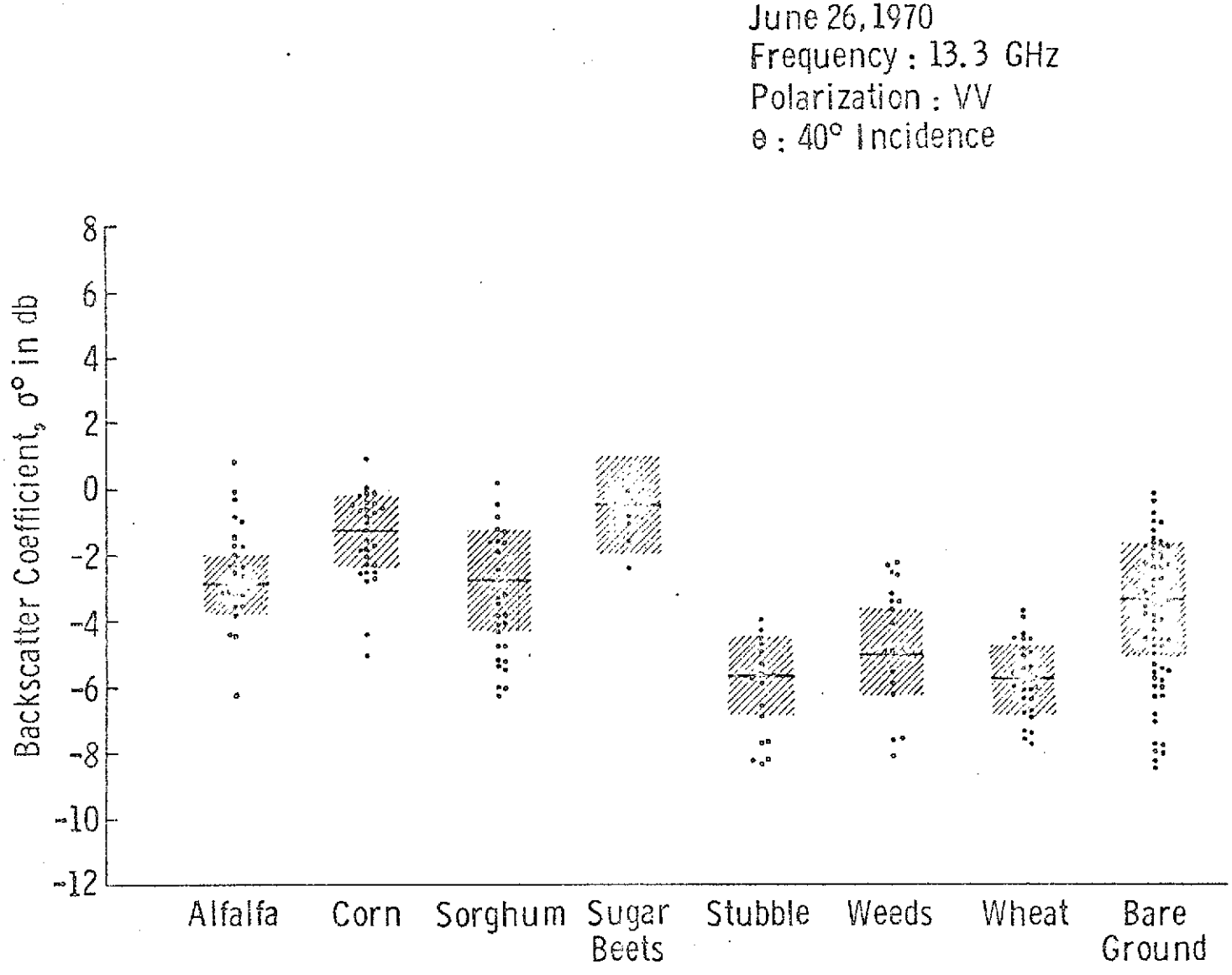

Figure 18D. Distribution of Mean Scattering Coefficients of Agricultural Fields.

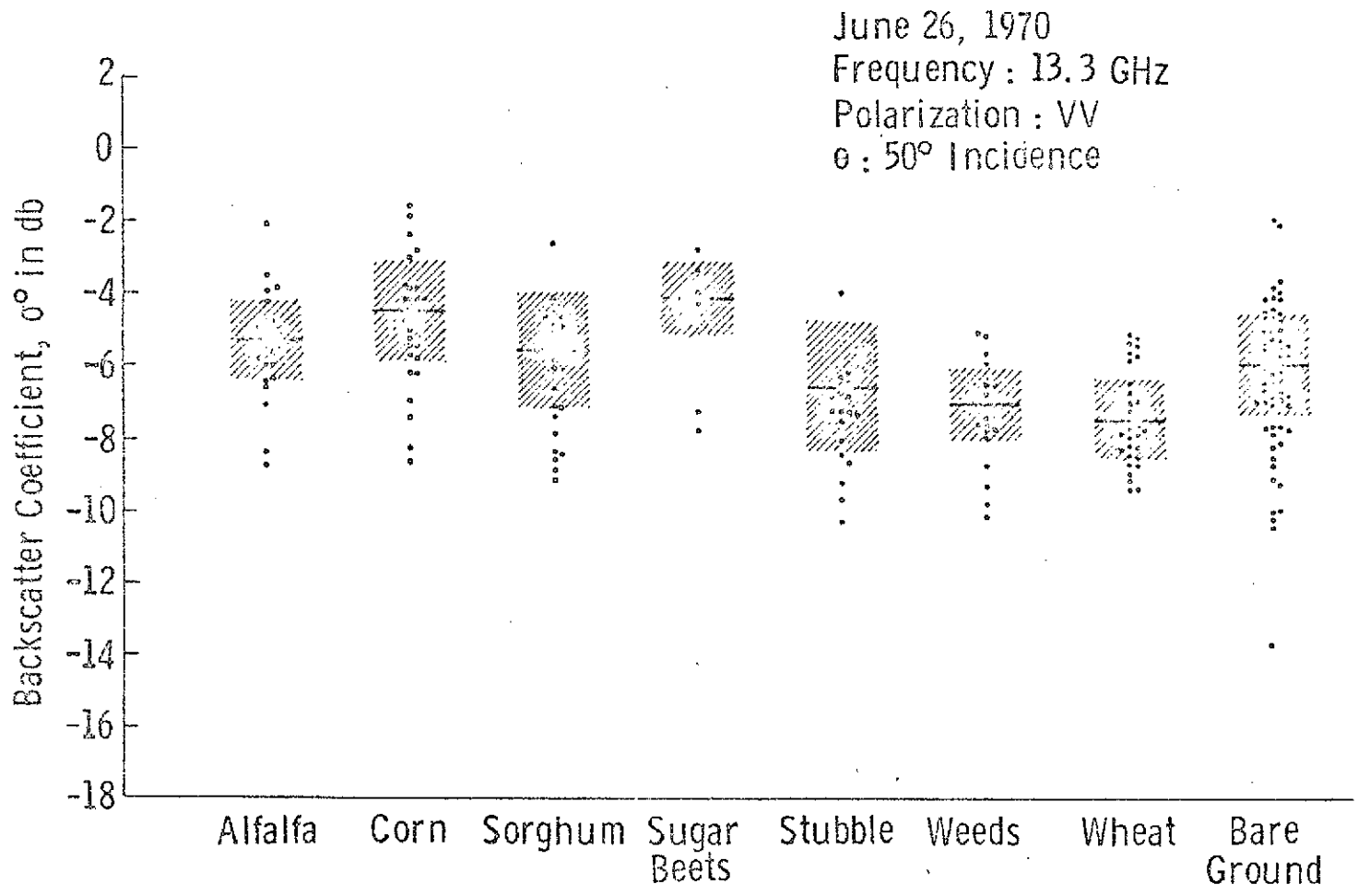

Figure 18E. Distribution of Mean Scattering Coefficients of Agricultural Fields.

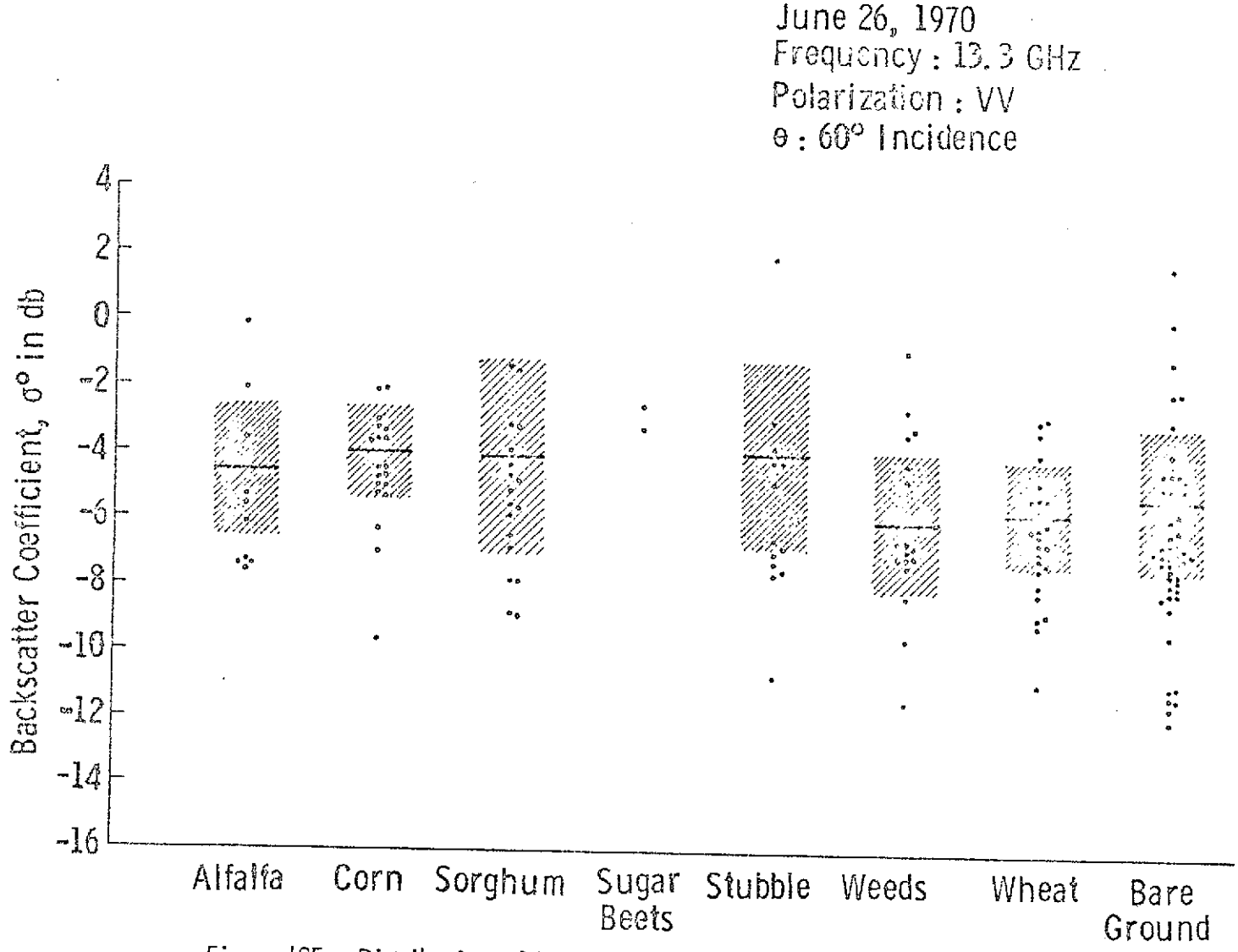

Figure 18F. Distribution of Mean Scattering Coefficients of Agricultural Fields.

From the histograms especially at 30° and 40° incidence, it seemed that a hint of clustering can be made among the crop considered. The usually irrigated crops of corn, sorghum and sugar beets exhibited higher returns than the much drier wheat stubbles, weeds, and grain wheat which were mostly ripe and dry at the time the data were collected. The categories of alfalfa and bare ground fell somewhere in between.

It was also observed that while the averages of all the categories of crops fell within a total spread of only 5 dB, the overlapping of the different categories was very significant, a same conclusion as drawn from the Ohio State farmland data. The entire range of the NASA/MSC agricultural terrain data was less than 15 dB.

400 MHz data were taken simultaneously in some of the sea ice and agricultural farmland experiments. It was reported [12] that at 400 MHz, first-year ice (1 to 3 feet thick) gave the strongest return and open water areas could also be differentiated. The result for farmland, however, is as yet inconclusive.

The observations for farmland discussed here were made in late June. Conclusions should not be generalized to other months. Images at 35 GHz in September, for example, show much greater crop contrast.

2.5 NASA Imaging Radar Measurements

The University of Kansas researchers also studied radar images taken by the Westinghouse APQ-97 imaging radar system over the Garden City test site [16]. Experiments were conducted in 1964 and 1965 in the later part of the growing season to determine the potential of radar as a remote sensor in agriculture.

The frequency of operation of this real-aperture airborne imaging radar was 35 GHz and the portion of the imagery analyzed had an approximate range of incidence angle from 50° to 67°. For calibration, a large sheltered, walled pond in the test site was used. The film density value of the imaged pond, once adjusted to the antenna pattern, served as a basis for comparison with imagery made on subsequent flights.

Four flights were made: October and November of 1964, and August and September of 1965. In the statistical analysis of the data, the individually small October and November data were combined. Histograms of the type shown in Figure 19 were obtained. The mean photographic density for each crop is

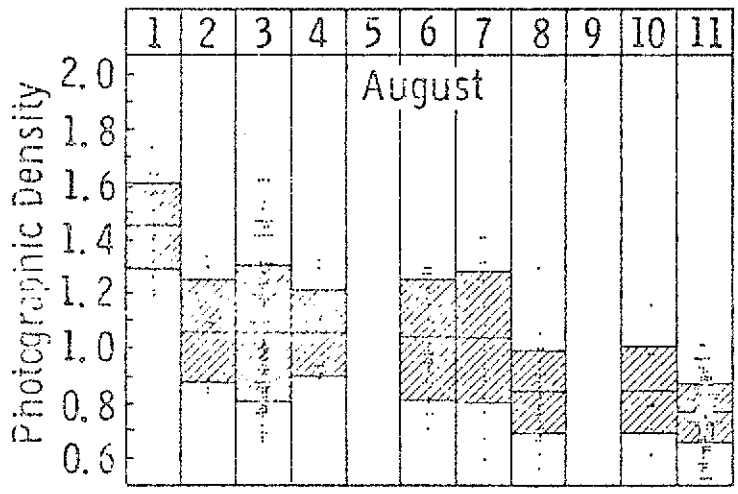

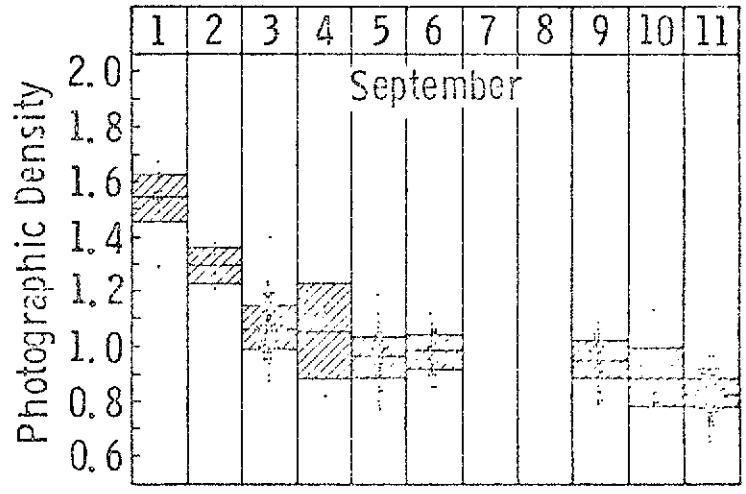

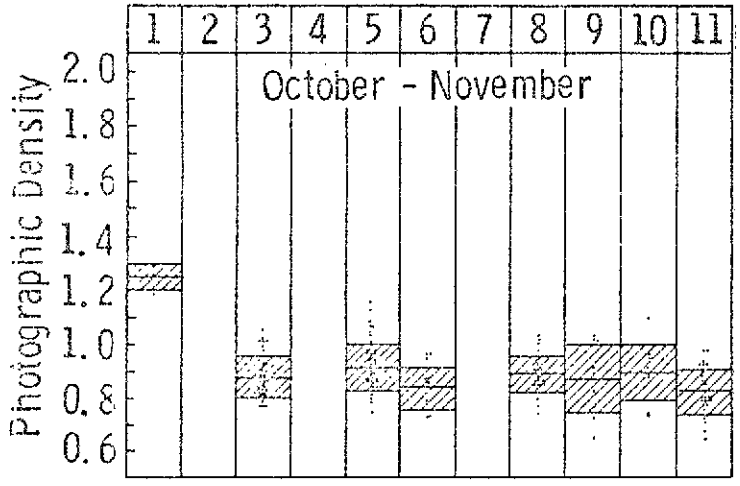

1 - Sugar Beets
2 - Corn
3 - Grain Sorghum
4 - Sudan
5 - Wheat
6 - Alfalfa
7 - Weeds
8 - Wheat Stubble
9 - Stubble and Weeds
10 - Pasture
11 - Bare

Figure 19. Mean Values and Values within One Standard Deviation by Crop for K_a-Band Imagery. Polarization H. (From Simonett, et al.)

shown by the center line and the shaded region represents the range of one standard deviation. The vertical axis is photographic density which, when multiplied by 10, gives the relative backscatter cross-section in dB. Since the imager is a non-calibrated sensor, the σ^{o} values thus obtained are not absolute.

In the set of histograms obtained late in the growing season, the backscatter shows a much greater crop contrast. Sugar beets had a consistantly higher return than all the other crops, and corn could also be easily identified due to its moderately high return in September. Bare ground exhibited low backscatter, and wheat, alfalfa, stubble, etc. were still indistinguishable from each other. The range of signals from different fields was about 10 dB.

2.6 Other Measurement Programs

The programs discussed so far were conducted in the frequency bands of X band up through Ka band. A host of other measurement programs were available in the open literature and a brief description of each is provided in the following paragraphs.

In the early 1950's Sandia Corporation of Albuquerque, New Mexico conducted a series of near vertical radar return experiments over different terrain surfaces ranging from desert, farmland, and forest to lakes, snow cover and cities [17-19]. These data were analyzed extensively at the University of New Mexico.

The Sandia data, although extensive in the variety of targets examined, were limited severely by the range of incidence angles employed which only extended from vertical incidence to 30^{o} (see Figure 20). The frequencies employed were 400 and 3800 MHz.

Another leading institution involved in terrain backscatter experiments is the U. S. Army Engineer Waterways Experiment Station in Vicksburg, Mississippi. An experiment was conducted in 1966 to determine the effect of moisture content on the dielectric properties of laboratory-prepared soil samples [20]. A cart containing the soil samples was placed at the axis of a large wooden arch along which multi-frequency radar could gather the radar response of the soil under test for different viewing angles.

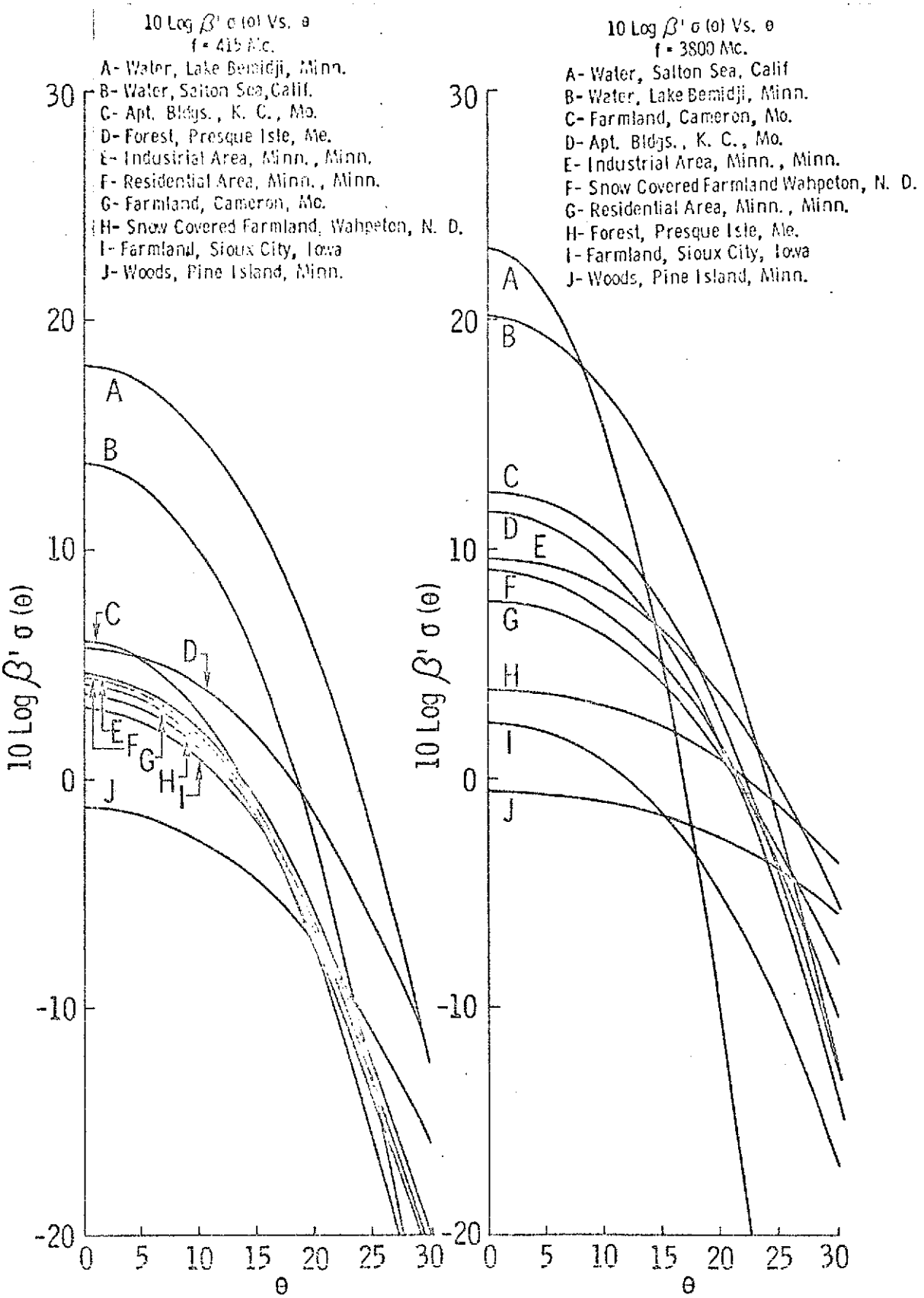

Figure 20. Relative plots of σ° vs. θ for various terrain types. (After Janza, et al.[16])

A swept-frequency technique was developed and tested by Lundien in 1971 at Waterways Experiment Station to measure the reflectivity and optical thickness of layered materials [21] thus providing a means of estimating the physical thickness and dielectric constant of layers such as highways. The mobile experiment set-up was housed in a boom truck system similar to the one at Ohio State.

Besides aircraft and mobile boom trucks, another favorite radar platform for researchers investigating the scattering properties of terrains is television towers and water towers. The Swedish Research Institute of National Defense is studying the backscattering properties of the ground with the aid of a tower mounted X band search radar [22, 23]. Their investigation is coordinated with an aircraft program [24] and the main emphasis in both programs is to determine the level and amplitude distribution of backscattered signals at low grazing angles.

Another European institution interested in radar terrain backscatter phenomena is the Physics Laboratory of National Defence in the Netherlands [25]. An X band measuring radar and a Ka band survey radar were mounted on a television tower in the homogeneous agricultural area of Goes. Since each agricultural field in this area is usually planted with only one type of crop, the study of radar backscatter from a single vegetation type through a complete growing season is possible (see Figure 21). In addition to seasonal changes, the effects of local rainfall and varying wind speeds were also investigated (Figure 22). Unfortunately the incidence angles for these data are all very near grazing.

The Aerospace Corporation performed some experimental measurements in the 40-90 GHz range for terrain samples in a wet and dry condition [26]. The samples included asphalt, concrete, gravel, wood, sod, tall weeds, and smooth and rough water. The antennas were mounted on a tower and the samples were placed at the foot of the tower. In Figure 23, the backscatter coefficients of the samples were plotted against incidence angles with the assumption that the backscatter was frequency independent.

The Remote Sensing Laboratory at The University of Kansas is involved in studying the effects of frequency variations on radar terrain backscatter [27, 28]. The MAPS (Microwave Active and Passive Spectrometer) system is truck mounted and spans the entire C band (4-8 GHz); it has recently been expanded to the 2-18 GHz range. The range of angles is wide (0° - 70°) and all four polarizations are possible. Based on C band measurement data from four crop types, all of

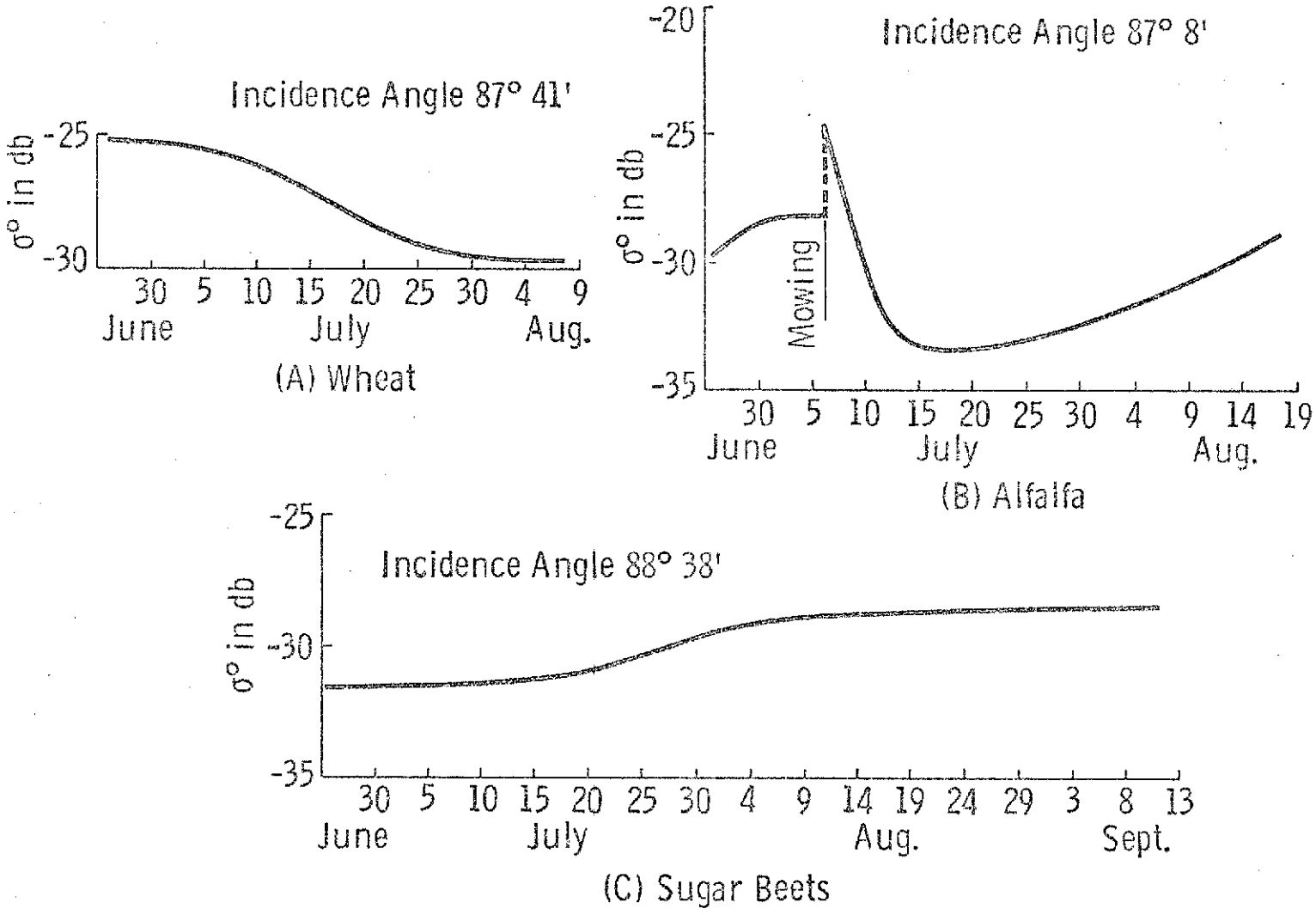

Figure 21. Variation of the Backscatter Mean Through the Season. Polarization HH. Frequency X-Band (after deLoor.)

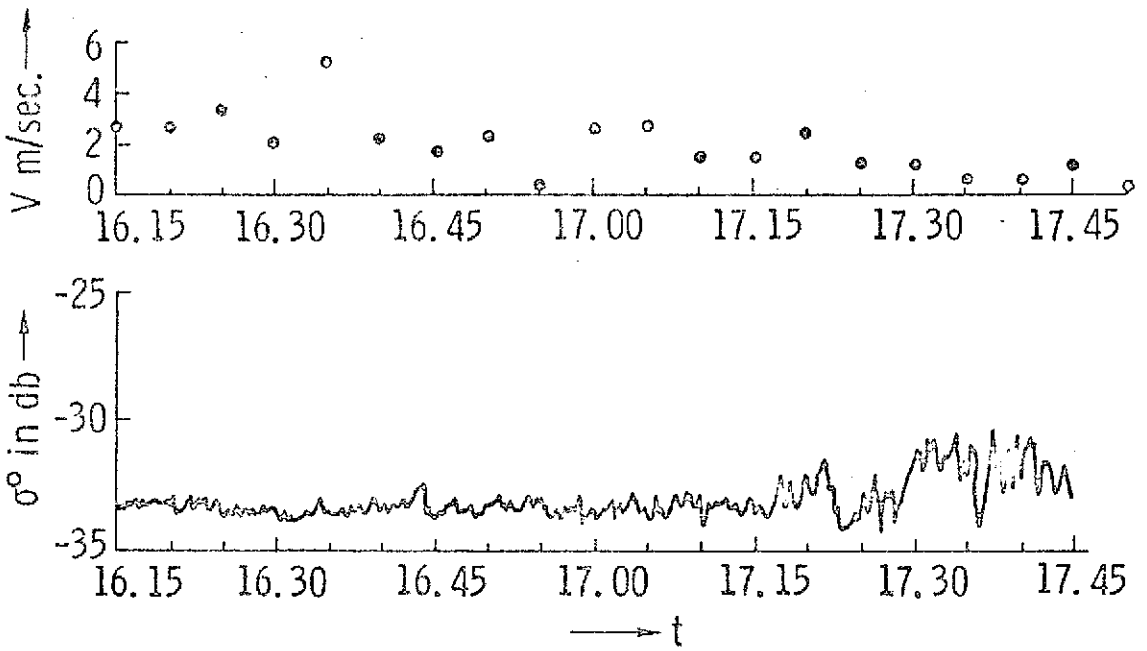

Long Term Fluctuation of the Mean at Low Wind Speeds (20 Sec. Averages). Polarization HH.

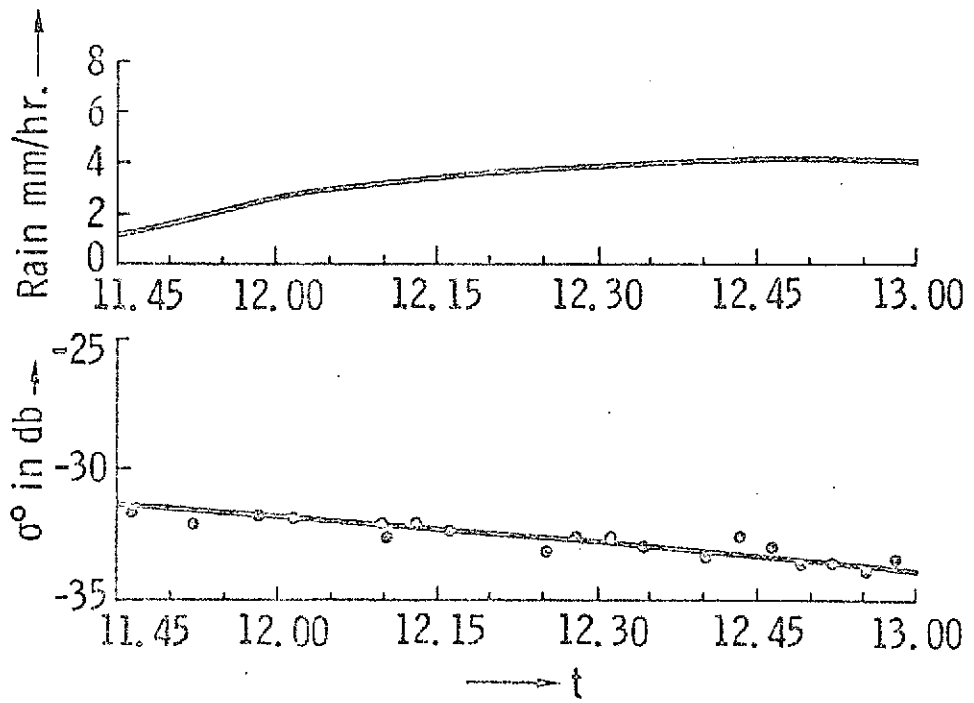

Dependency of the Mean on Rainfall. Polarization VV.

Figure 22. Effects of Weather on Backscatter. (After deLoor.)

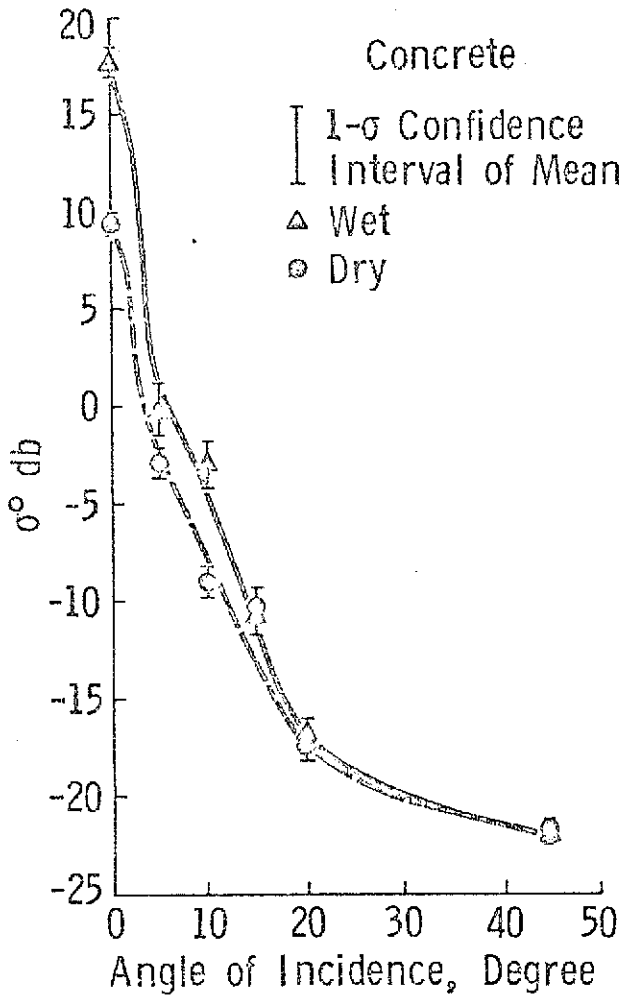

Figure 23A. Mean for wet and dry concrete. (After King, et al.)

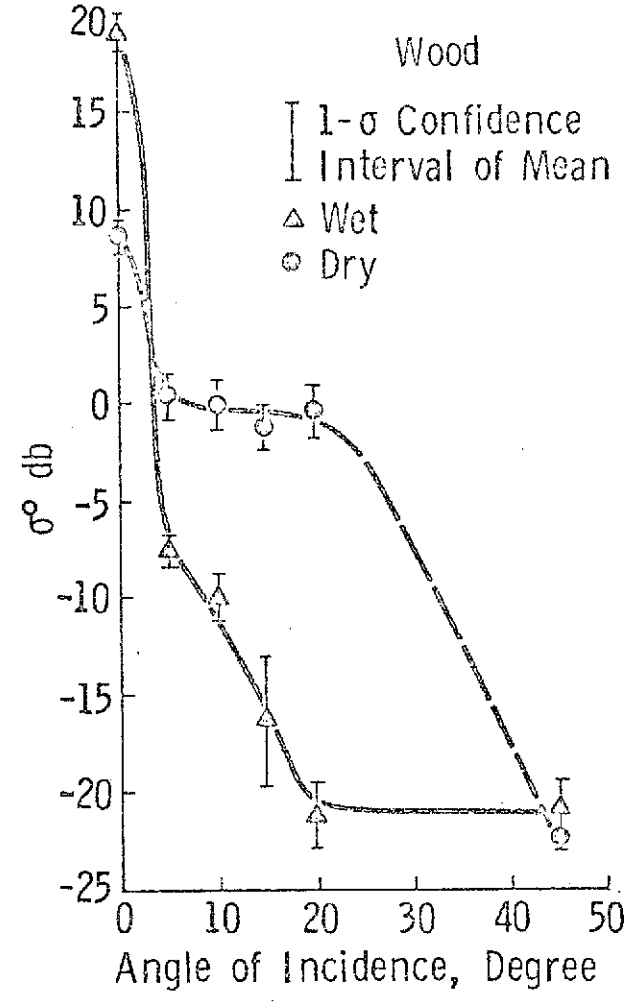

Figure 23B. Mean for wet and dry wood. (After King, et al.)

which were mature, it was found that the lower end of C band indicated the highest sensitivity to soil moisture at low incidence angles. On the other hand, proper crop identification can be best achieved by large angles of incidence at high frequencies.

The Jet Propulsion Laboratory of California Institute of Technology conducted aircraft and rocket flights in 1966 [29] over the Tularosa Basin area in New Mexico in an effort to simulate the return from the moon. Communications Research Center in Ottawa designed and tested a high resolution X band FM radar in a feasibility study of measuring the depth of snow and the thickness of fresh water ice [30].

Table 1 summarizes the radar terrain measurement programs mentioned above. The summary is tabulated by terrain categories, included in the tabulation are the principal investigators and their affiliation, the frequency of the sensor, the range of incidence angles investigated, and the type of platform used by the sensor.

TABLE 1

TERRAIN CATALOG FROM OPEN LITERATURE

Categcry	1st Author	Year	Affiliation	Platform	Frequency Bands	Sensor Viewing Angles (Incidence)
SEA ICE	Parashar	1973	KU	Aircraft	P, Ku	5° - 60°
	Rouse	1969	KU	Aircraft	Ku	5° - 60°
FARMLAND	Ulaby	1973	KU	Truck	C	0° - 70°
	King	1972	KU	Aircraft	P, Ku	5° - 60°
	de Loor	1972	Netherlands	Tower	X, Ka	80° - 89°
	Oliver	1969	Ohio State	Truck	L, X, Ku, Ka	10° - 80°
	Cullen	1969	KU	Aircraft	Ku	5° - 60°
	Eklund	1969	Sweden	Aircraft, Tower	X	60° , 85°, 89°
	Peake	1968	Ohio State	Truck	X	10° - 80°
	Simonett	1967	KU	Aircraft	Ka	45°
	Ericson	1966	Sweden	Aircraft	X	60° , 85°, 89°
	Linell	1966	Sweden	Tower	X	
	Cosgriff	1960	Ohio State	Truck	X, Ku, Ka	10° - 80°
	Reitz	1959	Goodyear	Aircraft	X	30° - 80°
	Edison	1959	Sandia Corp/UNM	Aircraft	P, S	0° - 30°
	Janza	1959	Sandia Corp/UNM	Aircraft	P, S	0° - 30°
FOREST	King	1970	Aerospace Corp.	Tower	mm	0° - 45°
	Eklund	1969	Sweden	Aircraft	X	60° , 85°, 89°
	Ericson	1966	Sweden	Aircraft	X	60° , 85°, 89°
	Newbry	1961	Goodyear	Aircraft	X	30° - 80°
	Edison	1959	Sandia Corp/UNM	Aircraft	P,S	0° - 30°
	Janza	1959	Sandia Corp/UNM	Aircraft	P, S	0° - 30°
	Reitz	1959	Goodyear	Aircraft	X	30° - 80°
	Ament	1958	NRL	Aircraft	P, L, S, X	10° - 90°
	Grant	1957	NRL	Bridge	X, K, Ka	0° - 80°
GRASSLAND	King	1970	Aerospace Corp.	Tower	mm	0° - 45°
	Reitz	1959	Goodyear	Aircraft	X	30° - 80°
	Grant	1957	NRL	Bridge	X, K, Ka	0° - 80°

TABLE 1

(Continued)

Category	1st Author	Year	Affiliation	Platform	Frequency Bands	Sensor Viewing Angle (Incidence)
SWAMPS	Ericson	1966	Sweden	Aircraft	X	60° , 85° , 89°
	Reitz	1959	Goodyear	Aircraft	X	30° - 80°
	Grant	1957	NRL	Bridge	X, K, Ka	0° - 80°
DESERT	Brown	1968	JPL-CIT	Rocket	L	(Rocket)
	Newbry	1961	Goodyear	Aircraft	X	30° - 80°
	Edison	1959	Sandia Corp/UNM	Aircraft	P, S	0° - 30°
	Janza	1959	Sandia Corp/UNM	Aircraft	P, S	0° - 30°
	Reitz	1959	Goodyear	Aircraft	X	30° - 89°
	Ament	1958	NRL	Aircraft	P, L, S, X	10° - 90°
VOLCANIC	Shultz	1969	Ohio State	Truck	L, X, Ku, Ka	10° - 80°
	Lundien	1967	KU	Aircraft	Ku	5° - 60°
	Masenthin	1967	KU	Aircraft	Ku	5° - 60°
RESIDENTIAL COMMERCIAL	Barnum	1971	Stanford	Moving Probe	K	65° - 85°
	Ericson	1966	Sweden	Aircraft	X	60° , 85° , 89°
	Newbry	1961	Goodyear	Aircraft	X	30° - 80°
	Edison	1959	Sandia Corp/UNM	Aircraft	P, S	0° - 30°
	Janza	1959	Sandia Corp/UNM	Aircraft	P, S	0° - 30°
	Ament	1958	NRL	Aircraft	P, L, S, X	10° - 70°
SNOW COVER	Venier	1972	CRC, Canada	Window & Bridge	K	Vertical
	Cosgriff	1960	Ohio State	Truck	X, Ku, Ka	10° - 80°
	Edison	1959	Sandia Corp/UNM	Aircraft	P, S	0° - 30°
	Janza	1959	Sandia Corp/UNM	Aircraft	P, S	0° - 30°
HIGHWAY PAVEMENT	Lundien	1971	Waterways Exp. Sta.	Truck	Sweep Frequency 0.2-7 GHz	Vertical
	King	1970	Aerospace	Tower	mm	0° - 45°
	Cosgriff	1960	Ohio State	Truck	X, Ku, Ka	10° - 80°

3.0 COMPARISON OF BACKSCATTER CROSS SECTIONS

In the previous section, the radar cross sections of various terrains were presented as they appear in the open literature. For ease of comparison, data that were presented in the projected cross section γ, were converted into the normalized cross section, σ^o, and all the antenna viewing angles were described in terms of incidence angle. In this section, the different terrain targets are grouped into nine different categories in the manner specified previously. The classification consisted of grasslands, farmland, forest and woods, desert, snow covered terrain, urban areas, swamps and marsh, road surfaces, and volcanic area.

To facilitate the comparison of the radar cross section from different terrains, a method of presentation similar to histograms is employed. The vertical axis represents the backscatter cross section, σ^o, in dB; and the various terrain categories are marked on the horizontal axis. The angle of incidence is the running parameter in these histograms. If the original data was given in the form of a curve (e.g. NRL aircraft data [1]) representing a whole class of terrain, the value registered on the histogram would be a straight line; if the data had a range of values (e.g. Goodyear data), the same range represented by shaded area would be given on the histogram.

The Skylab radiometer-scatterometer is capable of operating at five different antenna pitch angles, 0^o, 15.6^o, 29.4^o, 40.1^o, and 48.0^o. These angles, however, are not the true incidence angles with which the incident rays make with the mean ground surface. Due to the curvature of the earth, the effective incidence angles with respect to the mean ground surface are 0^o, 16.695^o, 31.629^o, 43.480^o and 52.550^o [31]. These were the angles used for extracting the backscatter cross section in plotting the various histograms.

3.1 Original Backscatter Cross-Sections

The radar terrain backscatter cross-sections were plotted in Figures 24A-E using the absolute values as they appeared in the literature. In each histogram the values are given together with the specifications as to the source of the data and the polarization states under which the data were obtained. Since only one

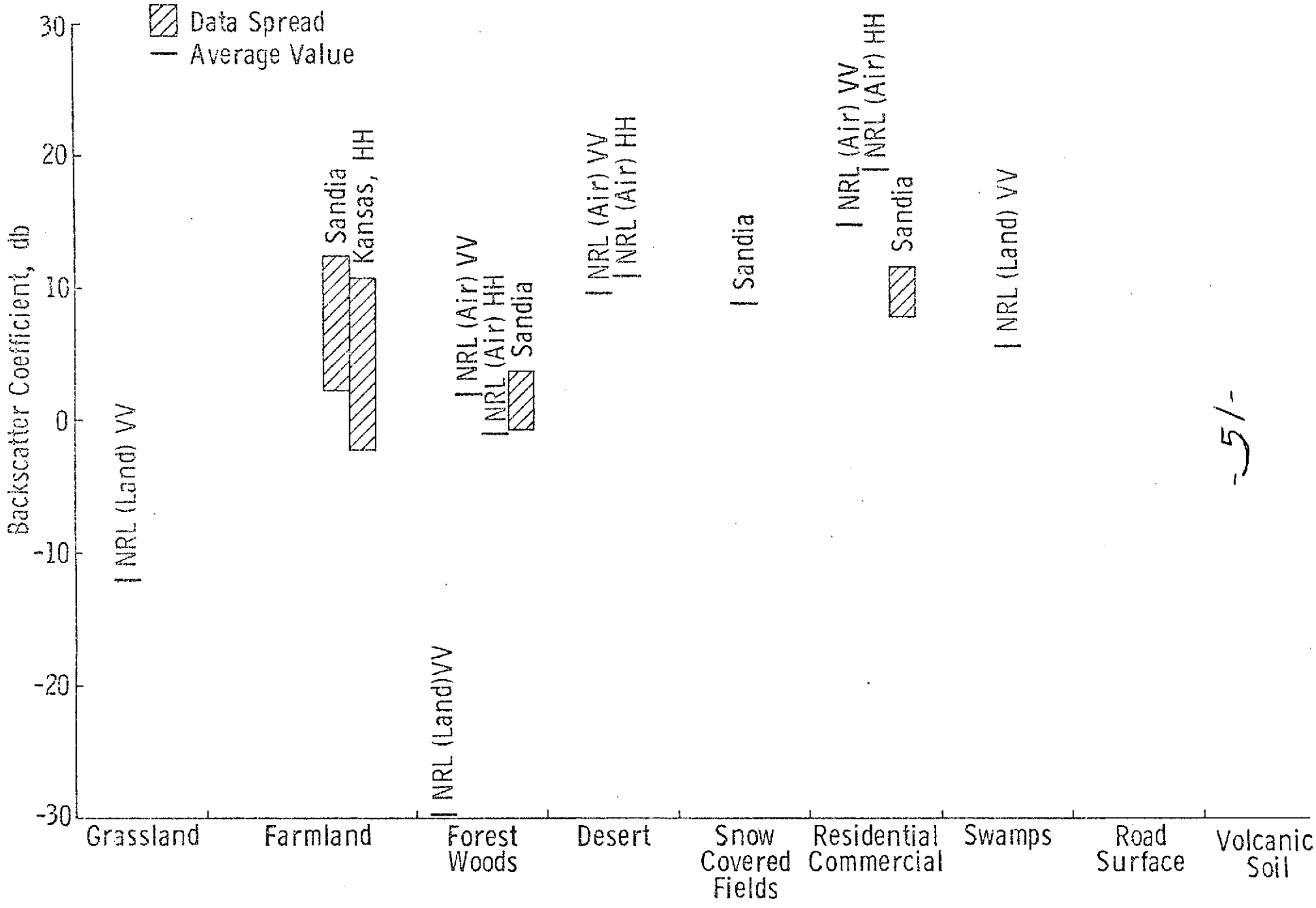

Figure 24A. 0° Incidence, Original Data.

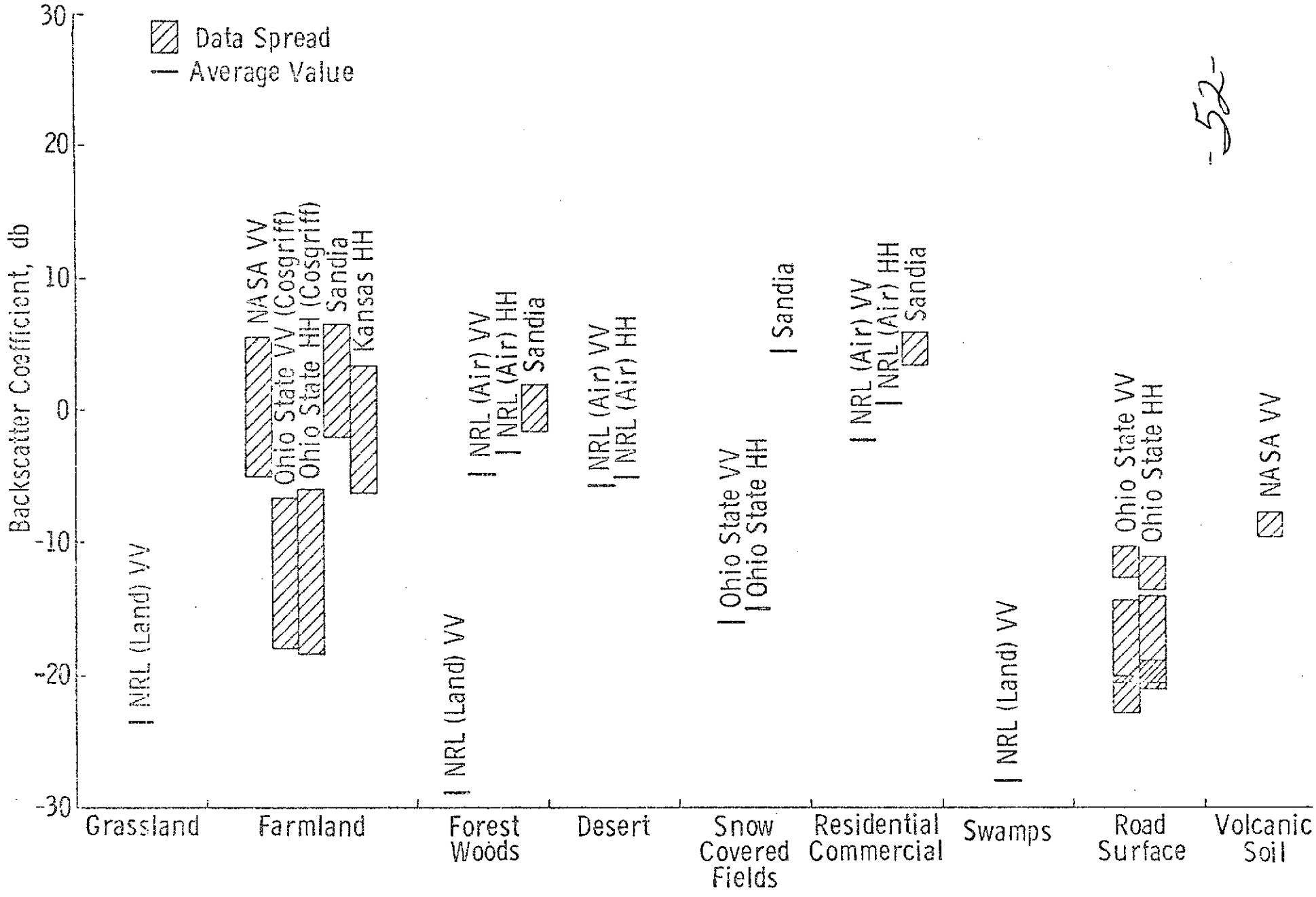

Figure 24B. 16° Incidence, Original Data.

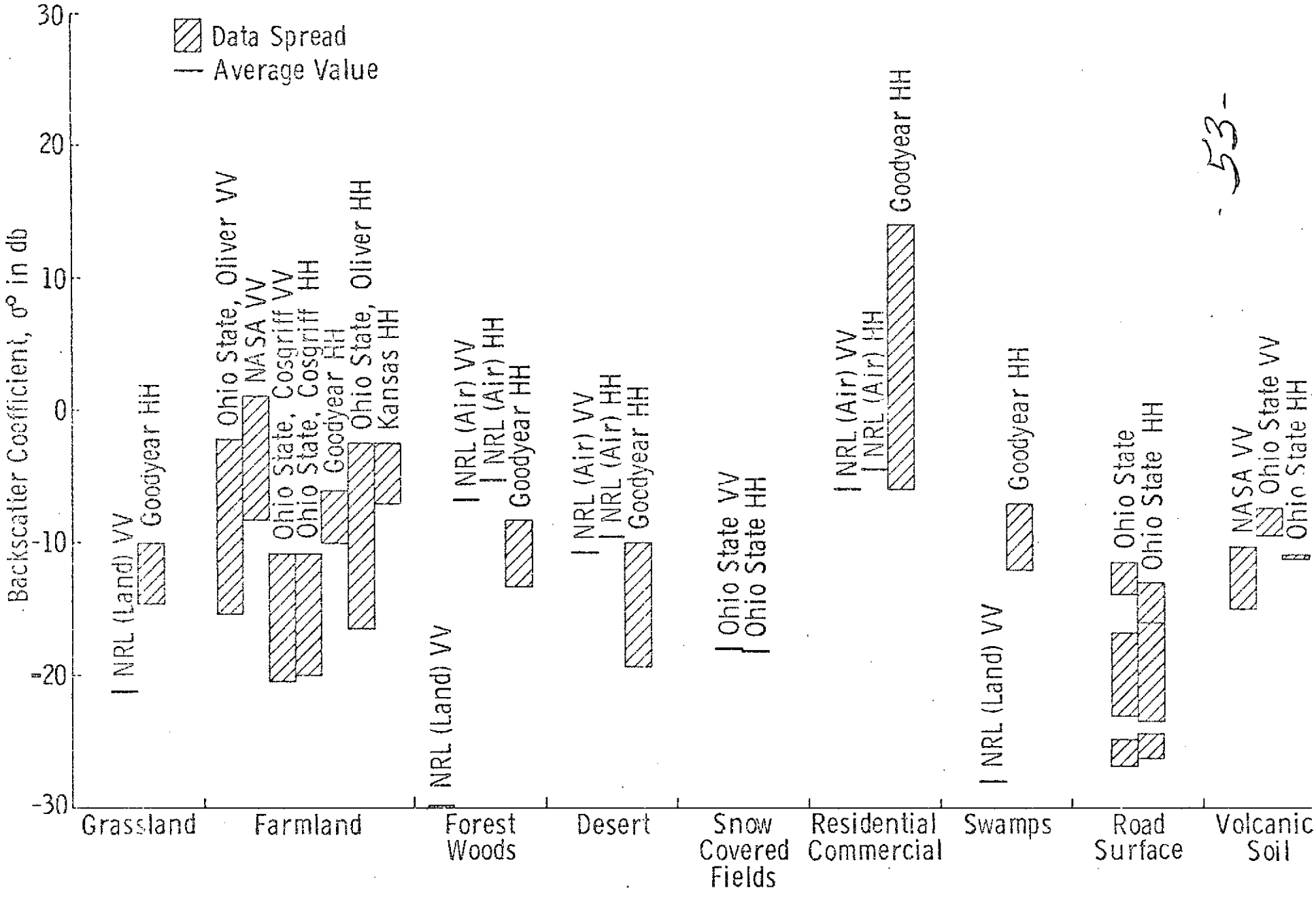

Figure 24C. 31° Incidence, Original Data.

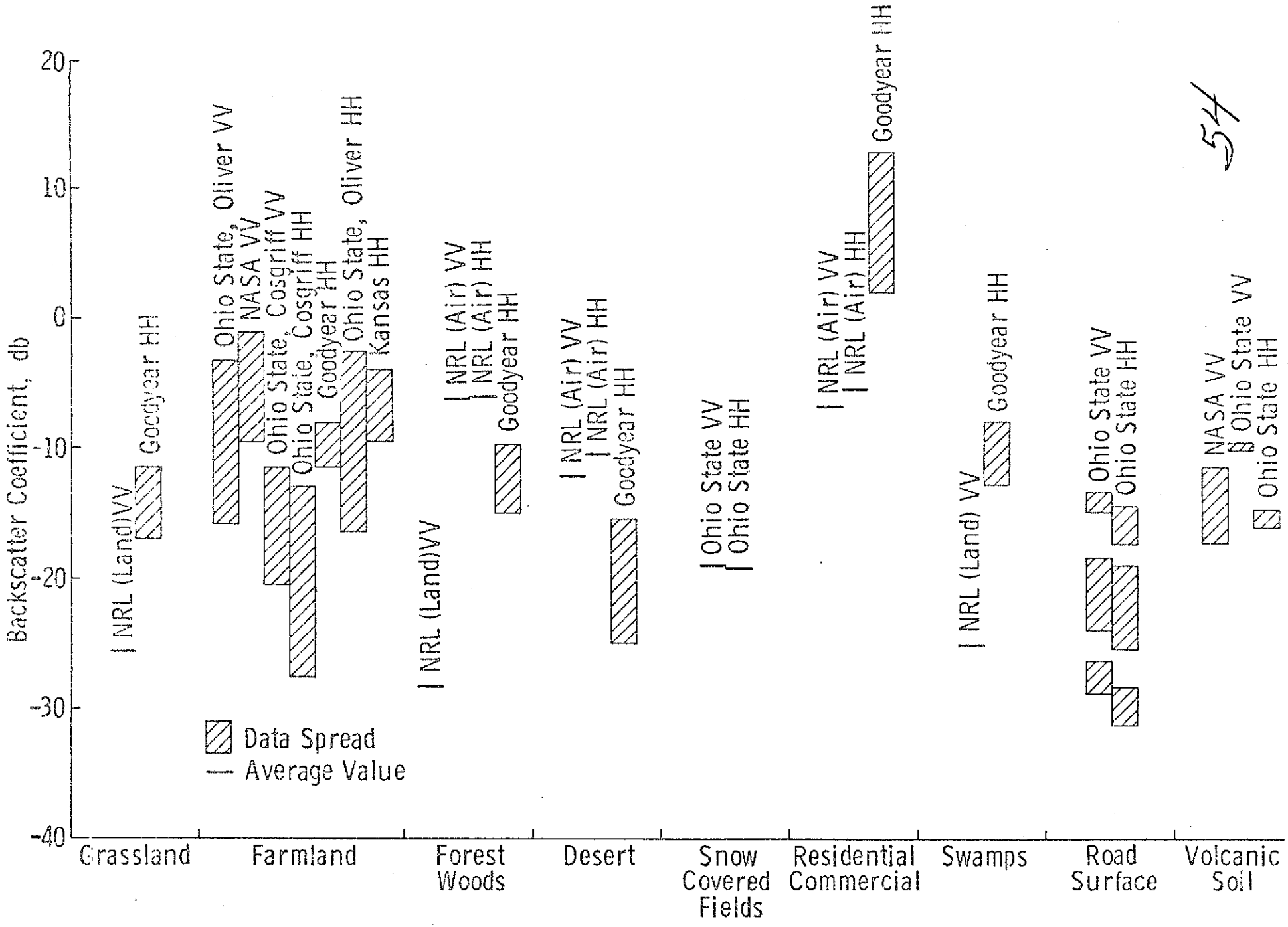

Figure 24D. 43° Incidence, Original Data.

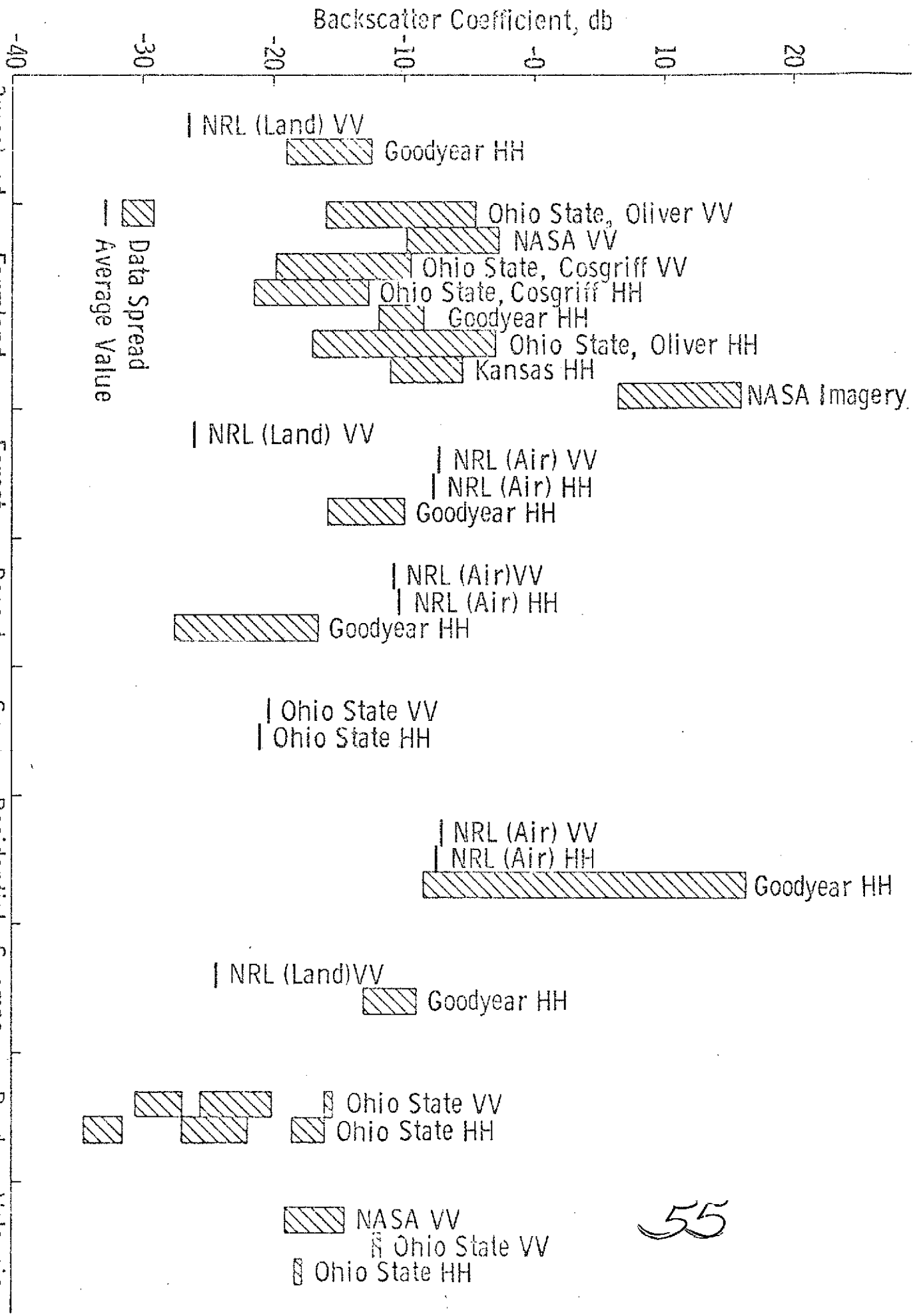

Figure 24E. 52° incidence, Original Data.

investigator (Ament, et al) obtained data in the cross-polarized mode, the cross polarization data were not included in the histograms. The data used in plotting these histograms were quoted from Ohio State, NRL, NASA and Goodyear, all of which obtained their data within or close to Ku band, the frequency band of the S-193. Sandia Corporation and The University of Kansas near-vertical-incidence data were also utilized for the reason that their experiments were conducted in a carefully controlled manner although the frequencies of operation were quite different from that of the S-193.

As evident in the histograms, the majority of the information was contained in angles of incidence greater than 30°. The amount of farmland data, exceeded by far those from the other terrain categories. Snow cover data from Ohio State was only for snow covered grass and hence should not be considered as representative of snow covered farmland. Snow backscatter obtained by Sandia Corporation, however, was for snow covered farmland in North Dakota. The three bands shown under road surfaces were gravel and cinder, asphalt, and concrete, in that order.

In general, the results quoted from different sources show good correlation for some categories; but in other categories, the discrepancies are large. For example, Cosgriff's Ohio State farmland data were completely separated from the NASA data although the terrains investigated were similar. The backscatter coefficients of wooded areas, as investigated by the bridge based and aircraft crews of NRL, showed a discrepancy as much as 20 dB at 43° incidence.

3.2 Normalizing The Data To One Incidence Angle

The large discrepancies discussed in the previous section prompted the idea of normalizing the backscatter cross-sections to one particular incidence angle. Taking the backscatter cross-section in Figures 24a-e and normalizing all the data to their individual values at 52° incidence, the histograms as shown in Figures 25a-d were obtained. Figure 25e is not included since it is at the normalizing angle. The additional information specified in Figure 25 is the normalizing factors for the different terrains as investigated by different research teams. Sandia data, however, are lost as their largest angle of incidence is only 30°, so normalization at 52° is not possible.

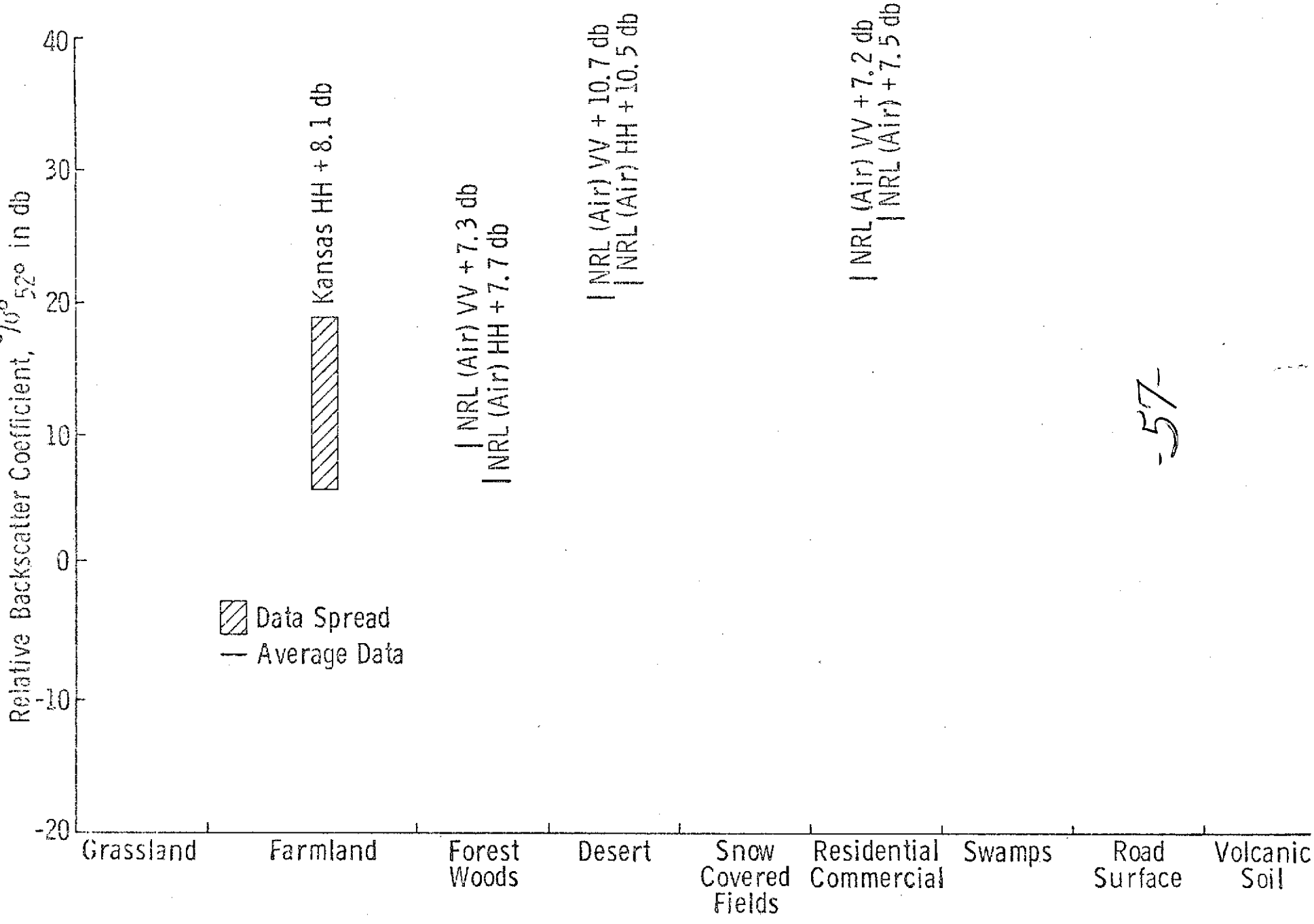

Figure 25A. 0° Incidence, Relative σ°

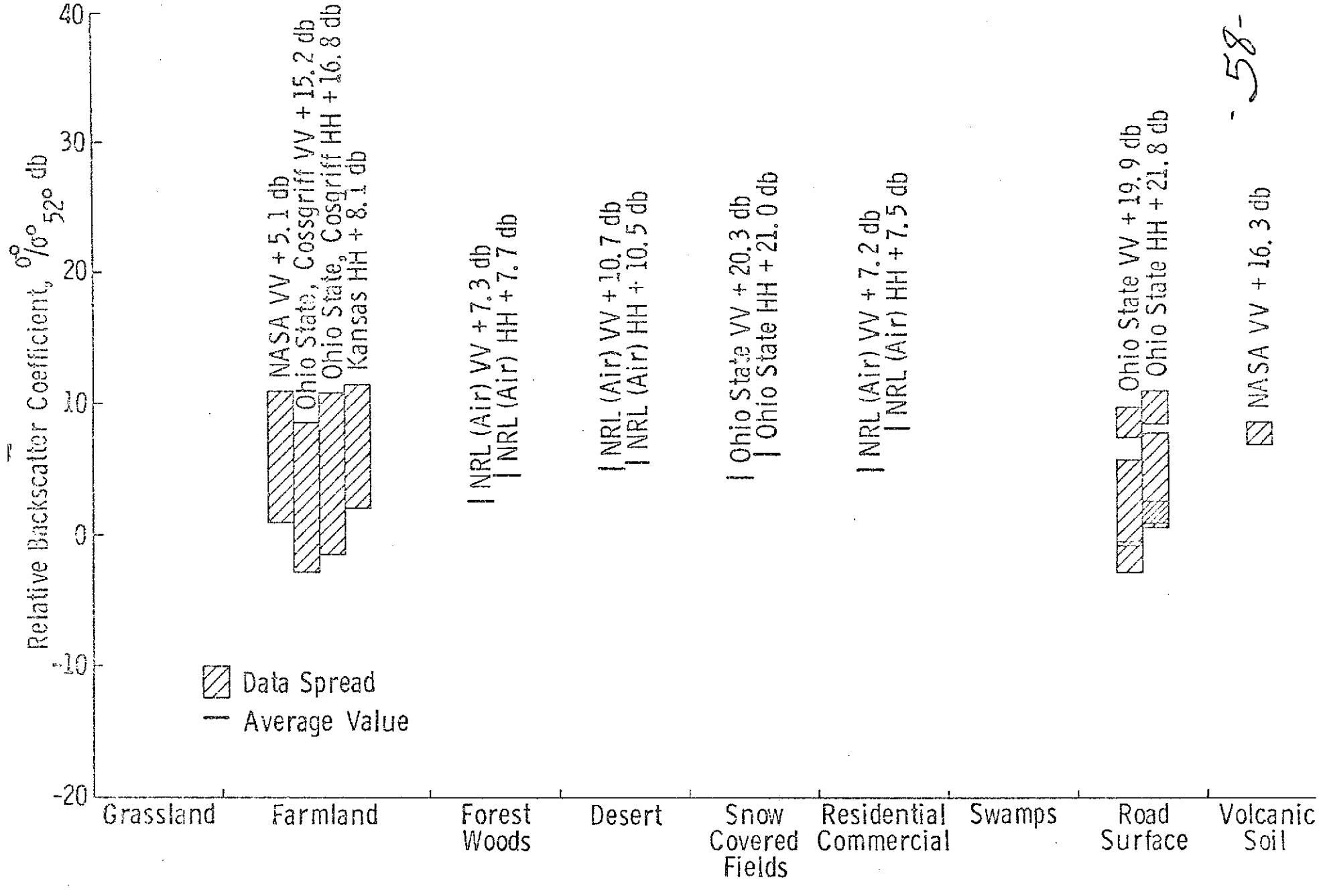

Figure 25B. 16° Incidence, Relative σ°

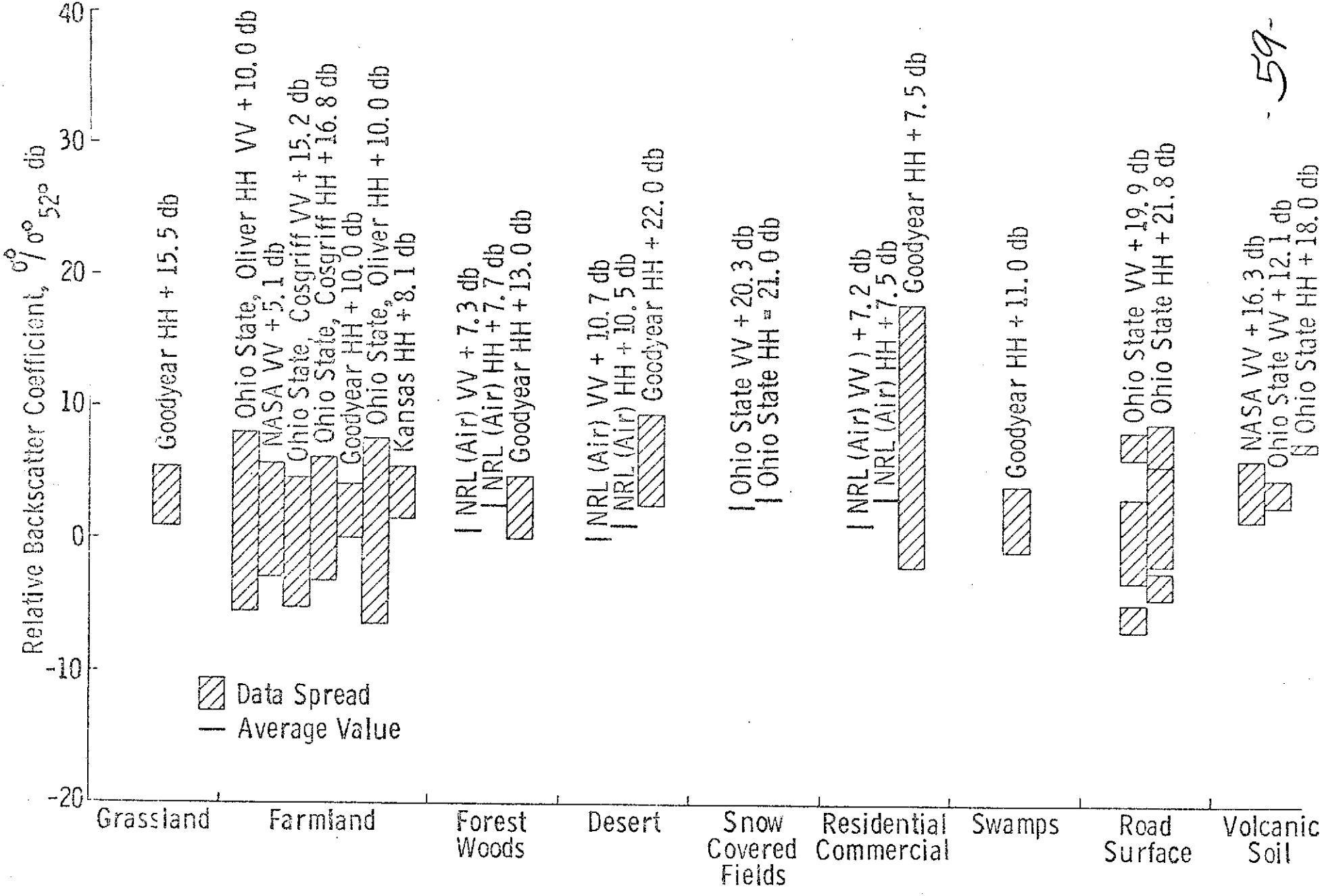

Figure 25C. 31° Incidence, Relative σ°

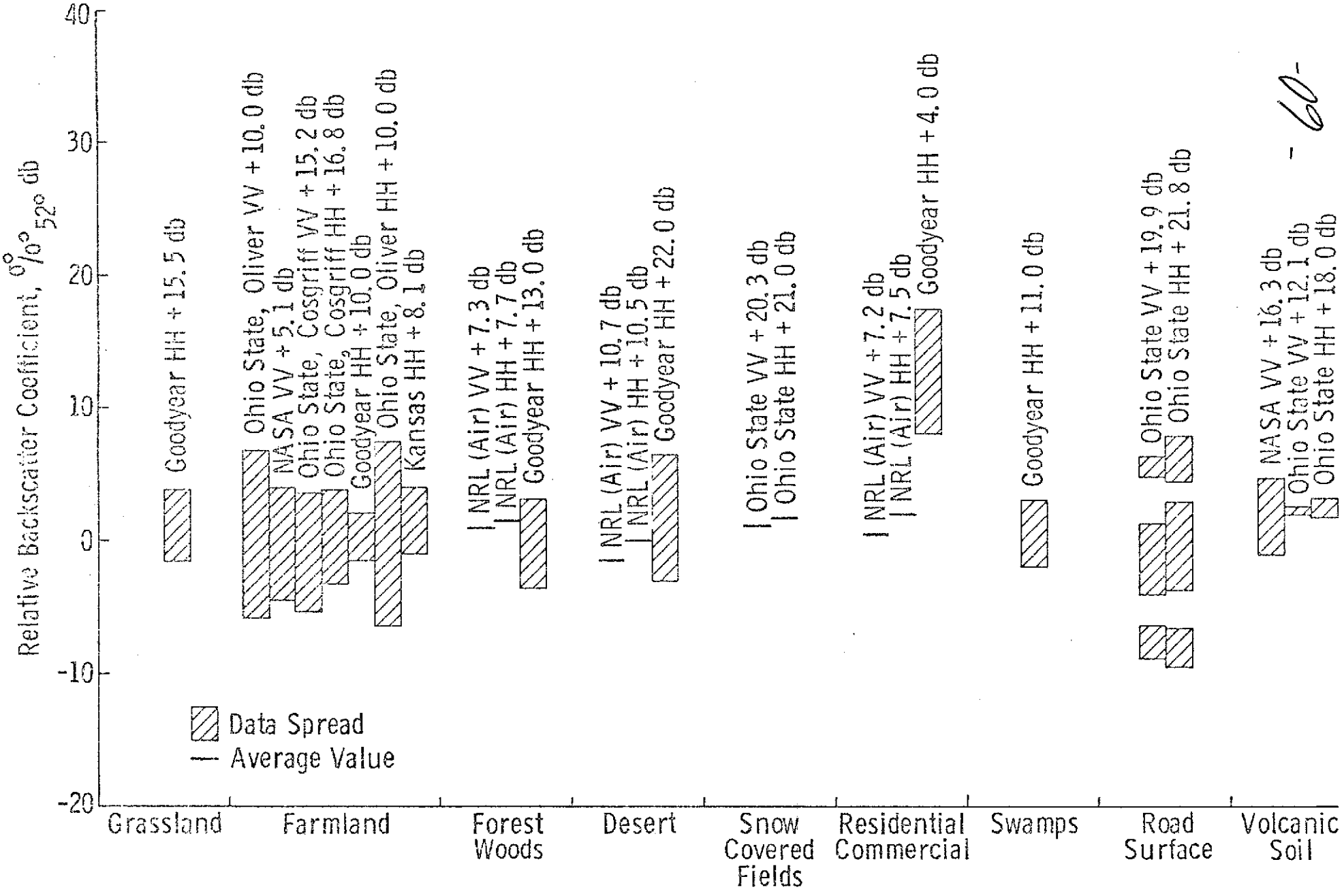

Figure 25D. 43° Incidence, Relative σ°

With the exception of the histogram at 0^{o} incidence, the only conclusion that can be drawn from this new set of presentations is that the variation among the land targets is greatly reduced.

At vertical indicence, only the Naval Research Laboratory had obtained data in the frequency range of interest. The values, however, should not be considered absolute but rather as an indication to the returns from different terrains relative to each other at this look angle. This is a necessary consequence of near vertical measurements with finite beamwidth or pulse length [32].

3.3 Normalizing The Data To One Terrain Category

Another approach in the data manipulation was to normalize all backscatter coefficient data to a common terrain category for which every research team had obtained results. Farmland was the obvious choice to make. Therefore, the horizontally polarized backscatter coefficient for farmland was normalized to 0 dB at 52^{o} incidence angle, and the other terrain backscatter coefficients were adjusted accordingly.

Figures 26A-E show the result of this transformation. It can be seen from these histograms that a definite hint of clustering begins to emerge. The relatively smooth target surfaces, such as concrete and desert, showed a low return at high angles of incidence. The return from the other terrain targets overlapped more or less with the return from the farmlands, but on the average volcanic areas gave higher returns at small angles of incidence and asphalt surface and grassland had less backscatter than the other vegetated targets at higher incidence angles.

The handicap in the interpretation of the histograms is that the data tend to concentrate in one or two categories. This is a direct consequence of the manner under which the experiments were conducted. As a result targets of interest such as croplands were investigated by every research team and other targets such as snow cover and swamps were hardly touched at all. To compare categories which had vastly different amount of coverage is difficult, to say the least. Further complications arise when results from more than one sensor system, which might have quite different sensitivity and dynamic ranges, are compared with one another.

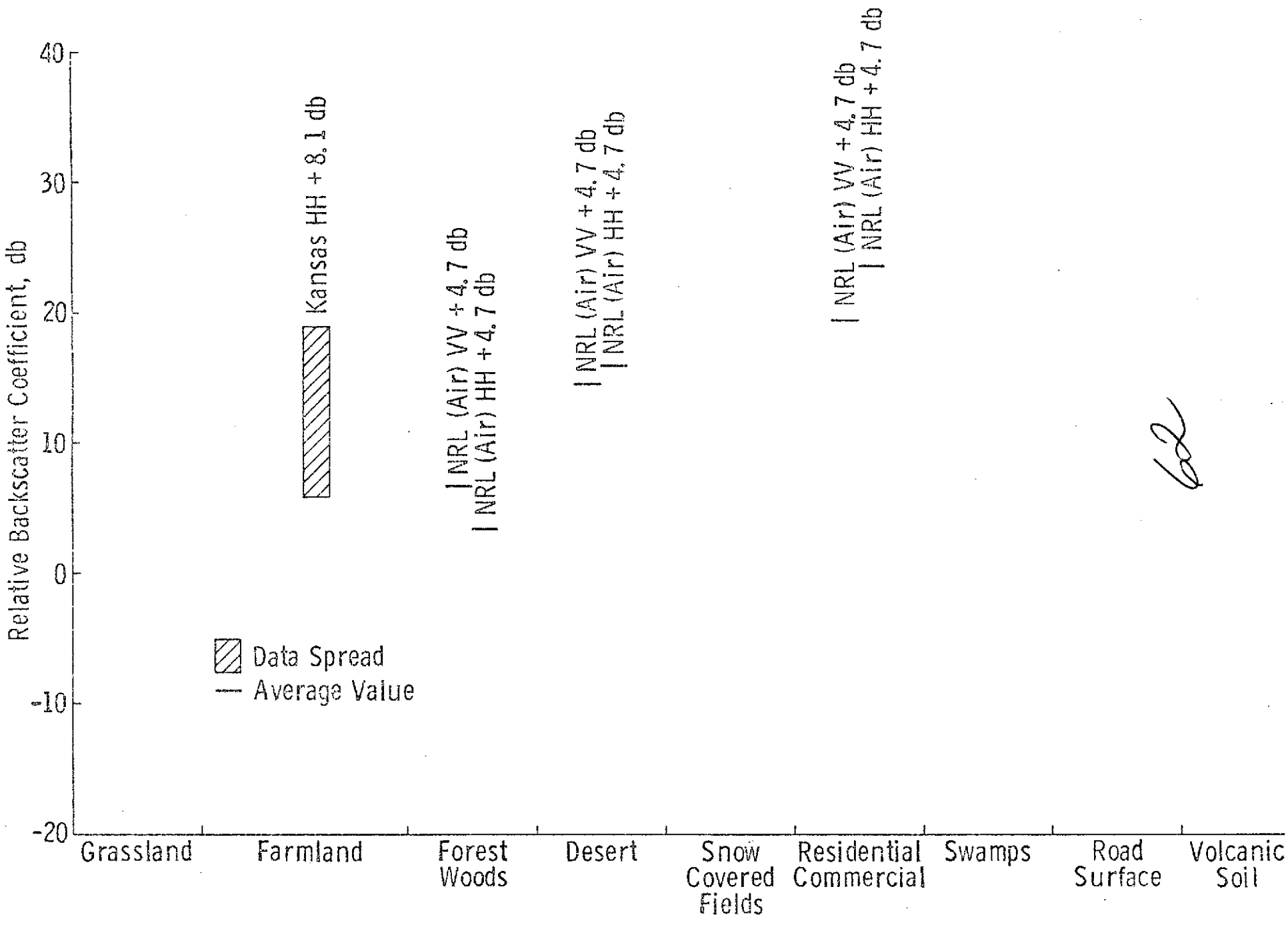

Figure 26A. 0° Incidence, Relative σ°, Normalized to Farmland Data at 52° HH Polarization.

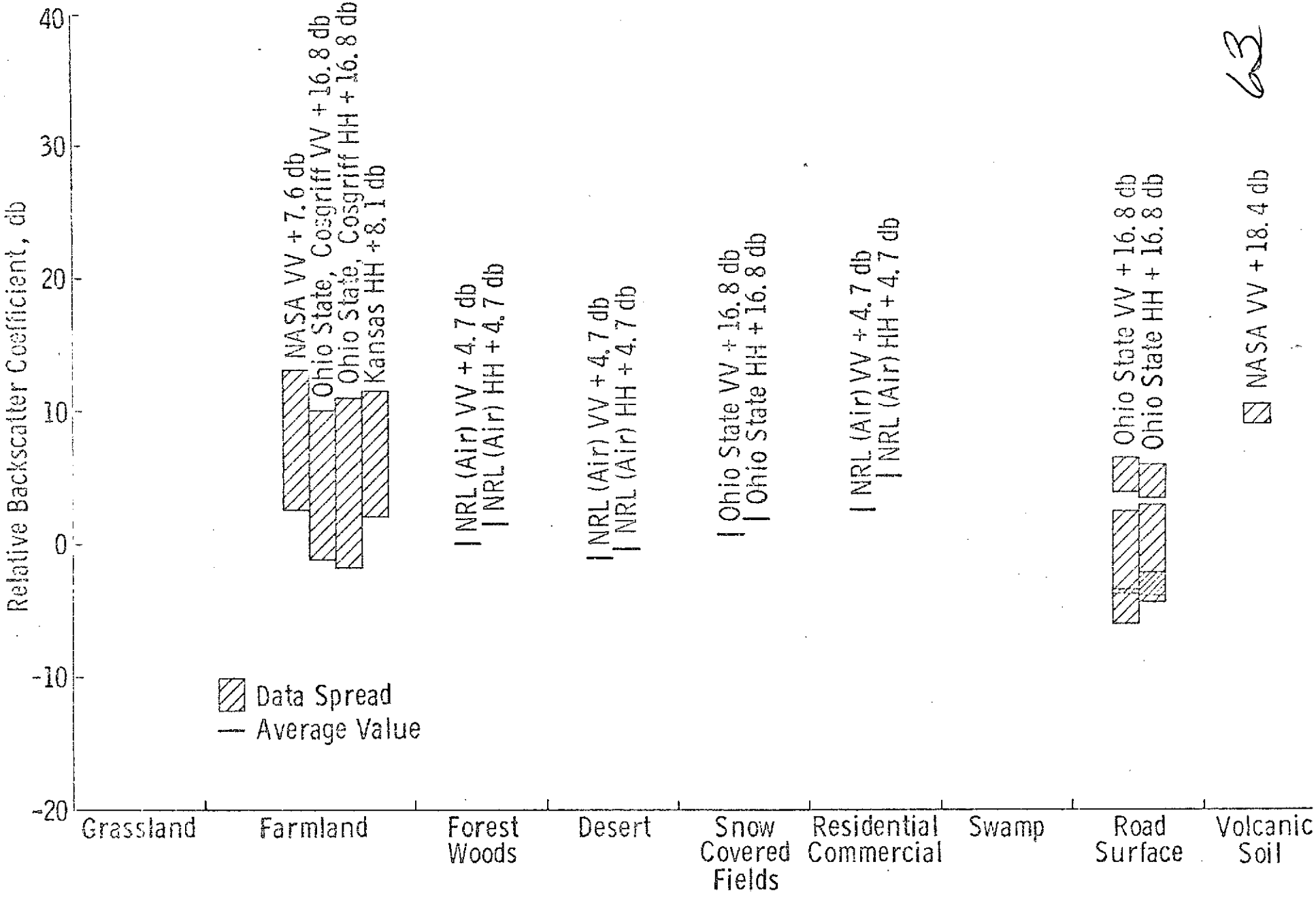

Figure 26B. 16° Incidence, Relative σ°, Normalized to Farmland Data at 52° HH Polarization.

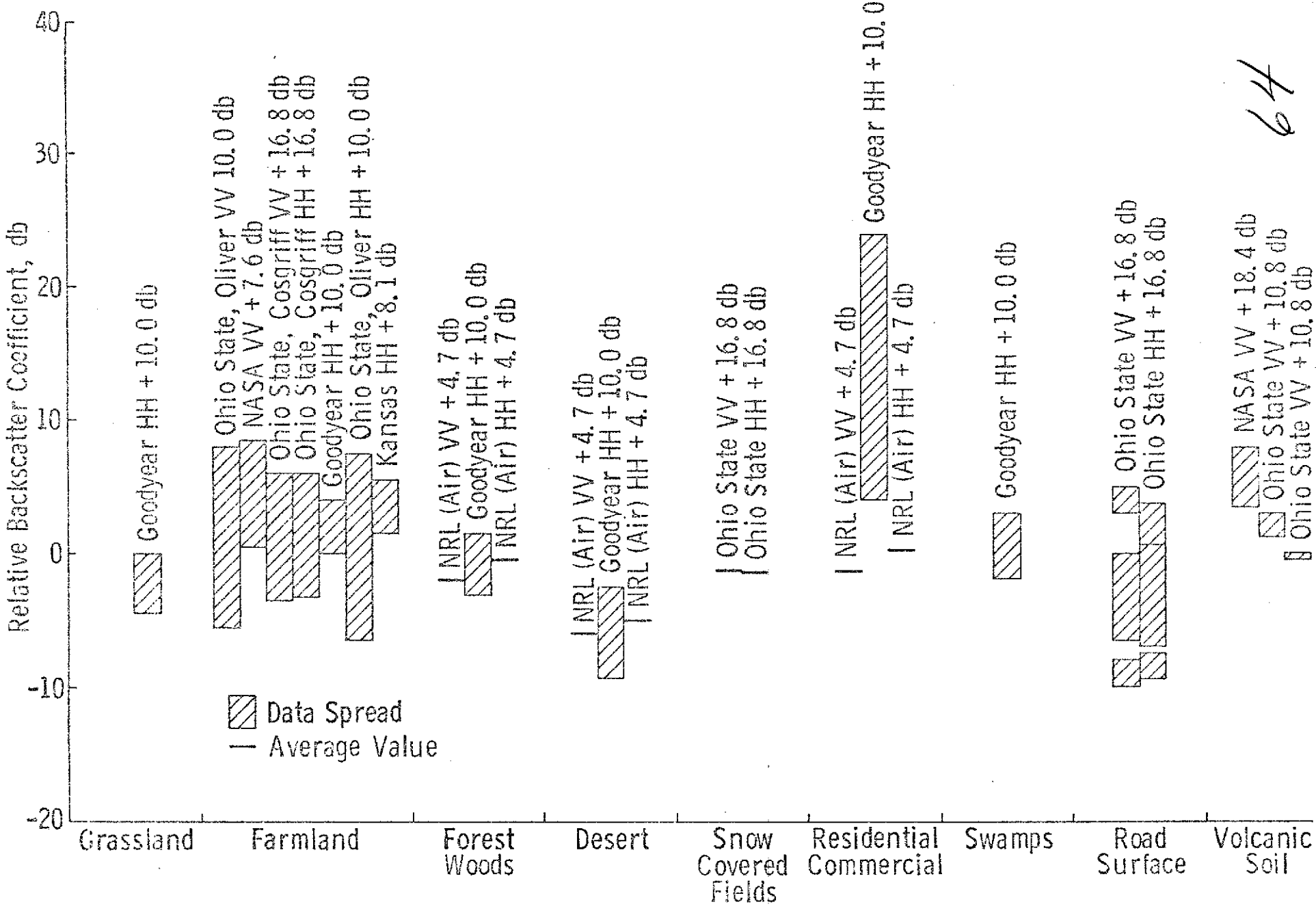

Figure 26C. 31° Incidence, Relative σ°, Normalized to Farmland Data at 52°, HH Polarization.

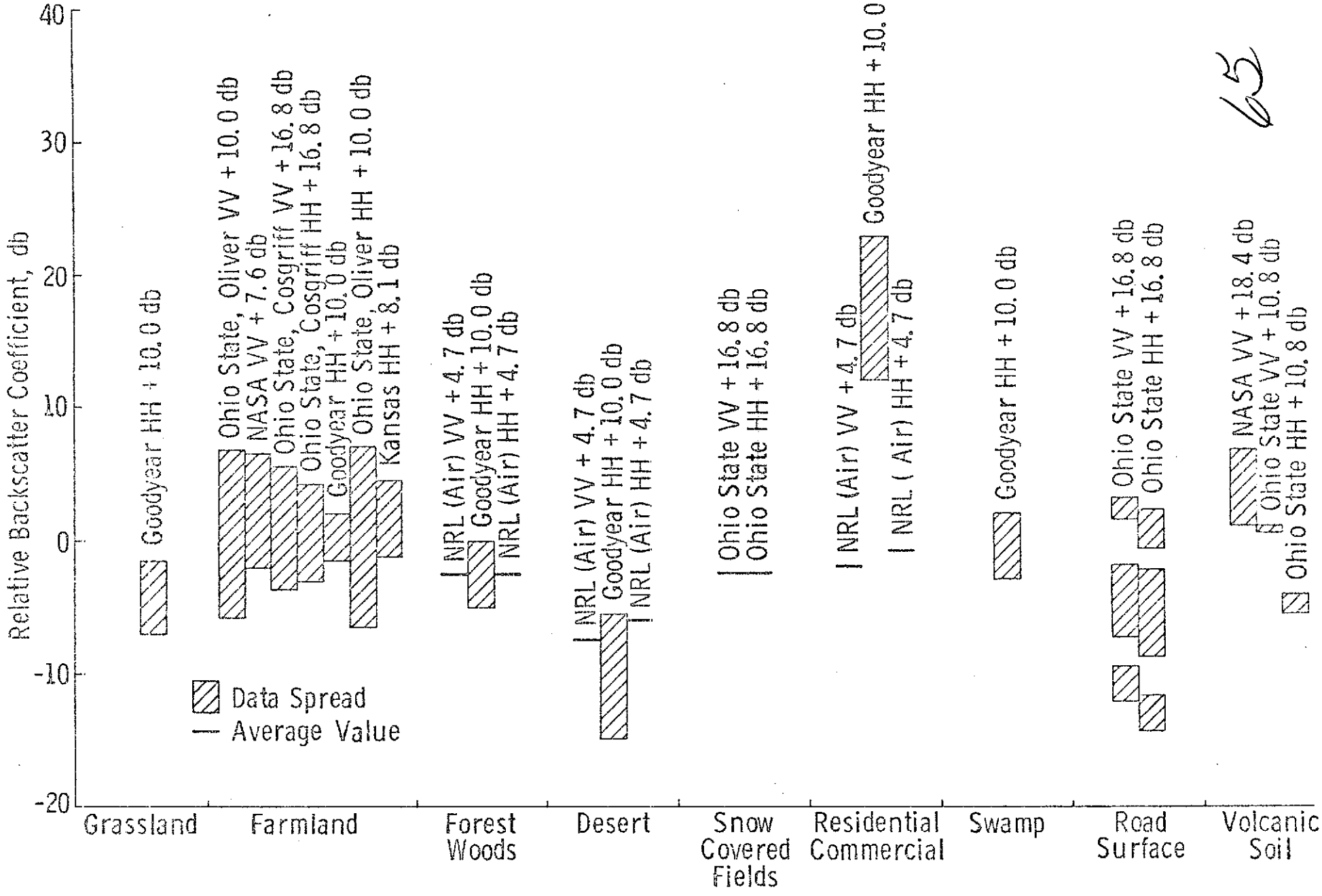

Figure 26D. 43° Incidence, Relative σ°, Normalized to Farmland Data at 52°, HH Polarization.

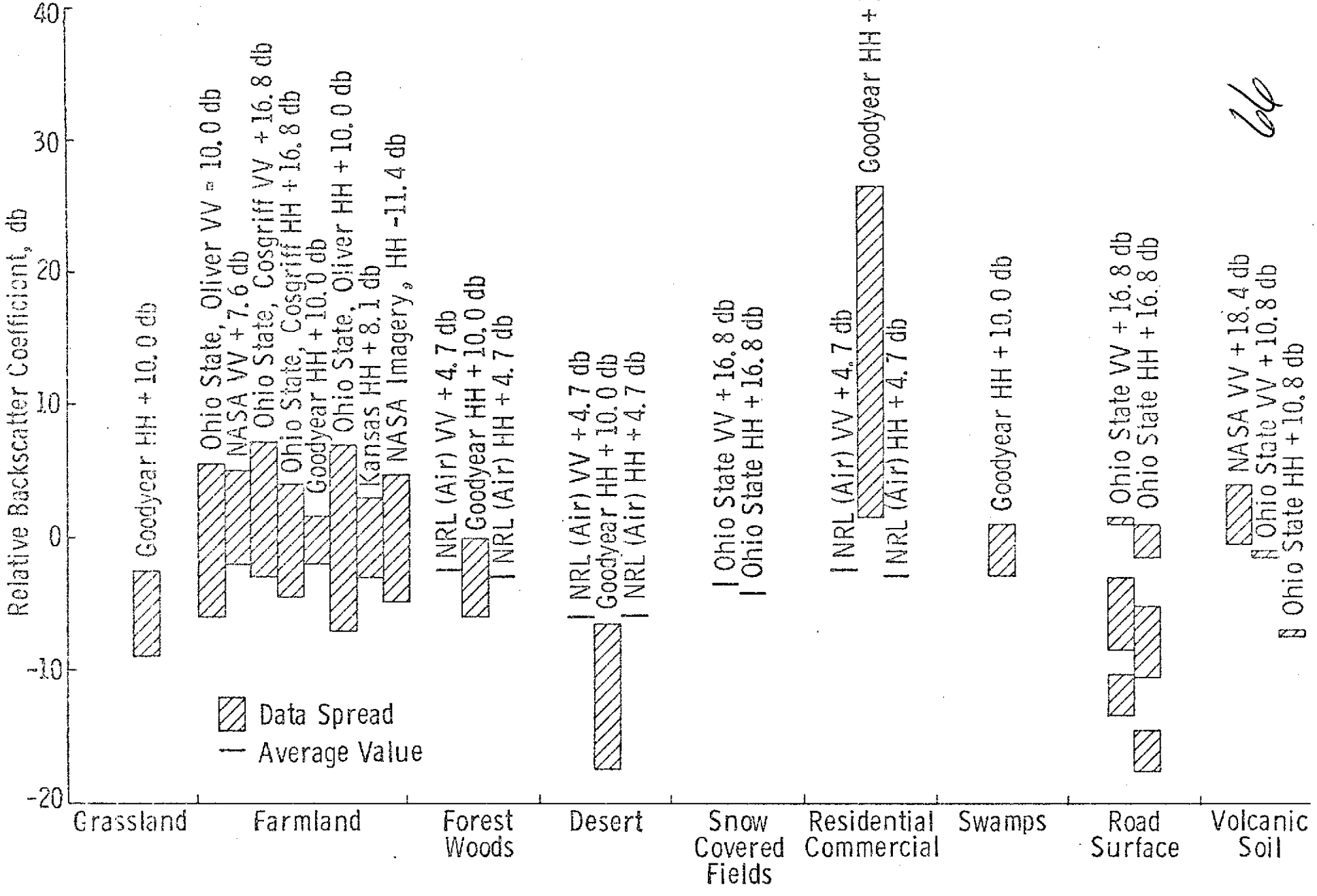

Figure 26E. 52° Incidence, Relative σ°, Normalized to Farmland Data at 52° HH Polarization.

4.0 CONCLUSION

A brief survey of previous radar terrain backscatter cross-section measurement programs was conducted and the result described. The main emphasis in the survey is in the area of sensors operating within or close to the specifications of the S-193 radscat. The only sources of data that fell within the prescribed domain are Naval Research Lab. aircraft and bridge-mounted programs, the Goodyear aircraft program, the Ohio State truck mounted program, and the NASA/Ryan airborne programs.

The data presentations were in three formats: the original data with their reported absolute values, the backscatter data normalized to one incidence angle, 52°, and data normalized to one terrain category, namely farmland, at 52°. In their original states, data taken by different research groups did not compare favorably with one another. The only way to differentiate different terrain categories was to examine one set of data obtained by the same sensor.

Even after normalizing to one incidence angle, the land targets could not be differentiated among themselves.

The most promising method of presentation seems to lie with the normalization of all data to farmland. Desert, road pavements, and volcanic areas can be separated; and, to a certain extent, grasslands and woods can be differentiated from the vegetated farmland.

The discussions in this report pointed out the obvious need for a coordinated research program. The S-193 radscat, with its tremendous potential area of coverage, should be a great asset in the study of backscatter phenomena from different terrain targets. In the words of the original proposal "it provides an unparalleled opportunity to collect scattering coefficient data... Although such observations cannot completely make up for the previous lack of data, use of S-193 on a single pass across the U. S. will permit acquisition and cataloging of a wider variety of backscatter data then reported in all the previous studies".

APPENDIX

EXPERIMENTAL DATA OF WIND-AFFECTED SEA BACKSCATTER

Measurements of the wind dependence of radar sea return have been conducted by many investigators in the past. The University of Kansas, under contract from NASA/MSC, studied the wind effect on ocean backscatter with a 13.3 GHz scatterometer. The Naval Research Laboratory has also conducted extensive measurements over a period of 30 years.

Altogether eight NASA ocean missions were flown in the period 1966-1971. Out of these, data from the two latest missions (Missions 119 and 156) were most reliable [33]. Figures A-1 and A-2 show the response of σ^o as a function of incidence angle θ plotted for several wind speeds for missions 119 and 156. The wind directions for both curves were upwind referenced to the aircraft flight direction. Both figures had been normalized such that σ^o at $\theta=10^o$ always appeared as 0 dB. The reason for normalization was to remove the effect of variability of the calibration signal in the scatterometer, thus allowing a comparison of data taken from both missions 119 and 156.

The normalized data from these two missions suggested a dependence on wind speed as governed by the following relationship

$$\sigma^o \propto W^{\alpha}$$

where σ^o is the backscattering cross-section, W the wind speed and α the wind speed exponent. For upwind flight direction and at the incident angle of 35^o, curve fitting showed the wind speed exponent to be 1.49, as shown in Figure A-3. In general, the exponent increased with incidence angle and was higher for upwind direction than for cross wind.

The results obtained by NRL were examined by researchers at NYU and The University of Kansas [34]. Extensive statistical analysis on two separately conducted NRL missions, the 1969 Northern Ireland (North Atlantic) mission and 1970 Bermuda (JOSS I) mission, showed that the ocean backscatter exhibited wind speed dependence similar to that obtained by the NASA 13.3 GHz scatterometer.

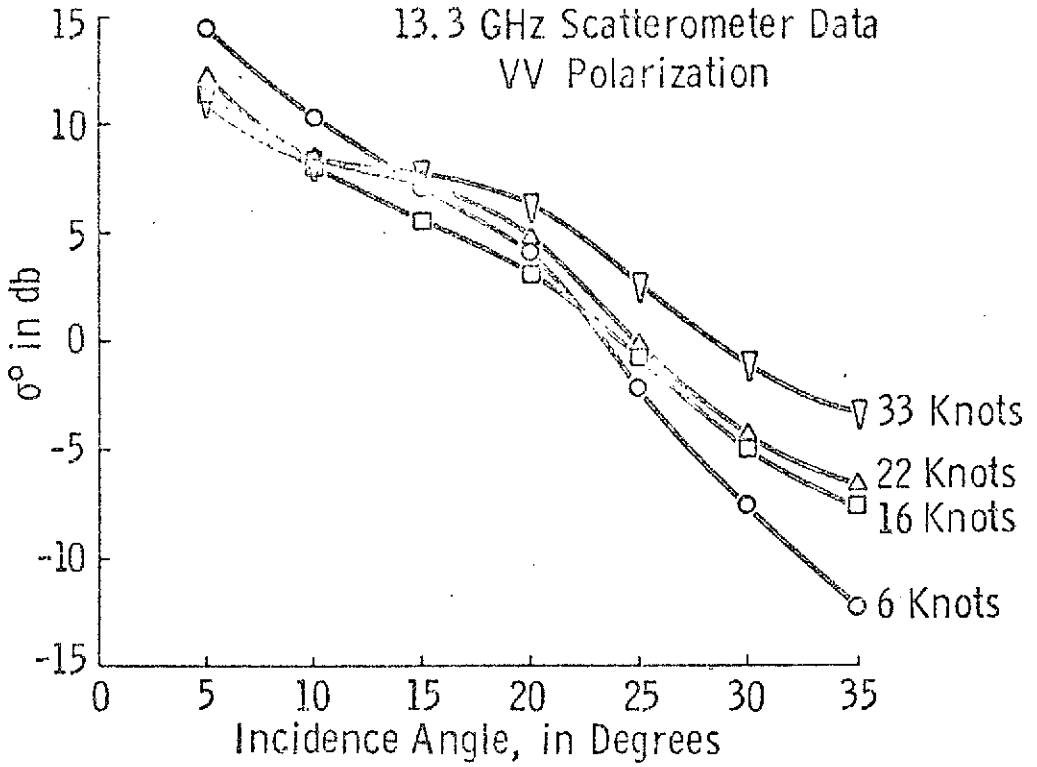

Figure A-1a. Upwind Radar Scatterometer Ocean Data, Mission 119. (After Bradley)

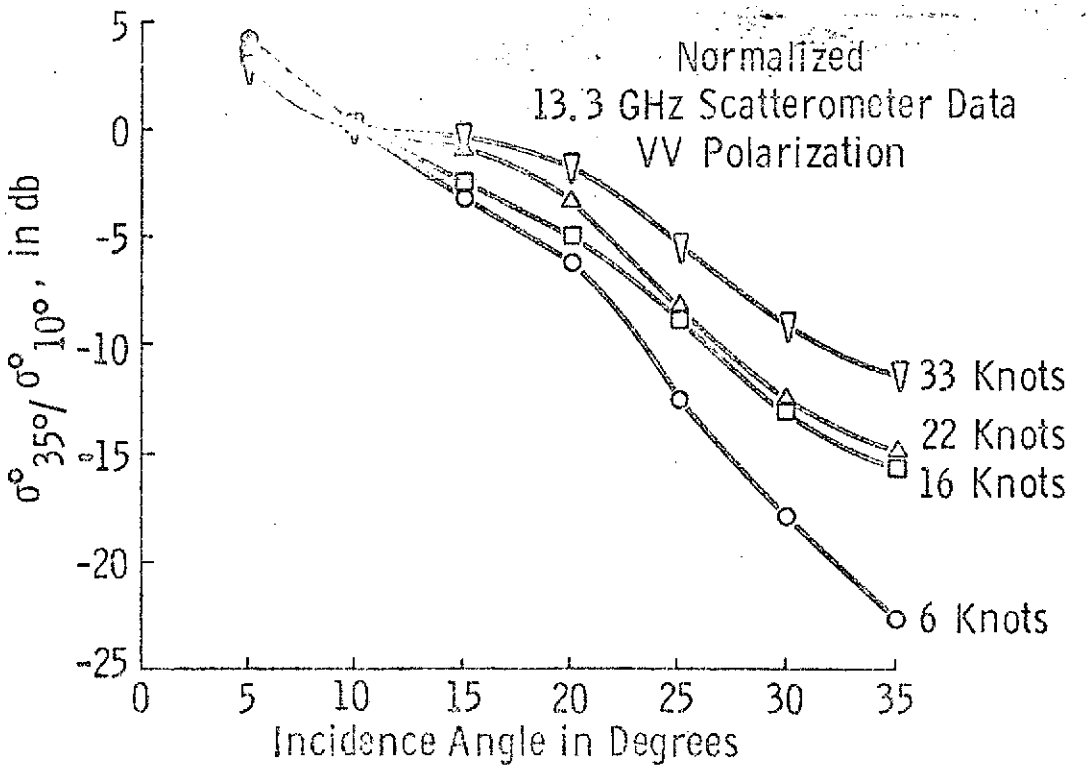

Figure A-1b. Normalized Upwind Radar Scatterometer Ocean Data, Mission 119. (After Bradley)

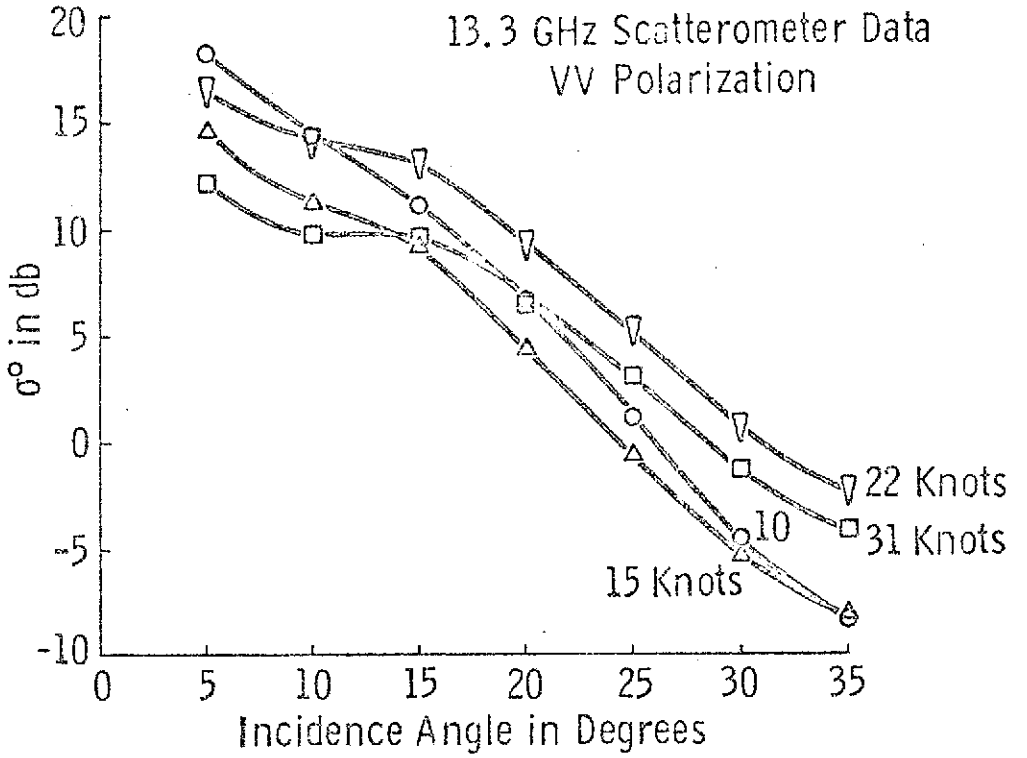

Figure A-2a. Upwind Radar Scatterometer Ocean Data, Mission 156.

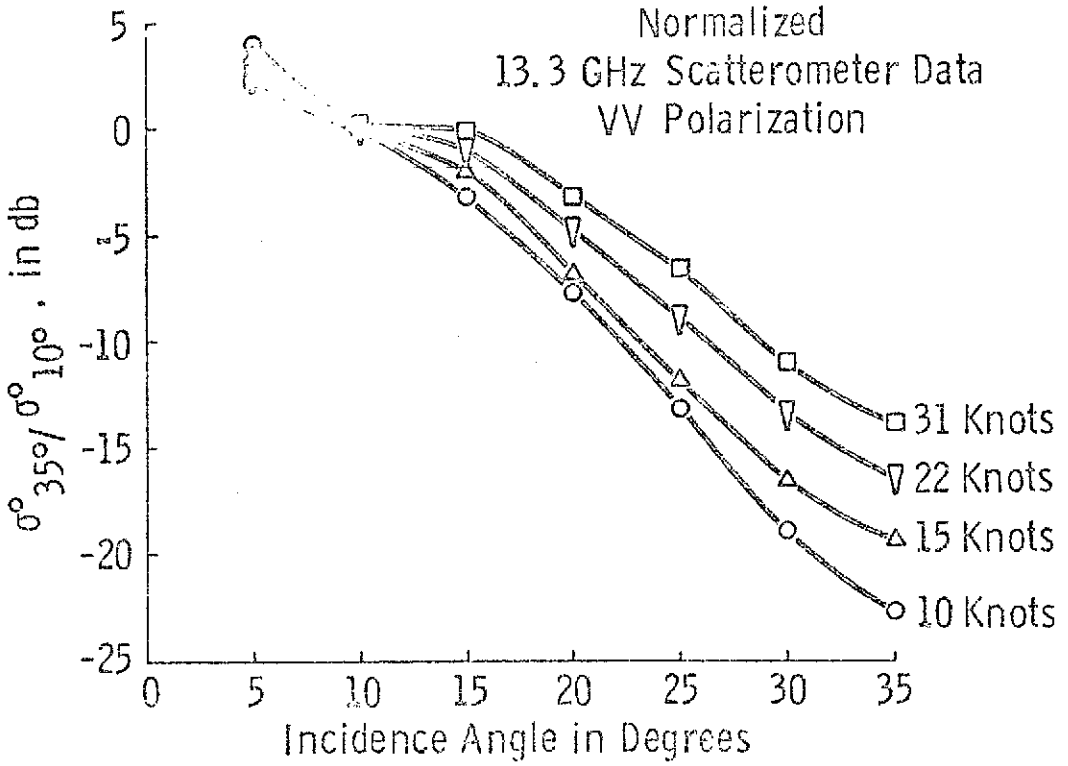

Figure A-2b. Normalized Upwind Radar Scatterometer Ocean Data, Mission 156.

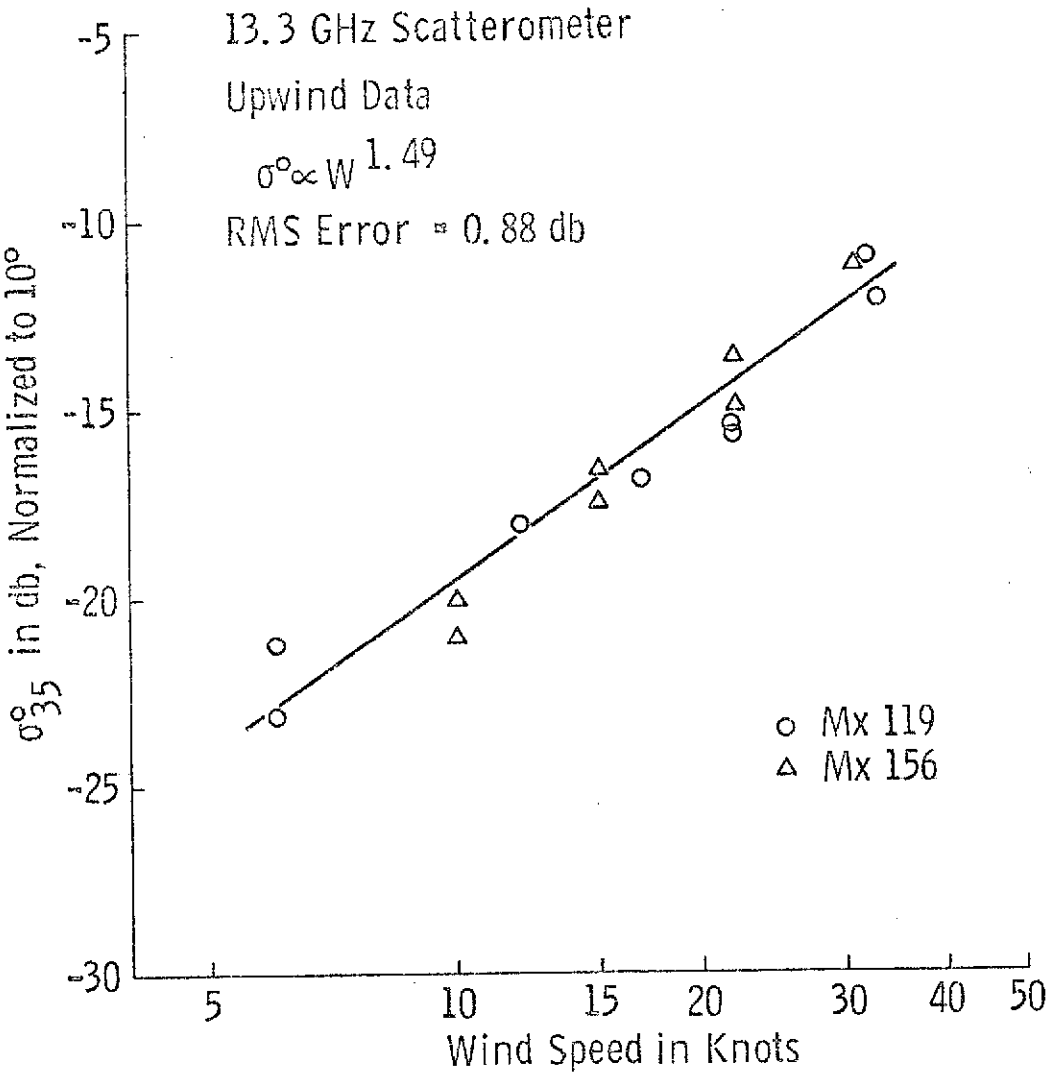

Figure A-3. Relationship between σ^o and Ocean Wind Speed. Upwind Direction. (After Bradley)

The absolute level of return from the North Atlantic mission, however, was lower than that from JOSS I. Sample graphs from X band data at 30° incidence are shown in Figure A-4 where the bias between the data for the two missions is readily apparent. Generally larger separations were observed for VV polarized data than HH polarized data, and similar separations were observed when like polarized data upwind and downwind were compared. When this bias was removed (Figure A-5) the wind dependence remained unchanged with a growth law of approximately 1.1. This power law relationship was established without normalizing the data to some incidence angle. The exponents vary with respect to both incidence angle and polarization. In general, vertical polarization yields a higher return. Some samples of the adjusted NRL σ^o vs incidence angle curves are shown in Figures A-6 and A-7.

In summary, the NASA/MSC and the adjusted NRL data can be grouped as shown in Table A-1. Comparison between the two sets of data should be done with caution since the 13.3 GHz data were normalized and the 8.9 GHz data were not.

TABLE A-1

	Polarization	Freq.	25°	30°	35°	60°
NASA	VV	13.3 GHz	1.12		1.49	
NRL	VV	8.9 GHz		1.0		1.3
NRL	HH	8.9 GHz		1.1		1.5

Power Law Exponents in the Relation Between Radar Backscatter and Windspeed, based on Upwind Data (from Moore, et al[35]).

This brief discussion of radar sea return is far from exhaustive. This subject has been studied by so many workers around the world that a comprehensive summary would be larger than this entire report!

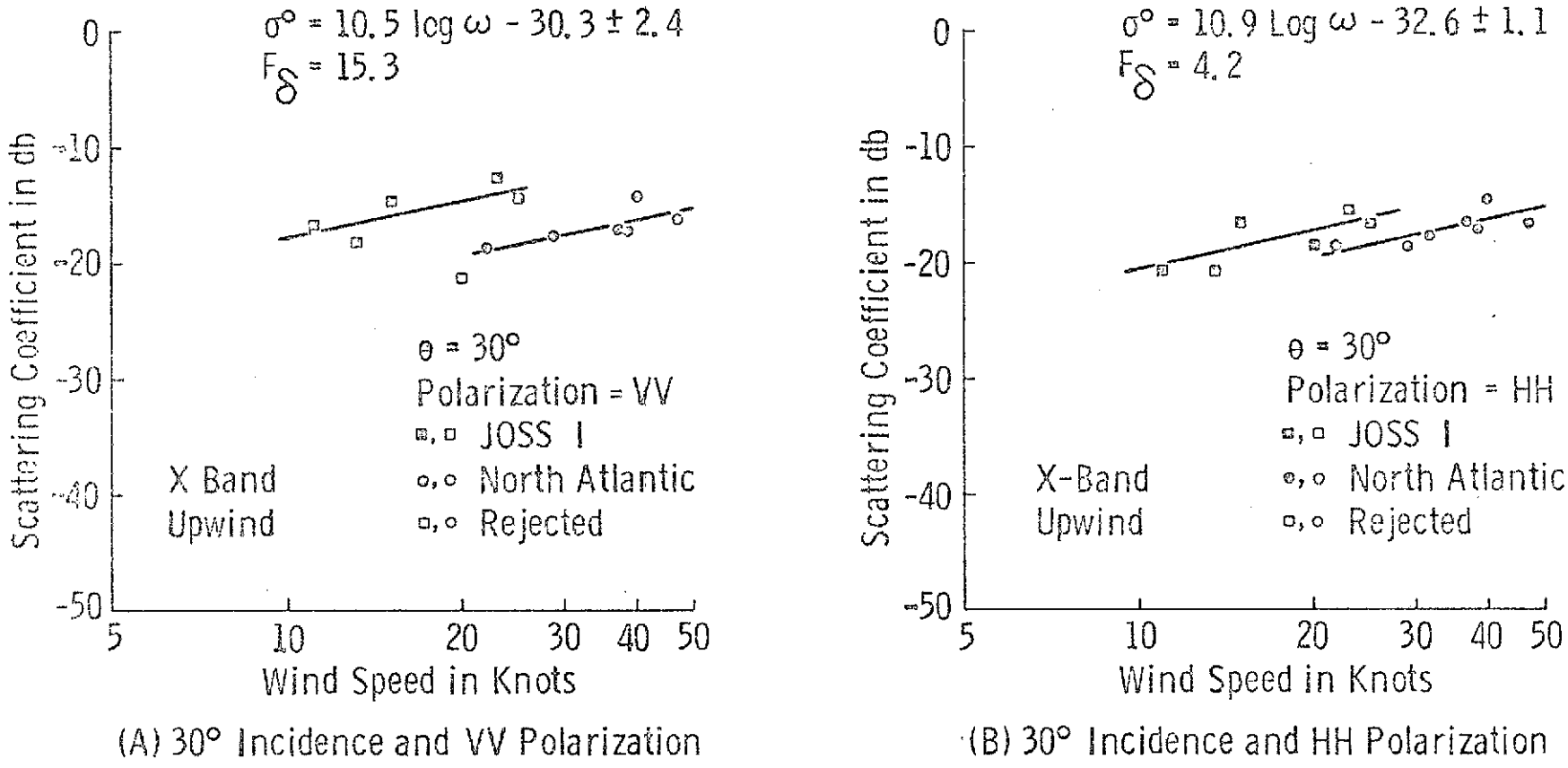

Figure A4. The Wind Response of NRL X-Band Data Showing Separation between Two Separately Conducted Missions. (Courtesy of J. P. Claassen and H.S. Fung)

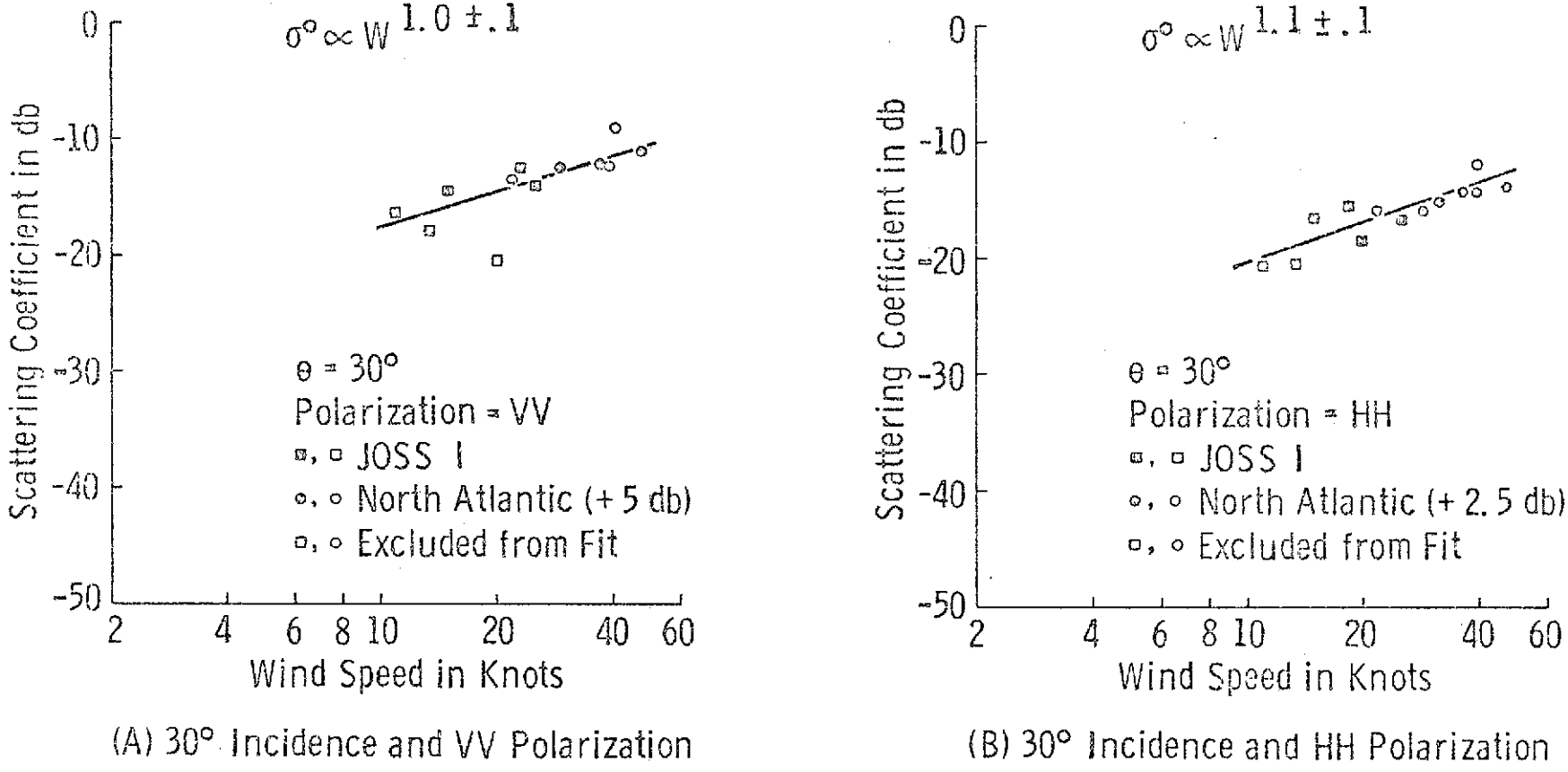

Figure A-5. The Wind Response of NRL Scatterometric X-Band Data with Apparent Bias Removed and Under Listed Conditions. (After Moore, et al.[35])

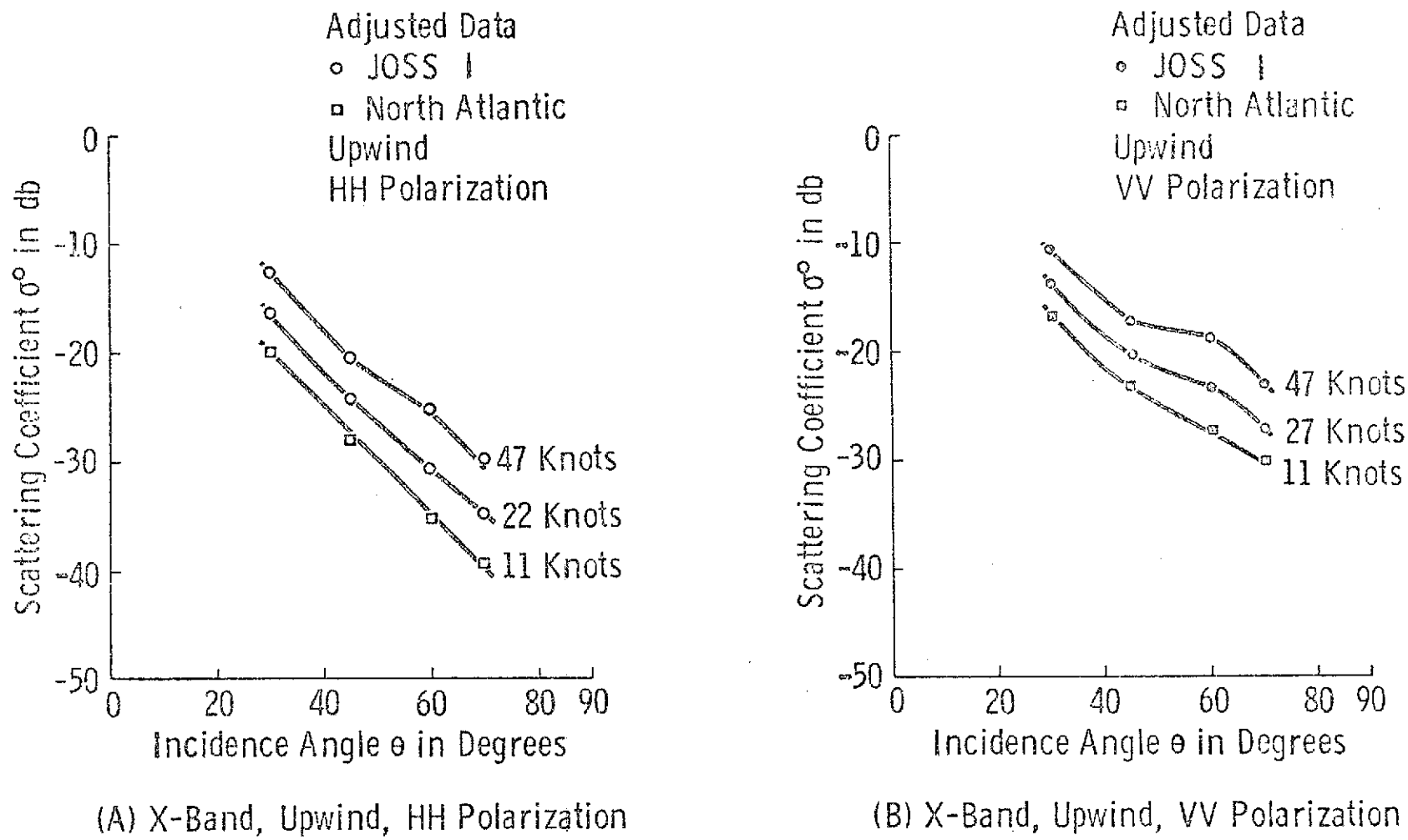

Figure A-6. σ° vs. θ Plots of Adjusted NRL Ocean Data for X-Band Upwind Cases.
(Courtesy of J. P. Claassen and H. S. Fung)

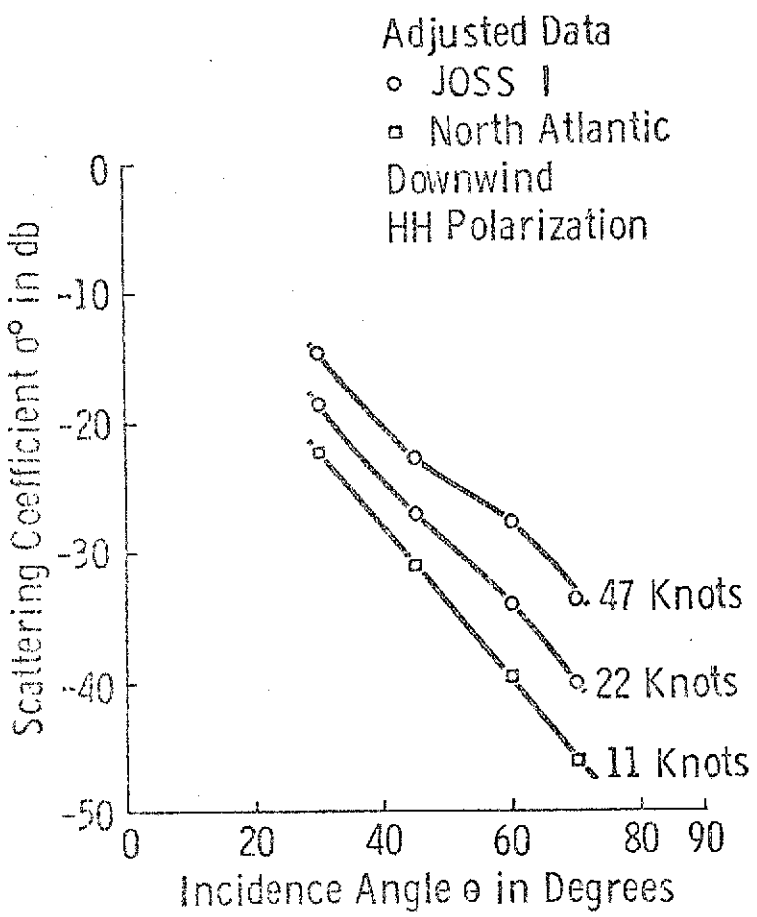

(A) X-Band, Downwind, HH Polarization

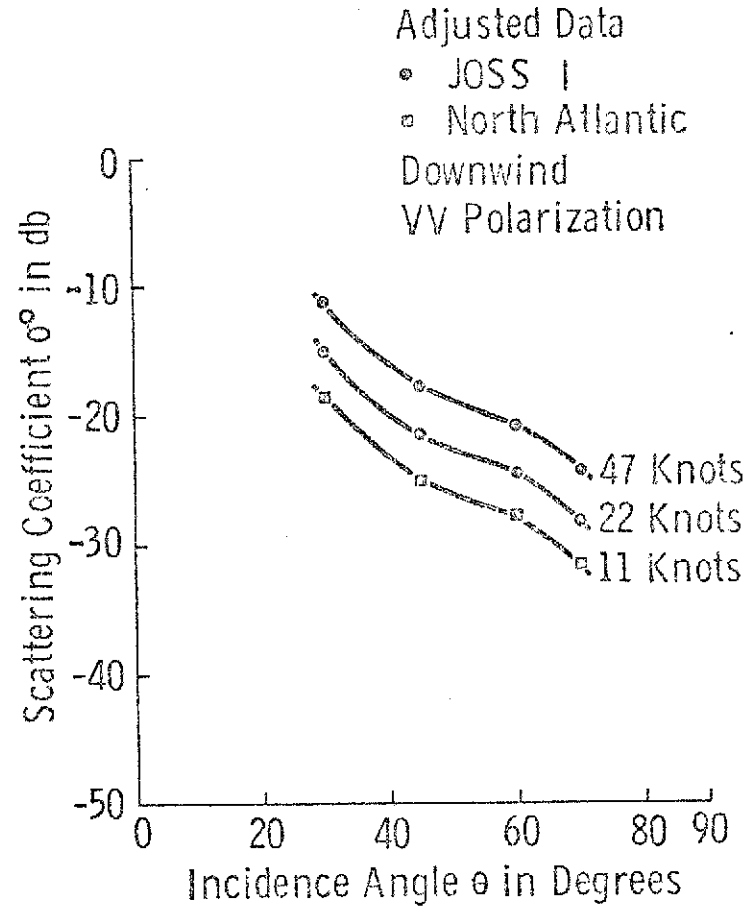

(B) X-Band, Downwind, VV Polarization

Figure A-7. σ° vs. θ Plots of Adjusted NRL Ocean Data for X-Band Downwind Cases.
(Courtesy of J. P. Claassen and H. S. Fung)

REFERENCES

[1] Ament, W. S., F. C. MacDonald and R. D. Shewbridge, "Radar Terrain Reflections for Several Polarizations and Frequencies," Trans. 1959 Symp. Radar Return, Pt. 2, May 11-12, 1959.

[2] Grant, C. R. and B. S. Yaplee, "Backscattering from Water and Land at CM and MM Wavelength," Proc. IRE, pp. 976-982, July, 1957.

[3] Reitz, E. A., et al., "Radar Terrain Return Study Final Report-Measurement of Terrain Backscattering Coefficients with an Airborne X-band Radar," Goodyear Aerospace Corp. Report GERA-463, September, 1959.

[4] Newbry, L. E., "Terrain Radar Reflectance Study," Photogrammertic Engineering, pp. 630-637, 1961.

[5] Cosgriff, R. L., W. H. Peake and R. C. Taylor, "Terrain Scattering Properties for Sensor System Design-Terrain Handbook II," Antenna Lab, Ohio State University, Columbus, Ohio, May, 1960.

[6] Oliver, T. L. and W. H. Peake, "Radar Backscattering Data for Agricultural Surfaces," Ohio State University ElectroScience Lab, Technical Report 1903-9, February, 1969.

[7] Shultz, C. H., R. L. Oliver and W. H. Peake, "Radar Backscattering Data for Surfaces of Geological Interest," Ohio State University Electroscience Lab, Technical Report 1903-7, December, 1969.

[8] Peake, W. H. and S. T. Cost, "The Bistatic Echo Area of Terrain at 10 GHz," 1968 WESCON Technical Papers, August, 20-23, 1968.

[9] Masenthin, H. W., "Scatterometer Data Analysis Technique," University of Kansas Center for Research, Inc., CRES Technical Report 118-3, July, 1967.

[10] Lundien, J. R., "Analysis of Scatterometry Data from Pisgah Crater," University of Kansas Center for Research, Inc., CRES Technical Report 118-2, August, 1967.

[11] Rouse, J. W., Jr., "Arctic Ice Type Identification by Radar," Proceedings IEEE vol. 57, no. 4, pp. 605-614, April, 1969.

[12] Parashar, S. K., "Investigation of Radar Discrimination of Sea Ice," The University of Kansas Center for Research, Inc., CRES Technical Report 185-13, December, 1973.

[13] Cullen J. M. and G. A. Bradley, "The Correlation of Radar Scatterometer Data with Aerial Terrain Photography," University of Kansas Center for Research, Inc., CRES Technical Report 118-13, April, 1969.

[14] Dickey, F., C. King, J. C. Holtzman, R. K. Moore, "Moisture Dependency of Radar Backscatter from Irrigated and Non-Irrigated Fields at 400 MHz and 13.3 GHz," accepted for publication in January, 1974 issue of IEEE Trans. on Geoscience Electronics.

[15] King, C., "Agricultural Terrain Scatterometer Observations with Emphasis on Soil Moisture Variation," University of Kansas Center for Research, Inc., CRES Technical Report 177-44, 1973.

[16] Simonett, D. S., J. E. Eagleman, A. B. Erhart, D. C. Rhodes and D. E. Schwartz, "The Potential of Radar as a Remote Sensor in Agriculture: A Study with K-band Imagery in Western Kansas," University of Kansas Center for Research, Inc., CRES Technical Report 61-21, March, 1967.

[17] Edison, A. R., F. J. Janza, R. K. Moore and B. D. Warner, "Radar Cross-Sections of Terrain Near Vertical Incidence at 415 Mc," University of New Mexico Engineer Experiment Station, Technical Report EE-15, 1959.

[18] Janza, F. J., R. K. Moore, and B. D. Warner, "Radar Cross-Sections of Terrain Near Vertical Incidence at 415 Mc, 3800 Mc and Extension of Analysis to X-band," University of New Mexico Engineer Experiment Station Technical Report EE-21, March, 1959.

[19] Edison, A. R., R. K. Moore, and B. D. Warner, "Radar Terrain Return Measured at Near Vertical Incidence," IRE Trans., PGAP, pp. 246-254, May, 1960.

[20] Lundien, J. R., "Terrain Analysis by EM Means - Radar Responses to Laboratory Prepared Soil Samples," U. S. A. E. Waterways Experiment Station Technical Report 3-693, September, 1966.

[21] Lundien, J. R., "Materials Analysis by Swept-Frequency Radar Interrogation," U. S. A. E. Waterways Experiment Station Technical Report, June, 1971.

[22] Linell, T., "An Experimental Investigation of the Amplitude Distribution of Radar Terrain Return," Swedish Res. Inst. of Natl. Def. Report, October, 1966.

[23] Eklund, F., "Experimental Investigation of Scattering from Irregular Surfaces," Swedish Def. Res. Inst. Report, 1969.

[24] Ericson, L. O., "Terrain Return Measurement with an Airborne X-band Radar Station," Swedish Res. Inst. of Natl. Def. Report, October, 1966.

[25] de Loor, G. P. and A. A. Jurriens, "Radar Ground Returns, Part I: The Radar Backscatter of Vegetation," Physics Lab of the Natl. Def. Res. Organization TNO (Dutch), Report Ph. L. 1972-73, January, 1972.

[26] King, H. E., C. J. Zamites, D. E. Snow, and R. I. Colliton, "Terrain Backscatter Measurements at 40 to 90 GHz," IEEE Trans. PGAP, vol. AP-18, no. 6, pp. 780-784, November, 1970.

[27] Ulaby, F. T., "Radar Measurement of Soil Moisture Content," University of Kansas Center for Research, Inc., CRES Technical Report 177-35, April, 1973, also to be published in March, 1974 issue of IEEE Trans. PGAP.

[28] Ulaby, F. T., "Radar Response to Vegetation," University of Kansas Center for Research, Inc., CRES Technical Report 177-42, September, 1973.

[29] Brown, W. E., "Radar Studies of the Earth," Proc. IEEE, vol. 57, no. 4, pp. 612-620, April, 1969.

[30] Venier, G. O. and F. R. Cross, "An Experimental Look at the Use of Radar to Measure Snow and Ice Depth," Comm. Res. Center Technical Memorandum, July, 1972.

[31] Sobti, A., "A Simulation Study of the S-193 Radscat in Orbit," University of Kansas Center for Research, Inc., CRES Technical Report 190-2, May, 1973.

[32] Moore, R. K., "Ground Echo," Radar Handbook, M. I. Skolnik, ed., McGraw Hill, 1970.

[33] Bradley, G. A., "Remote Sensing of Ocean Winds Using a Radar Scatterometer," Ph. D. Thesis, University of Kansas Center for Research, Inc., September, 1971.

[34] Claassen, J. P., H. S. Fung, R. K. Moore and W. J. Pierson, Jr., "Radar Sea Return and the RADSCAT Satellite Anemometer," Proc. 1972 IEEE Conf. Engin. in Ocean Environ., Newport, Rhode Island, September 13-15, 1972.

[35] Moore, R. K., J. P. Claassen, A. K. Fung, S. Wu, and H. L. Chan, "Toward RADSCAT Measurements over the Sea and their Interpretation," Proc. AAFE Principal Investigator's Review, NASA Langley Research Center, Hampton, Virginia, October, 1971, pp. 115-140.